EVALUATING METAMORPHIC PRESSURE-TEMPERATURE-TIME PATHS ALONG MILFORD SOUND, FIORDLAND, NEW ZEALAND

by

HANNAH FAITH DICKSON

HAROLD STOWELL, COMMITTEE CHAIR
KIMBERLY GENAREAU
DELORES ROBINSON
JOSHUA SCHWARTZ

A THESIS

Submitted in partial fulfillment of the requirements
for the degree of Master of Science
in the Department of Geological Sciences
in the Graduate School of
The University of Alabama

TUSCALOOSA, ALABAMA

2022

ABSTRACT

Fiordland, New Zealand offers an opportunity to study exposures of mid- to- lower crust that contain evidence for high temperature and pressure processes occurring beneath magmatic arcs. This thesis presents pressure, temperature, and time paths for rocks along Milford Sound to better understand the tectonic history and timing of metamorphism within and adjacent to the Anita Shear Zone. Samples analyzed are from St. Anne Point to near Milford Village here named the Milford Sound Transect. Rocks from the Thurso Gneiss (18MSNZ510a), Milford Geiss (15NZ51), Pembroke Granulite (05NZ12), and Camp Oven Creek Paragneiss (15NZ63), from west to east along the Milford Transect yielded garnet Sm-Nd ages of 99±7, 93±5, 122±2, and 119±8 Ma. Mineral assemblage diagrams and thermobarometry indicate somewhat higher pressures and temperatures in the central and eastern parts of the Milford Transect. Rocks in the Anita Shear Zone (18MSNZ511b; 18MSNZ510a) equilibrated at 9.5 to 11 kbar at temperatures of 650-700 ºC and 525 – 625 ºC, respectively. East of the Anita Shear Zone (15NZ51) peak metamorphism reached 10.5 to 11 kbar at 625-675 ºC. These new P-T-t data, with P-T data from Czertowicz and others (2016) and Klepeis and others (1999) provide a direct temporal link between garnet growth, high pressure metamorphism, and shear zone fabrics. Further east, samples 05NZ12, and 15NZ63 equilibrated at; 11-16 kbar at 640 – 725 ºC; and 8.5-13.5 kbar at 525- 625 ºC, respectively. Our new data delineates a ~ 7 km wide zone of < 100 Ma 9.5 to 11 kbar metamorphism along the western, and a ~8 km wide zone of > 11 kbar >100 Ma metamorphism along the eastern part of the Milford Transect. Garnet age differences between 15NZ51 and 05NZ12 of ca. 30 m.y., higher between them is compatible with possible fault

separation. I infer a fault or shear zone separating the young (<100 Ma) medium pressure (9.5 to 11 kbar) metamorphism along the eastern Milford Transect and the considerably older (122 to 126 Ma) Pembroke Granulite metamorphism at higher pressure (>11 kbar).

DEDICATION

This thesis is dedicated to my parents, Billy and Chris for supporting me throughout my life, and my cats Annie and Emmy for keeping me sane.

LIST OF ABBREVIATIONS AND SYMBOLS

Mineral Abbreviations after Kretz (1983):

Ab	Albite
And	Andalusite
Bt	Biotite
Camp	Clinoamphibole
Chl	Chlorite
Cpx	Cinopyroxene
Czo	Clinozoisite
Grt	Garnet
Hbl	Hornblende
Ilm	Ilmenite
Ky	Kyanite
Ms	Muscovite
Oamp	Orthoamphibole
Pl	Plagioclase
Qtz	Quartz
Rt	Rutile
Sil	Sillaminte
Tt	Titanite
Zrn	Zircon

Garnet End Members:

Alm Almandine (Fe)

Grs Grossular (Ca)

Prp Pyrope (Mg)

Sps Spessartine (Mn)

ACKNOWLEDGEMENTS

I would like to formally thank everyone who has helped me throughout my time completing my thesis research. Dr. Harold Stowell, committee chair of this thesis, has been an excellent mentor throughout my graduate degree and I am most indebted to him for his research expertise on metamorphic petrology and geochronology and wisdom on all subjects of life. I would also like to thank my thesis committee members, Dr. Delores Robinson, Dr. Kimberly Genareau, and Dr. Joshua Schwartz for their expertise, knowledge, and editing. I must also thank my friends in the RadIs Laboratory, Savanna Gutapfel, Ian Anderson, and Elizabeth Bollen whose friendship and support I am most grateful for. Robert Holler of the Alabama Analytical Research Center was very helpful in training and helping with technical issues on the EPMA.

I would also like to express my appreciation for the financial support I have received while completing this thesis: The University of Alabama Graduate School Research and Travel Funds, The W. Gary Hooks Endowed Geology Fund, Department of Geological Sciences Research Scholarship. I am also thankful for the support from the National Alumni Association Tag Graduate Fellowship and 3 years of support through various teaching assistant positions in geological sciences. These positions provided meaningful and rewarding teaching experiences I am grateful to have had.

CONTENTS

LIST OF TABLES

LIST OF FIGURES

INTRODUCTION

Fiordland, New Zealand is one of the few locations worldwide that allow observation of mid- to lower -crustal rocks containing evidence for high temperature and pressure processes occurring beneath magmatic arcs (e.g., Tulloch et al., 2009). This exhumed crustal block contains numerous plutons of intermediate composition which intrude Paleozoic metasedimentary rocks. The dominantly Mesozoic plutons can be grouped into paired belts of older mid-crustal plutons on the east and younger lower crustal plutons on the west. The Fiordland crustal block is currently exhuming due to transpression along the Cenozoic Alpine Fault or underthrusting of oceanic crust of the Tasman Sea (e.g., Norris and Toy, 2014). Although displacements along the Alpine Fault *sensu stricto* are likely < 45 Ma (Sutherland, 1999), there may have been older faults in a broader zone of deformation (e.g., Sutherland, 1999). The Anita Shear Zone, which parallels the Tasman Sea coastline in northern Fiordland (Fig. 1), may represent a transpressional precursor to the Alpine Fault (Blattner 1991) or part of the subhorizontal Doubtful Sound Shear Zone to the south (Hill, 1995a, 1995b). Therefore, P-T-t paths for metamorphic rocks in the Anita Shear Zone which include both subhorizontal and subvertical foliations are important for reconstructing the tectonic history (Klepeis et al., 1999).

The purpose of this study is to determine the timing and conditions of metamorphism across the Anita Shear Zone and adjacent rocks exposed in a transect along Milford Sound from St. Anne Point to Milford Village in northern Fiordland, New Zealand (Milford Transect) (Fig. 1). Emphasis is on the ages of garnet and the pressure-temperature-time paths for rocks in and adjacent to the Anita Shear Zone. The Anita Shear Zone is an inactive zone of highly deformed

rocks that parallels the currently active Alpine Fault and forms the western boundary of the lower crustal Fiordland block of Zealandia (Klepeis et al., 1999; Claypool et al., 2002). Metamorphism of rocks in the Anita Shear Zone is complex, and the timing of amphibolite facies mineral growth is proposed to be Paleogene to Neogene based on recent titanite U-Pb, zircon U-Pb, and white mica Ar^{40}/Ar^{39} geochronology from this zone (Simon 2017; Czertowicz et al., 2016; Claypool et al., 2002). These ages and estimated mid-crustal pressures (Klepeis et al., 1999), indicate that the Anita Shear Zone may contain rocks with similarities to the those currently deep along the Alpine Fault and evidence for the earliest right lateral displacement along the western edge of the South Island (Wood, 1972).

This study utilizes garnet Sm-Nd ages from a suite of five samples along Milford Sound (Fig. 1) to determine the timing of garnet growth. Previous titanite and white mica populations are predominantly Miocene in age; however, metamorphic zircon rims within the Anita Shear Zone have Cretaceous and Paleozoic ages (Simon 2017). The new garnet age results presented here combined with P-T estimates provide new insights into the tectonic history of the Anita Shear Zone and initial extension associated with the separation of Zealandia from Australia.

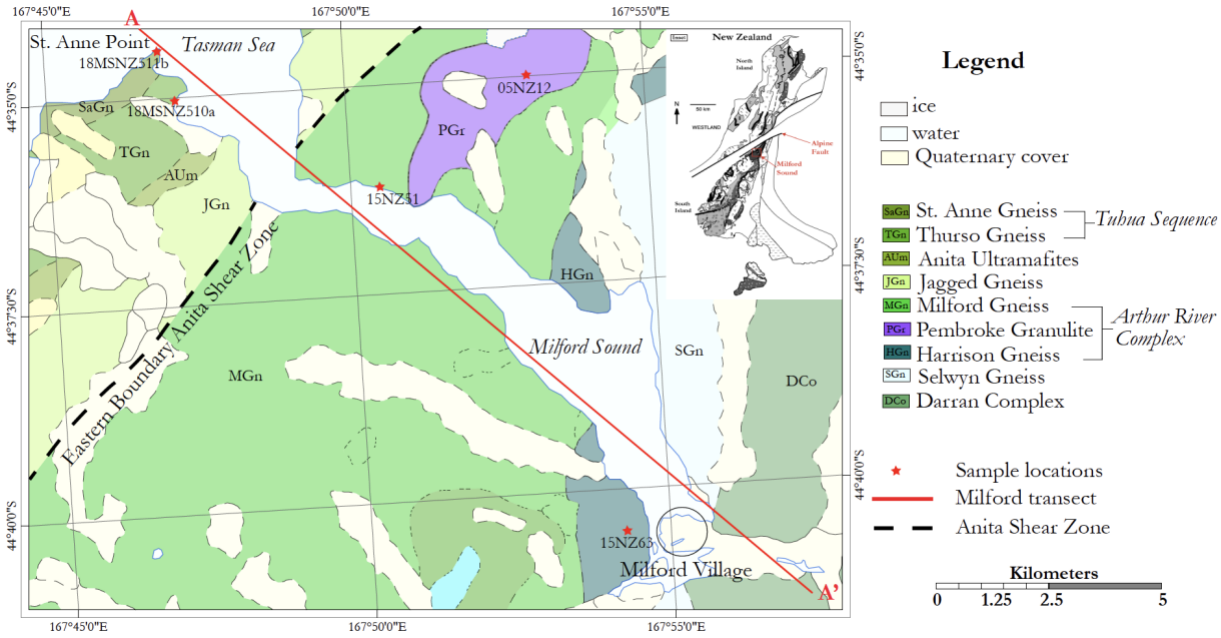

Figure 1. Simplified geologic map of the Milford Sound area with sample locations from this study. Geology is from Klepeis (unpublished) and Turnbull et al. (2010). Inset map is modified from Hollis et al. (2004). Bold red line defines the Milford Transect discussed in this study.

Regional Geology

Zealandia, a largely submerged continent that includes all of New Zealand (Mortimer et al., 2017), was part of the convergent margin of Gondwana during Late Cretaceous time (Klepeis et al., 2016). Subduction of the Pacific plate beneath the eastern edge of Gondwana and arc-magmatism formed the western and eastern provinces of Fiordland (Mortimer, 2008). Zealandia broke away from the Gondwana margin when the Tasman Sea opened at ca. 83 Ma and seafloor spreading began (Gaina et al., 1998). The Alpine Fault is a Tertiary right lateral transpressional fault that links the southwestern and northwestern boundaries of Zealandia. It connects subduction along the Hikarangi Trough to the north with subduction initiation along the Puysegur Trench to the south. The Alpine Fault is an 850 km long, continental dextral strike-slip fault that accommodates some 60-90% of the obliquely convergent motion between the Pacific and Australian Plates in South Island, New Zealand (Barnes et al., 2005). Late Quarternary strike- slip displacement rate is 27±5 mm/year (Barnes et al., 2005). As a result of oblique subduction ca. 25 Ma, the Alpine Fault was formed (Klepeis et al., 2019).

The Anita Shear Zone, subparallel to the Alpine Fault, is a 4 to 5 km wide 30 km long zone of intensely deformed amphibolite- facies rocks (Hill, 1995; Klepeis et al., 1999; Czertowicz et al., 2016) exposed east of the Alpine Fault. This shear zone is dominated by steep to subvertical NNE- striking foliation. Two fjiords, Milford Sound and Poison Bay in northern Fiordland provide almost continuous exposure across the Anita Shear Zone and its wall rocks along sections oriented orthogonal to its NNE strike. The Anita Shear Zone and the Alpine fault have similarities that include their steep to subvertical orientations and their NNE strike. Milford Sound, the study area, exposes the following sequences of rock from west to east: Tuhua Sequence, Anita Ultramafites, Jagged Gneiss, Milford Gneiss, Arthur River Complex, and the

Darran Complex (Fig. 1). The Tuhua Sequence includes the St. Anne Gneiss and Thurso Gneiss. The Arthur River Complex includes the Milford Gneiss, Harrison Gneiss, and Pembroke Granulite.

Lithological units within the Anita Shear Zone include the St. Anne Gneiss, Thurso Gneiss, Anita Ultramafites, and the Jagged Gneiss. (Fig. 1). The western boundary of the shear zone is located within schistose and mylonitic rocks of the St. Anne Gneiss which shows a transition from sheared to unsheared rocks from west to east (Hill, 1995b). The Thurso Gneiss lies entirely in the Anita Shear Zone and consists of calc-silicate gneisses, marble and mafic mylonites with compositional layering parallel to the shear zone fabric. The Anita Ultramafites also lie entirely in the Anita Shear Zone, and are dominantly composed of layered harzburgite and dunite. The Jagged Gneiss contains fine-grained mylonitic foliation and extreme flattening of enclaves, dikes, and pegmatite resulting in compositional banding (Hill, 1995b).

The Anita Shear Zone contains evidence for three deformation events (Klepeis et al., 1999), defined as D_2, D_3, and D_4. D_2 and D_3 deformation events are categorized as amphibolite facies deformation events, whereas D_4 is categorized as greenschist facies deformation events. D_2 foliations are subhorizontal to gently east- or west- dipping compositional layering. D_3 foliations are subvertical, NNE- striking mylonitic foliations that transpose the older D_2 fabrics (Klepeis et al., 1999). D_4 is the youngest phase of deformation within the Anita Shear Zone and produced narrow subvertical greenschist facies shear zones that crosscut D_2 and D_3 structures. D_4 is best developed in the St. Anne Gneiss, the western boundary of the shear zone (Klepeis et al., 1999). Peak metamorphic conditions during D_2 were 11.9±1.1 kbar and 581±34°C, whereas, peak metamorphic conditions during D_3 were 8.7±1.2 kbar and 587±42°C (Klepeis et al., 1999). D_2 is interpreted as a simple shear- dominated event that accommodated lower crustal thinning

with ductile normal faulting that added to the thinning of the lower crust, decompression, and rapid isothermal exhumation of rocks during or after mid- Cretaceous extensional deformation (Klepeis et al., 1999). D_3 is interpreted as a major pure- shear dextral transpressional event that resulted from latest Cretaceous or early Tertiary oblique convergence during the last stages of the opening of the Tasman Sea (Klepeis et al., 1999). D_4 is interpreted to record an upper crustal reactivation by dextral strike- slip faults and narrow shear zones that strongly resemble late Tertiary deformation patterns associated with the southernmost segment of the Australian-Pacific transform plate boundary (Klepeis et al., 1999).

Czertowicz and others (2016) used garnet cores and inclusions to estimate metamorphic conditions for the Anita peridotite and surrounding gneisses at 675- 746 °C and sillimanite zone conditions (~2-7 kbar) (Stage I). Subsequent Stage II metamorphism produced high- Ca rims on garnet and crystallization of kyanite at or before burial to the base of thickened arc crust at ca. 686 °C and 11 kbar. Stage II was followed by extensive recrystallization and mylonitic deformation in the Anita Shear Zone (Stage III). Czertowicz and others (2016) include a zircon U-Pb age of 104 Ma from their sample SAP-1 collected <500 m west of 18MSNZ511b, which they interpret to reflect timing of metamorphism after Stage II.

Outside the Anita Shear Zone along Milford Sound, rocks preserve a complex history of deformation and in places, high pressure (12-13 kbar) granulite facies metamorphism (Blattner, 1991; Klepeis et al., 1999). Since these rocks are overprinted and deformed by the Anita Shear Zone, D_1 is interpreted to predate shear zone deformation (Klepeis et al., 1999). In the Pembroke Granulite, peak temperatures of garnet growth were > 680^{o}C at 11-14 kbar (Stowell et al., 2010).

The Arthur River Complex is a heterogeneous assemblage of orthogneisses and dikes and includes the Milford, Gneiss, Pembroke Granulite, and Harrison Gneiss. The Milford Gneiss

extends eastward from the shear zone 10 km and includes a variety of mafic to felsic gneisses. The mafic gneisses contain garnet porphyroblasts surrounded by eye- shaped leucosomes. Felsic veins are isoclinally folded with axial planes parallel to gneissic foliation. This unit is folded at the boundary of the Anita Shear Zone and transitions into the Jagged Gneiss. This contact is a gradational contact (Hill, 1995b). The Pembroke Granulite includes amphibolite, gabbroic gneiss, dioritic gneiss, trondhjemite veins, and adjacent garnet granulite reaction zones (Stowell et al., 2010). The Harrison Gneiss, which is part of the Arthur River Complex, is dioritic in composition and is dominated by west- dipping foliation (Daczko et al., 2001). Foliation is defined by flattened clusters of coarse amphibole and plagioclase grains with or without garnet, clinopyroxene, biotite and phengite (Daczko et al., 2001). Selwyn Gneiss is composed of hornblende diorite and garnet- biotite gneiss and is intruded by dikes (Claypool et al., 2002). The Darran Complex, east of the Arthur River Complex, and forms part of the Median Batholith (Daczko et al.,2001). The Darran Complex is composed of leucogabbros and diorites (Claypool et al., 2002; Bradshaw, 1989; Kimbrough et al., 1994; Mortimer et al., 1999).

Previous Geochronological Studies

Tulloch et al. 2009 and Stowell et al. 2010 presented zircon and garnet ages for the eastern part of Milford Sound. The zircon U-Pb ages are bimodal with peaks at 357 and 134 Ma (Tulloch et al. 2009). These authors interpreted the zircon data to indicate a ca. 134 Ma granulite facies metamorphic event after Paleozoic pluton emplacement in the Arthur River Complex. Sm-Nd garnet ages obtained from the Pembroke Granulite in Pembroke Valley, just north of Milford Sound range from ca. 126 to 109 Ma (Stowell et al., 2010). Stowell et al. interpreted the garnet Sm-Nd results to indicate that granulite facies metamorphism peaked at >680° C and 11 – 14 kbar between 126 and 123 Ma. Previous Sm-Nd garnet ages east of the Anita Shear Zone

suggest a younging trend from east to west along Milford Sound (Stowell et al., 2010; Stowell unpublished).

Prior studies identified at least 3 metamorphic events associated with widespread granitic intrusion have occurred in mid-to-lower crustal rocks in the Western Province of Fiordland (e.g., Bradshaw, 1989; Gibson and Ireland, 1995; Brown, 1996; Klepeis et al., 2003). These were defined as Paleozoic high-T at ca. 360 Ma; Cretaceous high-T and medium-P at ca. 135-125 Ma; and Cretaceous high-T and P (12-14 kbar) at 126-110 Ma. The WFO (Western Fiordland Orthogneiss) intruded the Arthur River Complex during the second Cretaceous event and caused crustal heating at high pressure (Bradshaw 1989; Gibson and Ireland, 1995; Brown, 1996; Klepeis et al., 2003). Zircon ages in the WFO range from 124- 121 Ma in the Worsely Pluton (Tulloch and Kimbrough, 2003; Hollis et al., 2004), 123-115 Ma in the Misty Pluton (Gatewood, unpublished; Klepeis and Allibone et al., 2009a), and 117- 114 Ma for the Malaspina Pluton (Tulloch and Kimbrough, 2003; Hollis et al., 2004).

Geochronological studies in the Anita Shear Zone include phengitic white mica ^{40}K-^{39}Ar, zircon U-Pb, titanite U-Pb, and garnet Sm-Nd ages. Phengitic white mica ^{40}K-^{39}Ar ages from the St. Anne Gneiss at Poison Bay record age clusters of 12-13 Ma and 20-30 Ma, which record two periods of mineral growth or recrystallization along with deformation in these shear zones during latest Oligocene- late Miocene (Claypool et al., 2002). Zircon U-Pb metamorphic ages (LASS-ICP-MS) from Anita Shear Zone at Milford Sound range from 112- 97 Ma and 280-300 Ma, which reflect Cretaceous and Paleozoic metamorphism (Simon 2017). Titanite U-Pb ages in the Anita Shear Zone record Miocene recrystallization with the oldest and most precise titanite crystallization ages of 19±1.3 Ma and 8.5±3.7 Ma (Simon 2017).

Research objectives for this study:

The overall objective for this thesis is to evaluate the tectonic significance and timing of deformation along the Anita Shear Zone. In this work, I divide the overall objective into 4 subcategories:

1) Determine the timing of garnet growth in the Anita Shear Zone

2) Evaluate a proposed decrease in peak metamorphic age from east to west along Milford Sound.

3) Construct metamorphic pressure- temperature- time paths for rocks along Milford Sound.

4) Determine if garnet along the Milford transect grew during the same metamorphic event.

I present data for a suite of five samples along Milford Sound and across the Anita Shear Zone. These are garnet bearing samples from the St. Anne Gneiss, Thurso Gneiss, Milford Gneiss, Pembroke Granulite, and Camp Oven Creek Paragneiss (samples 18MSNZ511b, 18MSNZ510a, 15NZ51, 05NZ12, and 15NZ63, respectively)(Fig. 1). The samples include porphyroblastic garnet schist, coarse garnet gneiss, and migmatitic garnet granulite (Fig. 2). In this study, I use metamorphic assemblage diagrams (MAD), thermobarometry, and garnet Sm-Nd ages to construct P-T-t paths in order to reconstruct conditions and timing of metamorphism.

METHODS

Petrography

Samples for this study were collected by Harold Stowell and other members of the Zealandia Academy of Petrochronology during the 2005, 2015, and 2018 field seasons in northern Fiordland, New Zealand. These samples were cut into rectangular rock tabs in the Rock Preparation Laboratory at the University of Alabama. Spectrum Petrographic and National Petrographic Service, Inc. produced thin sections for these tabs. Minerals and rock textures were identified and described using a standard petrographic microscope.

X-ray Fluorescence Spectrometry

Whole rock major element concentrations were determined by X- ray fluorescence spectrometry (XRF). Representative portions of each rock were selected for analyses and then pulverized with a ring and puck mill in the Spex Shatterbox at the University of Alabama. Powders were heated to 900°C to evaporate volatiles and calculate loss on ignition (LOI). Next, the rock powders were mixed with flux and fused into glass discs. XRF analyses were obtained using the PANalytical Epsilon 3^{XLE} at Louisiana State University. The resulting rock compositions were used for constructing MAD.

Electron Probe Microanalysis

Electron probe microanalysis was done at the University of Alabama's Analytical Research Center. Backscatter and X-ray images, and quantitative mineral compositions were determined on the JEOL 8600 Electron Probe Micro Analyzer (EPMA). Backscatter and X-ray images were obtained with the Bruker XFlash energy dispersive spectrometer (EDS) and JEOL wavelength dispersive spectrometers (WDS), respectively. Rock tabs were cut, polished, and carbon coated in preparation for analysis on the EPMA. The WDS were calibrated with multiple silicate mineral standards using Probe for Windows *Probewin 8.21* software (Donovan, 2007). For Si, Mg, Al, and Fe, the Smithsonian sourced standards were used and for Ti, Cr, C.M. Taylor sourced standards were used. Standards for analysis contained the following: Kakanui Pyrope, Kakanui Augite, Arneal Hornblende, Rutile, Chromite #5, Magnetite, Rockport Fayalite, Spessartine, Diopside #5a, Amelia Albite #4, and Orthoclase MAD-10. A 15 keV accelerating voltage and 200 nA beam current was used for garnet X-ray maps. Quantitative point analyses were calibrated using a 15 keV accelerating voltage and 20 nA beam current with count times of 30-45 seconds for Fe, Mg, Ca, Mn, Ti, Si, Al, Cr, Na, and K in garnet, plagioclase, biotite, muscovite, and amphibole.. A one micron beam diameter was used for all minerals, except plagioclase, where a 10 micron beam diameter was used in order to avoid Na "burn off". The resulting wt.% oxide compositions from this calibration were used to calculate mineral structural formulas and mole fractions of solid solution end members and were used in thermobarometry calculations.

Thermobarometry

Net-transfer and exchange thermobarometry was used for calculating the temperature and pressure of mineral equilibrium. Geothermometers which are sensitive to temperature with a

large change in enthalpy and entropy with small changes in volume and geobarometers which are sensitive to pressure with large changes in volume were employed. In this study, the garnet-hornblende and garnet-biotite geothermometers, and the garnet-biotite-plagioclase-muscovite geothermobarometer were utilized. Garnet- biotite and garnet-hornblende are both exchange thermometers that are based on the exchange of Fe and Mg between garnet and biotite, and garnet and hornblende (e.g., Ferry and Spear, 1978). The garnet-biotite-muscovite-plagioclase net transfer reaction involves a change of Al coordination from 6 to 4 and a change in Fe-Mg coordination from 8 to 6 (Ghent and Stout.,1981) making it pressure sensitive. Temperature and pressure estimates from these thermobarometers are used to augment and compare with P-T estimates MAD. Garnet- biotite- muscovite- plagioclase thermobarometry calibrations used in this study are described in Hodges and Crowley, 1985 and garnet- hornblende calibrations in Ravna, 2000. Thermobarometry reactions that used to calculate P-T estimates in this study are listed below:

Garnet-Biotite

(1) $Mg_3Al_2Si_3O_{12} + KFe_3AlSi_3O_{10}(OH)_2 = KMg_3AlSi_3O_{10}(OH)_2 + Fe_3Al_2Si_3O_{12}$

Garnet-Hornblende

(2) $3/5\ KCa_2(Mg)_5(Al,Si)_8O_{22}(OH)_2 + Fe_3Al_2Si_3O_{12} = Mg_3Al_2Si_3O_{12} + 3/5\ KCa_2(Fe)_5(Al,Si)_8O_{22}(OH)_2$

Garnet-Biotite-Muscovite-Plagioclase

(3) $3\ CaAl_2Si_2O_8 + KFe_3(AlSi_3)O_{10}(OH)_2 = Fe_3Al_2Si_3O_{12} + Ca_3Al_2Si_3O_{12} + KAl_2(AlSi_3)O_{10}(OH)_2$

Metamorphic Assemblage Diagram

THERIAK- DOMINO (De Capitani and Petrakakis, 2010) was used to construct MAD by forward modeling mineral stability based on whole rock compositions. Water content was estimated as the minimum amount needed to stabilize the observed mineral assemblages in granulite facies rocks based on temperature versus H_2O MAD (e.g., Stowell et al., 2010) or minimum for saturation below the solidus in pelitic rocks. These water contents were used to construct P-T MAD with garnet compositional isopleths. Phase diagrams were calculated in the MnNCKFMASHTOH chemical system which consists of Mn, Na, Ca, K, Fe, Mg, Al, Si, H, Ti, and O (Stowell et al., 2010, 2014). Mineral activity models were compiled and coded by Tinkham et al. (2001), using models form Holland and Powell (1998, 2003), White et al. (2007), and Diener and Powell (2012). The peak pressure and temperature conditions were estimated from the observed mineralogy, the P-T field for these minerals predicted from MAD and predicted and observed garnet compositions (e.g., Stowell et al., 2001). Garnet in lines on MAD are lines where garnet begins to grow under a certain P-T range with the given composition. Solidus lines are where a rock of that composition begins to melt.

Whole rock compositions from XRF analysis were converted into mole proportions of major elements for use in THERIAK-DOMINO. Modal percentages of important phases such as garnet were used to determine when each phase was growing or breaking down. Isopleths of the mole fractions of the end-member compositions for garnet were calculated and plotted to determine the equilibration P-T during metamorphism.

Garnet Sm-Nd Geochronology

The timing of garnet growth was determined by using Sm and Nd isotope ratios of garnet rims, garnet cores, bulk garnet, and whole rocks. Garnet, more than most other minerals, strongly

fractionates Sm over Nd, making it an excellent geochronometer for the isochron method (Baxter and Scherer, 2013). The technique relies on ^{147}Sm decay to the daughter product ^{143}Nd with a half-life of 1.06 Ga. Garnet isotope ratios are paired with isotopic measurements of the rock matrix (MTX) and whole rock (WR) to define the isochron.

Sample Preparation

Garnet samples were prepared as core and rim or bulk aliquots. Aliquots of garnet were obtained by drilling and chiseling rocks and larger grains. Garnet grains were then crushed for purification and dissolution.

Mineral inclusions in garnet that contain Sm and Nd can affect garnet ages since the Sm and Nd concentrations alter the isotopic ratios (e.g., Anczkiewicz and Thirlwall, 2003; Baxter and Scherer, 2013). Therefore, garnet is picked and leached to purify garnet aliquots. Inclusion-free garnet grains were hand picked under a 20x binocular microscope. Samples were sieved to 100-325 um and then leached in hot HNO_3, HF, and $HClO_4$. Rock and matrix samples were cleaned with acetone then powdered. Samples were then weighed and spiked for isotope dilution and then dissolved in HF and HNO_3. After samples were dissolved, fluorides were converted into chlorides with a series of HCl treatments. Bulk REE fractions were obtained by ion chromatography using BioRad polyprep columns. Sm and Nd aliquots from each sample, were obtained using 2-methylactic acid (MLA) ion chromatography columns. These methods are more fully described in Stowell et al. (2014, 2017).

Thermal ionization mass spectrometry

Sm and Nd isotope ratios were measured at the University of Alabama's RadIs Laboratory using the VG Sector 54 thermal ionization mass spectrometer (TIMS). Nd samples were loaded onto Re filaments and Sm samples were loaded onto Ta filaments. Nd isotope ratios

were measured using seven Faraday collectors in dynamic mode and Sm isotope ratios were measured using five Faraday collectors in static mode. The Nd and Sm isotope ratios and two sigma uncertainties were used in ISOPLOT (Ludwig, 2008) to calculate isochron ages. Neodinium standard JNdi values were $^{143}Nd/^{144}Nd = 0.512117 \pm 13$ ppm as compared to $^{143}Nd/^{144}Nd = 0.512115 \pm 7$ ppm reported by Tanaka et al. (2000) and BHVO-1 values were $^{143}Nd/^{144}Nd = 0.512960 \pm 9$ ppm and $^{147}Sm/^{144}Nd = 0.1500 \pm 0.0004$ as compared to $^{143}Nd/^{144}Nd = 0.512957 \pm 10$ ppm (Raczek et al., 2003) and $^{147}Sm/^{144}Nd = 0.1492$ to 0.1505 (Li et al., 2012). These values were averaged based on data from run times for samples used in this study May 2019- December 2020).

RESULTS

Rock compositions and petrography

Whole rock compositions obtained from XRF analysis and sample descriptions for samples 18MSNZ511b, 18MSNZ510a, 15NZ51, 05NZ12, and 15NZ63 are tabulated in Table 1. 18MSNZ511b composition resembles an average pelite (Shaw, 1958). 18MSNZ510a composition resembles a basalt. 15NZ51 composition is similar to a diorite. 05NZ12 composition resembles a dioritic gneiss. 15NZ63 composition resembles a diorite (Shaw, 195**8)**. The rock compositions were used in THERIAK- DOMINO for calculating MAD. Lithological units, peak assemblages, and rock types for samples are tabulated in Table 2. Hand sample scans and some outcrop photographs are shown in Fig. 2.

Table 1. Whole rock compositions and sample locations for samples along the Milford transect.

	18MSNZ511b	18MSNZ510a	15NZ51	05NZ12	15NZ63	Standard deviation	USGS AGV-2
Latitude	45°16'37.35"	45°15'59.20"	45°14'55.62"	44°35'18.40"	45°11'1.58"		
Longitude	17°44'35.59"	17°44'48.64"	17°47'27.65"	167°53'24.29"	17°48'51.12"		
Oxide-wt %							
SiO2	61.45	50.91	n.d.	51.85	65.12	7.05	59.30
Al2O3	15.63	17.92	n.d.	18.11	14.23	1.87	16.91
Fe3O3	10.35	12.55	n.d.	10.54	9.90	1.18	6.69
MnO	0.10	0.17	n.d.	0.16	0.39	0.13	n.d.
MgO	4.78	5.36	n.d.	4.44	1.50	1.72	1.79
CaO	1.68	8.33	n.d.	8.27	3.32	3.42	5.20
Na2O	1.35	3.15	n.d.	4.62	3.10	1.34	4.19
K2O	2.15	0.66	n.d.	0.41	2.02	0.90	2.88
TiO2	0.87	0.47	n.d.	1.04	0.76	0.24	1.05
P2O5	0.00	0.05	n.d.	0.14	0.18	0.08	0.48
Total	98.36	99.57	n.d.	99.58	100.52		98.49

*n.d. = not determined

*Oxide-wt% collected at LSU and UA

Table 2. Lithologic units, peak mineral assemblages, and rock types for the five samples along the Milford Transect.

Sample	Lithological unit	Peak Assemblage	Rock type
18MSNZ511b	St. Anne Gneiss	Grt, Pl, Bt, Qtz Ky, Rt	Garnet- biotite- muscovite schist
18MSNZ510a	Thurso Gneiss	Grt, Hbl, Qtz, Rt, Bt, Pl, Czo, Tt	Garnet amphibolite
15NZ51	Milford Gneiss	Grt, Pl, Hbl, Bt, Rt, Qtz, Cpx	Garnet amphibole gneiss
05NZ12	Pembroke Granulite	Pl, Grt, Cpx, Hbl, Qtz, Bt, Rt	Dioritic gneiss
15NZ63	Camp Oven Paragneiss	Grt, Pl, Bt, Czo, Rt, Qtz	Garnet gneiss

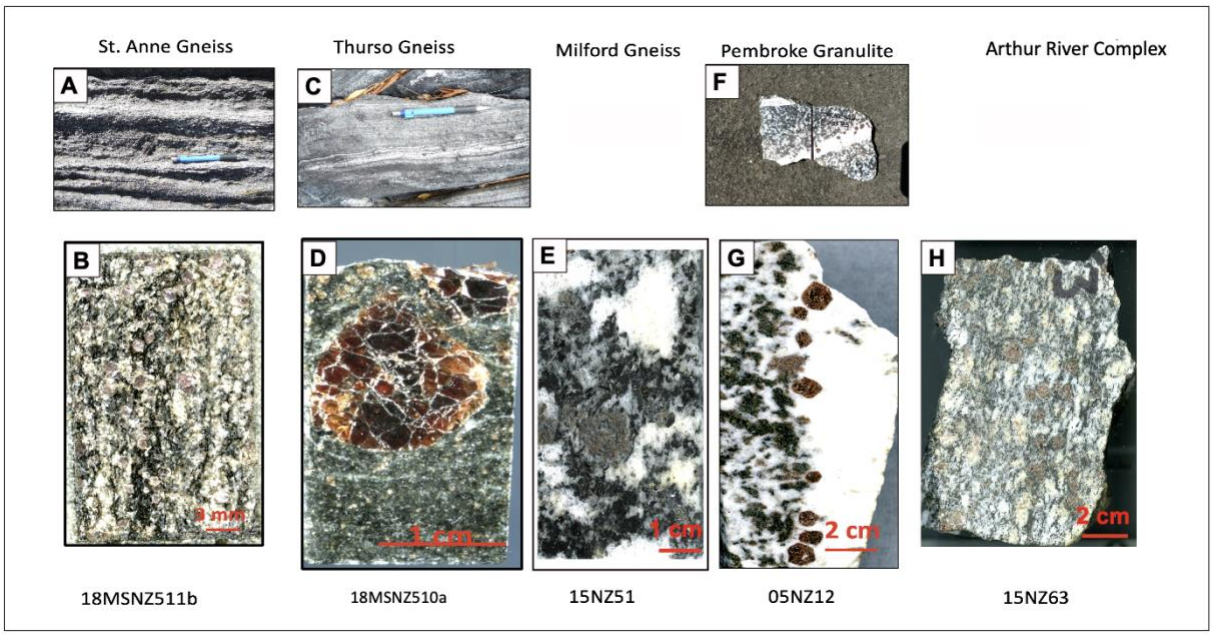

Figure 2. Outcrop and hand sample photos of samples along the Milford transect, Fiordland New Zealand. (A) St. Anne Gneiss outcrop photo showing compositional layering and the typical schistose foliation. (B) St. Anne Gneiss polished sample showing abundant garnet which is common throughout the outcrop. (C) Thurso Gneiss outcrop photo showing gneissic foliation. (D) Thurso Gneiss polished sample showing large 1 cm garnets and smaller 0.3 – 0.5 mm garnets found throughout rock. (E) Milford Gneiss polished sample showing 1 cm garnets with inclusions of hornblende and pyroxene and gneissic foliation present throughout this sample. (F) Pembroke granulite hand sample showing the leucosome, garnet reaction zone, and host rock in this sample. (G) Pembroke Granulite polished sample highlights 1 cm garnets that were dated in this study. (H) Camp Oven Creek Paragneiss sample showing ~1 cm garnets found throughout rock and gneissic foliation.

18MSNZ511b

Sample 18MSNZ511b is a pelitic schist which contains 1-4 mm anhedral garnet in a matrix of muscovite, biotite, and plagioclase. Matrix minerals are 0.1 to 5 mm in maximum dimension. The rock has 2 mm plagioclase and quartz veins parallel to foliation (Fig. 2). 18MSNZ511b contains garnet, biotite, muscovite, plagioclase, quartz, rutile, kyanite, apatite, and opaques (Fig. 3). Garnet are 2- 6 mm in diameter, anhedral, and compose about 15- 20% of the rock. Garnets have rutile inclusions concentrated around rims, biotite inclusions in garnet rims, and quartz inclusions found in both garnet core and rim. Biotite and muscovite are found together throughout this rock, but muscovite is found cross cutting biotite indicating late growth. Kyanite in this sample is found as anhedral 0.2 mm grains and is found in the matrix. Based on these textures, I interpret the peak mineral assemblage to be garnet, plagioclase, biotite, quartz, kyanite, and rutile.

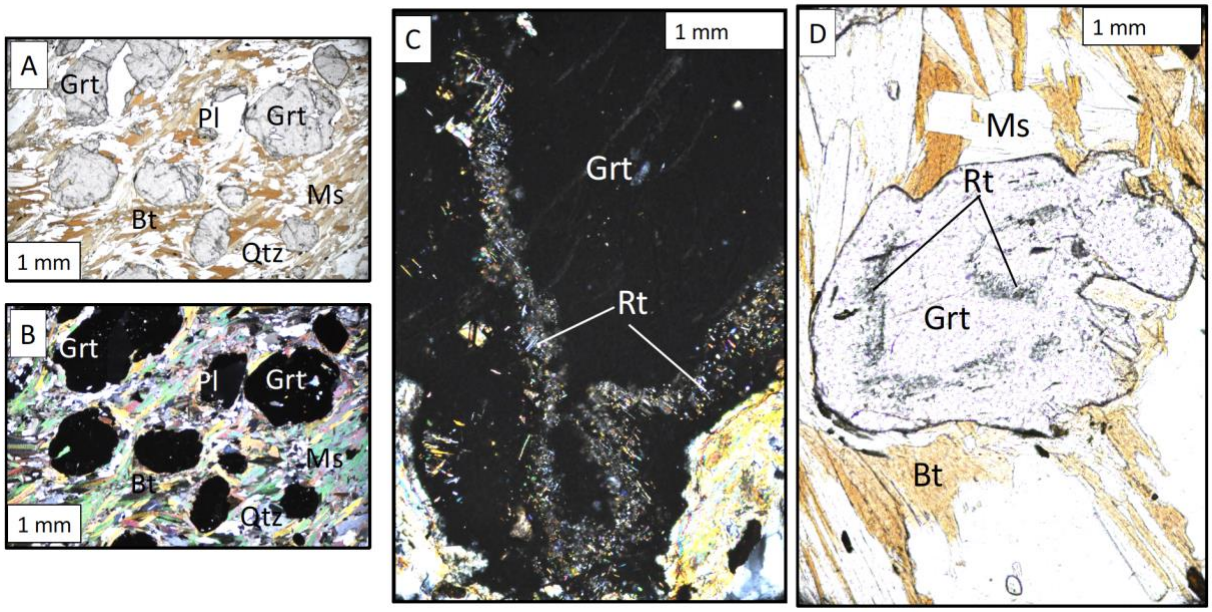

Figure 3. Representative photomicrographs of 18MSNZ511b, Milford Sound New Zealand. (A) Plane polarized light photomicrograph showing garnet surrounded by a biotite and muscovite rich matrix. (B) Crossed polarized light photomicrograph showing the alignment of biotite and muscovite. (C) Crossed polarized light photomicrograph of garnet with rutile inclusions concentrated in the rims. (D) Plane polarized light photomicrograph of an anhedral garnet with rutile inclusions in core and rim.

18MSNZ510a

Sample 18MSNZ510a contains a range of 0.3 -1 cm subhedral garnet in a matrix dominated by plagioclase, hornblende, and clinozoisite. This sample has a weak gneissic foliation and plagioclase and quartz veins parallel to foliation (Fig. 2). It contains garnet, biotite, hornblende, clinozoisite, titanite, plagioclase, rutile, and quartz (Fig. 4). This sample is fine-grained with small garnets that are 1-2mm and larger garnet 1 cm in diameter. Garnet mode varies from 2- 10 % of this rock. Garnets are subhedral to anhedral and include aligned rutile, hornblende near the rims, and quartz throughout. Biotite is found in the matrix and aligned with foliation while hornblende and clinozoisite are found as subhedral-euhedral grains throughout the matrix. Titanite is only found in the matrix in this sample. Quartz and plagioclase lenses are found throughout this sample. Based on these textures, I interpret the peak mineral assemblage to be garnet, biotite, hornblende, quartz, rutile, plagioclase, clinozoisite, and titanite.

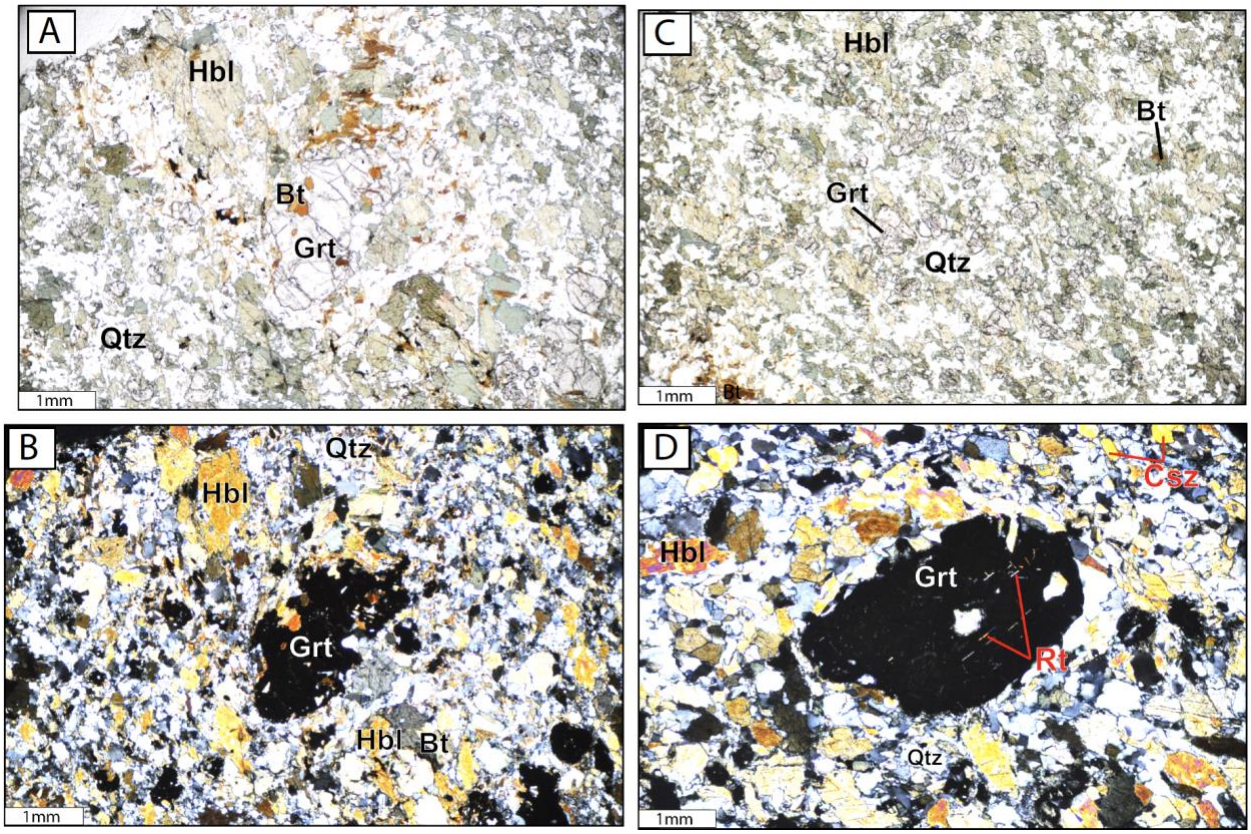

Figure 4. Representative photomicrographs of 18MSNZ510a, Milford Sound New Zealand. (A) Plane polarized light photomicrograph of surrounded by a biotite and hornblende rich matrix. (B) Crossed polarized light photomicrograph showing the anhedral garnet grains. (C) Plane polarized light photomicrograph of garnet with biotite, hornblende, and quartz found throughout the matrix. (D) Cross polarized light photomicrograph showing rutile needles in garnet.

15NZ51

Sample 15NZ51 contains 0.5 to 1.4 cm anhedral fractured garnets in a gneissic rock matrix. Garnet, biotite, hornblende, quartz, plagioclase, clinozoisite, clinopyroxene, and rutile and sparse opaques (tentatively identified as pyrite) were identified in thin section (Fig. 5). Garnet comprises 10 - 15% of the rock and contains inclusions of biotite, amphibole, quartz, and plagioclase. Garnet are surrounded by curved halos of hornblende and pyroxene indicating likely rotation of the porphyroblasts. Based on these textures, I interpret the peak mineral assemblage to be garnet, plagioclase, hornblende, biotite, rutile, quartz, and clinopyroxene.

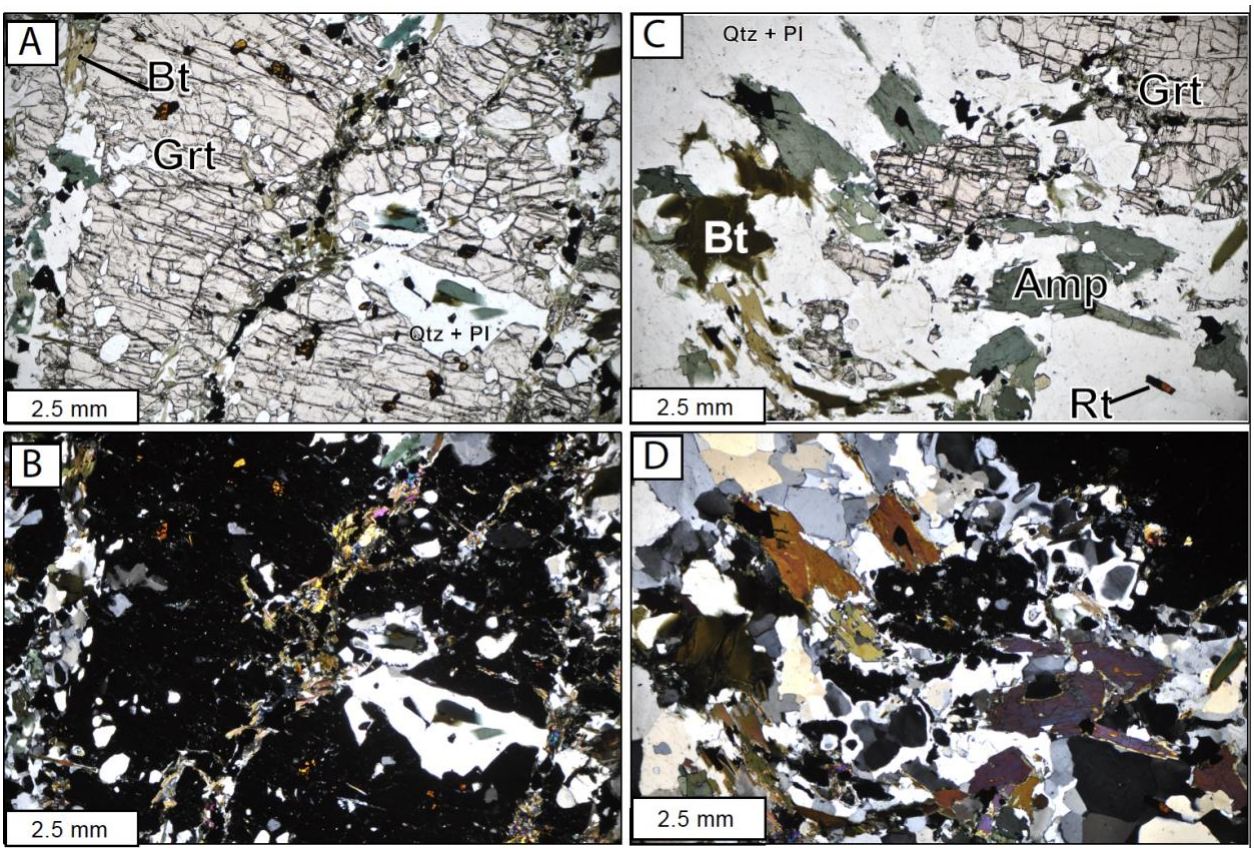

Figure 5. Photomicrographs of sample 15NZ51, Milford Sound New Zealand. (A) Representative plane polarized light photomicrograph of garnet surrounded by hornblende and pyroxene. (B) Crossed polarized light photomicrograph showing the anhedral garnet grains with inclusions of quartz, plagioclase, and biotite. (C) Plane polarized light photomicrograph showing hornblende and biotite and the rim of a garnet. (D) Cross polarized light photomicrograph showing quartz and plagioclase adjacent to garnet.

05NZ12

Sample 05NZ12 contains a range of 0.2 to 1 cm subhedral- euhedral garnet with the largest grains adjacent to a trondhjemite vein of plagioclase and quartz. This vein, or leucosome, is bordered by a selvage of the largest garnet grains and a garnet reaction zone dominated by biotite and clinopyroxene, and a host rock with biotite, plagioclase, pyroxene, and hornblende (Fig. 6). 05NZ12 contains garnet, plagioclase, rutile, clinoamphibole, biotite, quartz, hornblende, clinopyroxene, and clinozoisite (Fig. 7). Garnets contain crystallographically aligned rutile needle in the garnet cores. Garnet makes up 1 – 10% of this rock. Based on these textures, I interpret the peak mineral assemblage to be plagioclase, biotite, garnet, clinopyroxene, hornblende, rutile, and quartz.

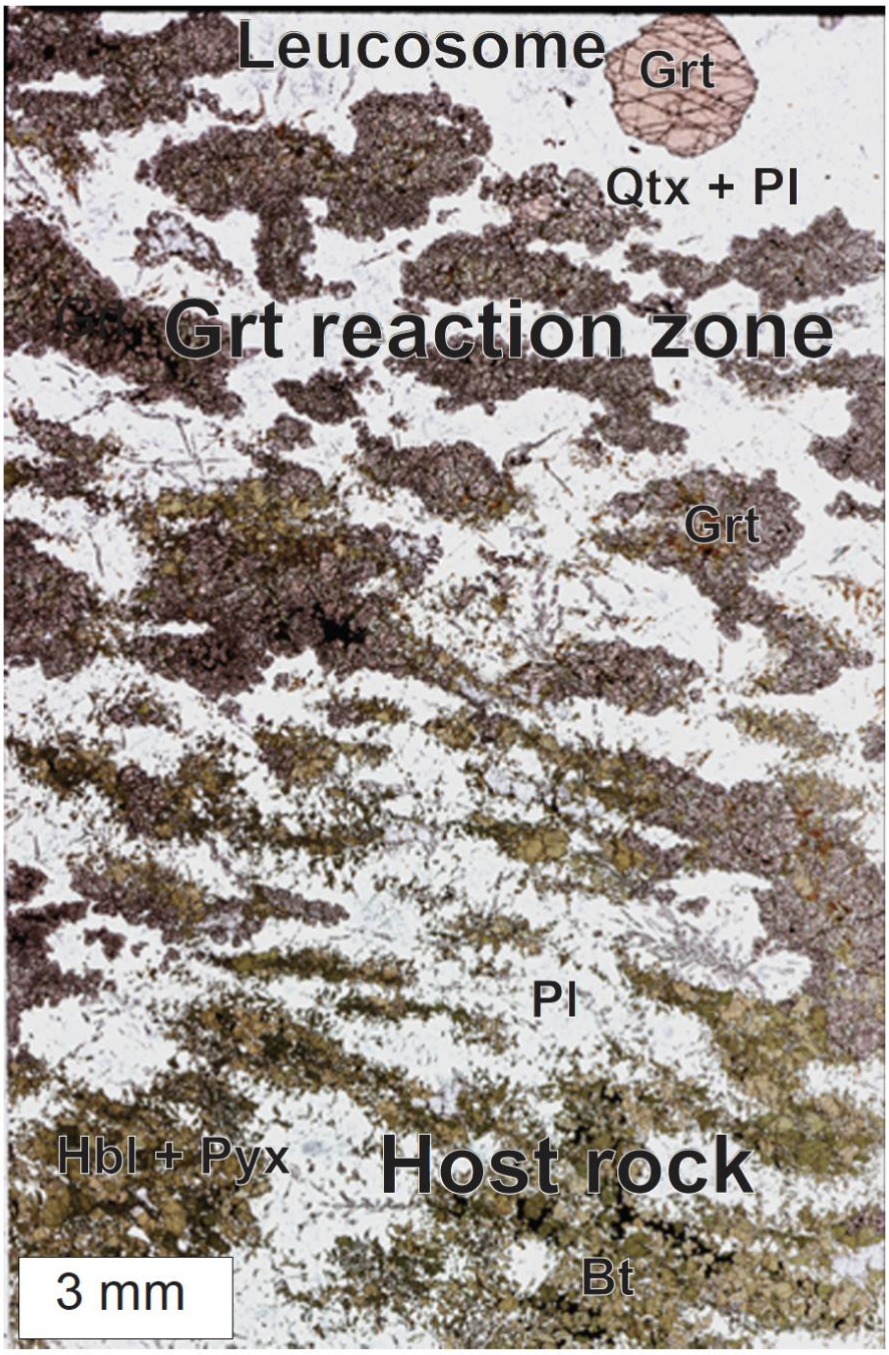

Figure 6. Thin section scan of 05NZ12 from Pembroke Granulite near Milford Sound New Zealand. Image shows the clearly defined host rock, garnet reaction zone, and leucosome.

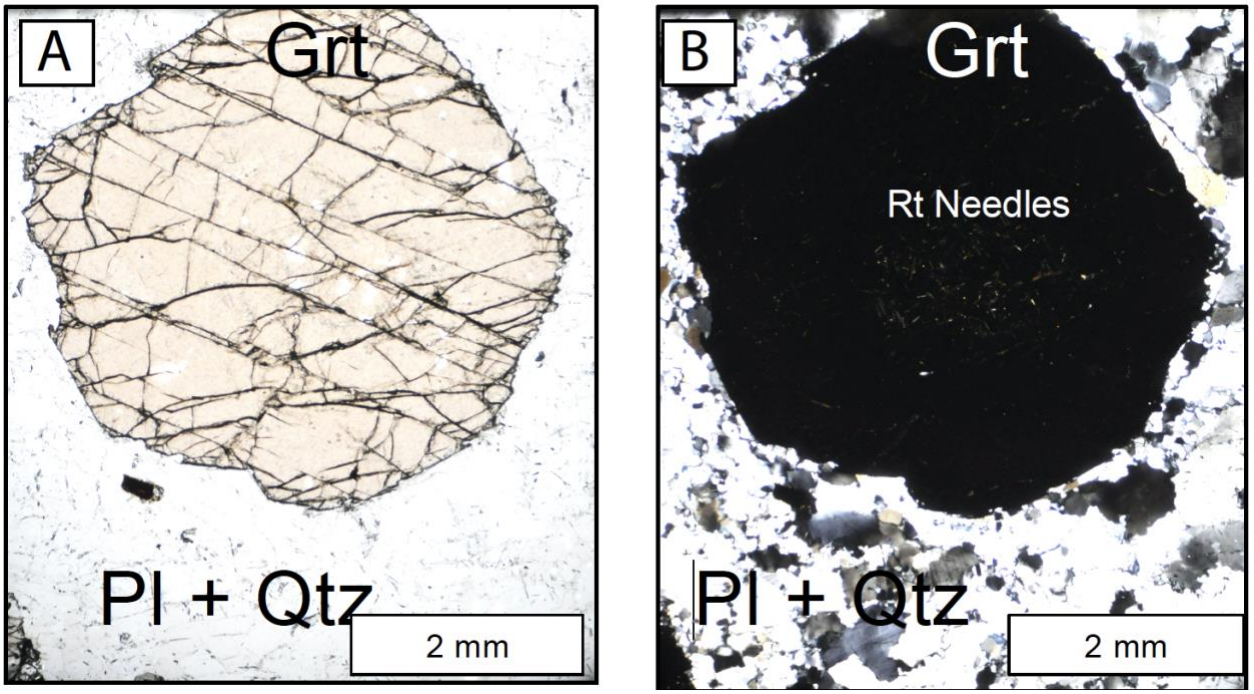

Figure 7. Photomicrographs of sample 05NZ12. (A) Plane polarized light photomicrograph showing an inclusion free garnet from the leucosome vein selvage surrounded by plagioclase and quartz. (B) Crossed polarized light photomicrograph showing rutile needles concentrated in the core of the garnet.

15NZ63

Sample 15NZ63 contains 2- 7 mm subhedral garnets in a medium-grained matrix. This gneissic sample contains garnet, muscovite, biotite, plagioclase, clinozoisite, titanite, apatite and zircon (Fig. 8). Garnet makes up 15-25% of this rock and contains quartz inclusions throughout. Biotite is generally aligned with gneissic layering and is cross cut by muscovite grains. Clinozoisite is found exclusively in the matrix with greater amounts of plagioclase and quartz. Based on these textures, I interpret the peak mineral assemblage to be garnet, plagioclase, biotite, rutile, and quartz.

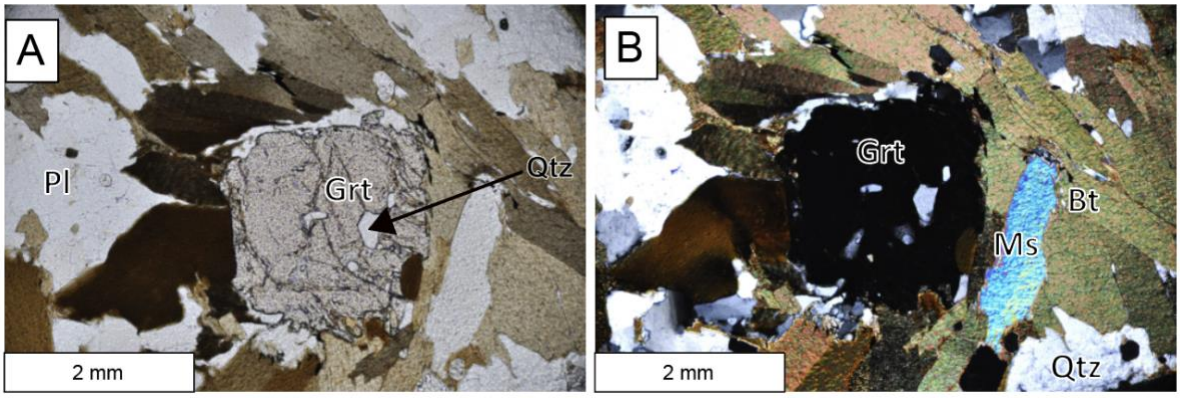

Figure 8. Photomicrographs of sample 15NZ63. (A) Plane polarized light photomicrograph showing a representative section of sample in thin section. Garnet is found throughout the sample and is surrounded biotite. (B) Crossed polarized light photomicrograph showing the anhedral garnet grains with inclusions of quartz.

Mineral Compositions

Garnet Zoning

Major element mineral compositions and Kα X-ray intensity maps were determined by EPMA for five samples along Milford Sound. The Kα X-ray intensity maps were used to place quantitative analyses along lines through the compositional centers of garnet grains. Additional spot analyses were obtained in the cores and along the rims of all minerals used for thermobarometry. Mineral formulas were calculated on the basis of twelve oxygen for garnet, eight for plagioclase, twenty- three for hornblende, and twenty- two for biotite and muscovite. All analyses were filtered in order to remove non-stoichiometric and other questionable data. Lines of spot analyses across garnet grains, plotted as mole fractions of end members, are presented in order to evaluate zoning.

18MSNZ511b

Garnet in sample 18MSNZ511b has complex zoning which is illustrated in the Kα X-ray maps (Fig. 9) and the quantitative analyses (Fig. 10). Calcium is significantly lower in the core and increases towards the rims of all garnets, based on line scan point analyses. Magnesium is fairly uniform throughout the center of grains and decreases at the rims. Iron is weakly zoned with little or no variation across grains. The Mg/(Mg+Fe) ratios decrease from core to rim, suggestive of diffusion and or decreasing temperature. Manganese is weakly zoned with very slightly higher concentrations in the cores of grains. All of the garnet grains contain healed fractures with compositional alteration, resulting in complex zoning. X-ray maps also reveal that garnet has inclusions of allanite, which contains high amounts of REE Ce, Y, and La.

I interpret the complex garnet zoning (Figs. 9, 10) to reflect near complete modification of any growth zoning. This is inferred from the low Mn cores and increase of Mn at garnet rims (Fig. 10). I tentatively infer that the high magnitude spikes in Mg, Ca, and Fe may be due to healed fractures; however, they could represent multiple rim resorption and growth events. The high Ca rims are tentatively interpreted to result from a change in pressure.

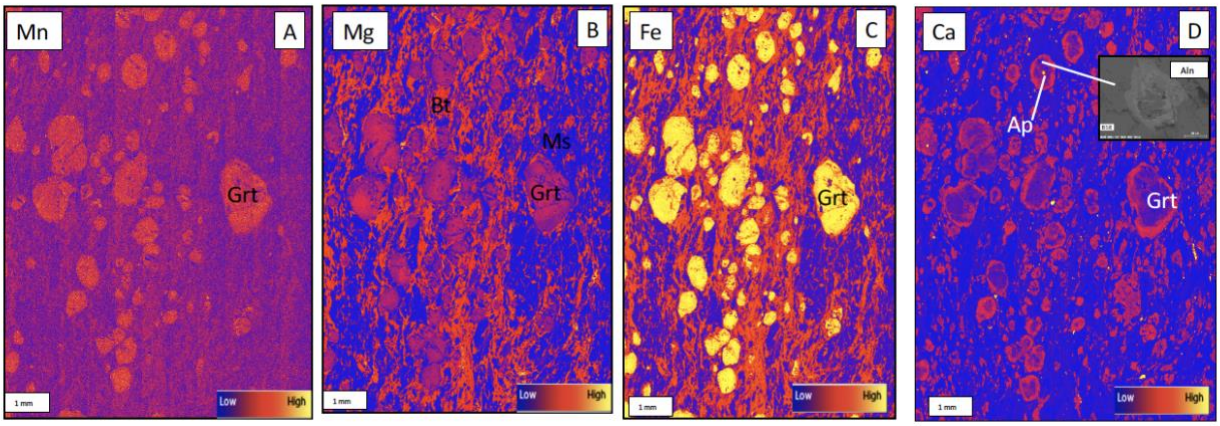

Figure 9. Compositional zoning in garnet from sample 18MSNZ511b. A-D. Manganese, Mg, Fe, and Ca Kα X-ray maps. Higher concentrations are shown in lighter warmer colors (red) and lower concentrations in darker cooler colors (purple). (D) includes an BSE image of an allanite found in garnet which also contained apatite.

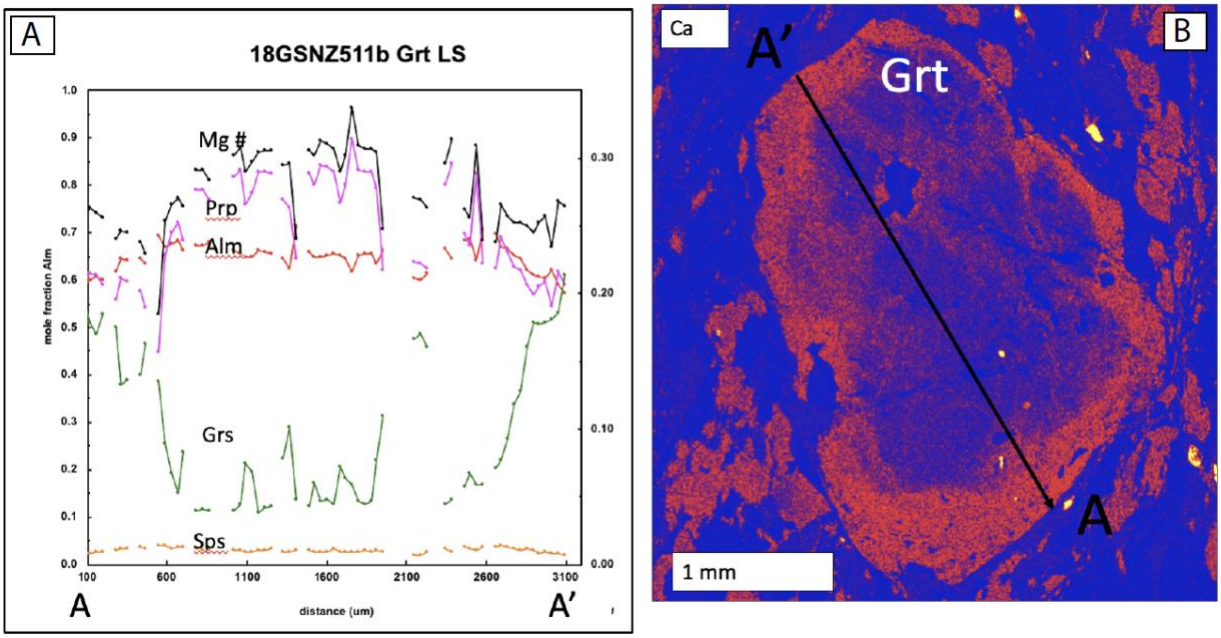

Figure 10. Garnet compositions for sample 18GSNZ511b, Milford Sound New Zealand. (A) Compositional zoning across garnet (60 analyses along A-A' shown in B). (B) Ca Kα X-ray map of garnet showing the line of analyses shown in (A). Higher concentrations are shown in lighter warmer colors (red) and lower concentrations in darker cooler colors (purple)

18MSNZ510a

Garnet in sample 18MSNZ510a has relatively little zoning. The Mg Kα X-ray map, shows no appreciable zoning and inclusions of hornblende in the large garnet (Fig.11). Calcium is weakly zoned with slight increases at the edge of the garnet grains and high values for inclusions of apatite. Fe Kα X-ray map shows titanite that is present in the matrix of this sample. Manganese is also nearly unzoned with a small increase within 1 mm from the edges of the garnet grain. The very weak zoning seen in the maps is confirmed by the quantitative analyses shown in Figure 12. The limited interior zoning is similar to that observed in garnet from 18MSNZ511b.

The broad core areas of garnet with little zoning may result from modification of any early growth zoning. The ca. 1 mm wide zones at garnet rims with increasing Mn and Ca up to the grain boundary (Figs. 11, 12) are interpreted as the last modification of garnet. The high Mn concentrations and anhedral grains are likely to reflect resorption of garnet with diffusion of Mn into the grain (Kohn and Spear, 2000). The calcium increases toward the rims may result from increased pressure during final equilibration. The overall lack of significant garnet zoning in grain interiors may result from diffusion at high temperature which erased any growth zoning.

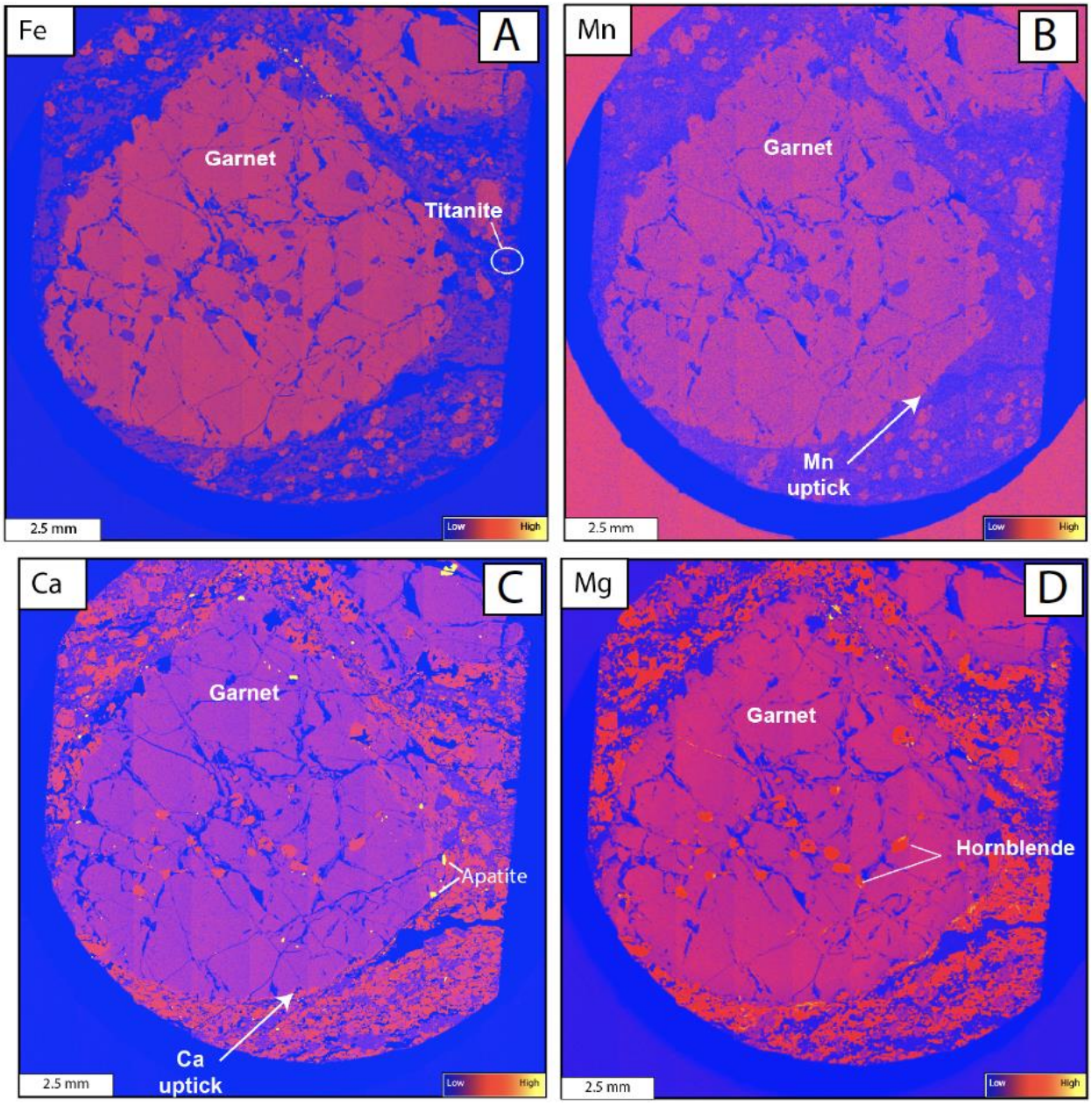

Figure 11. Compositional zoning in garnet from sample 18MSNZ510a. A-D. Iron, Mn, Ca, and Mg Kα X-ray maps. Higher concentrations are shown in lighter warmer colors (red) and lower concentrations in darker cooler colors (purple).

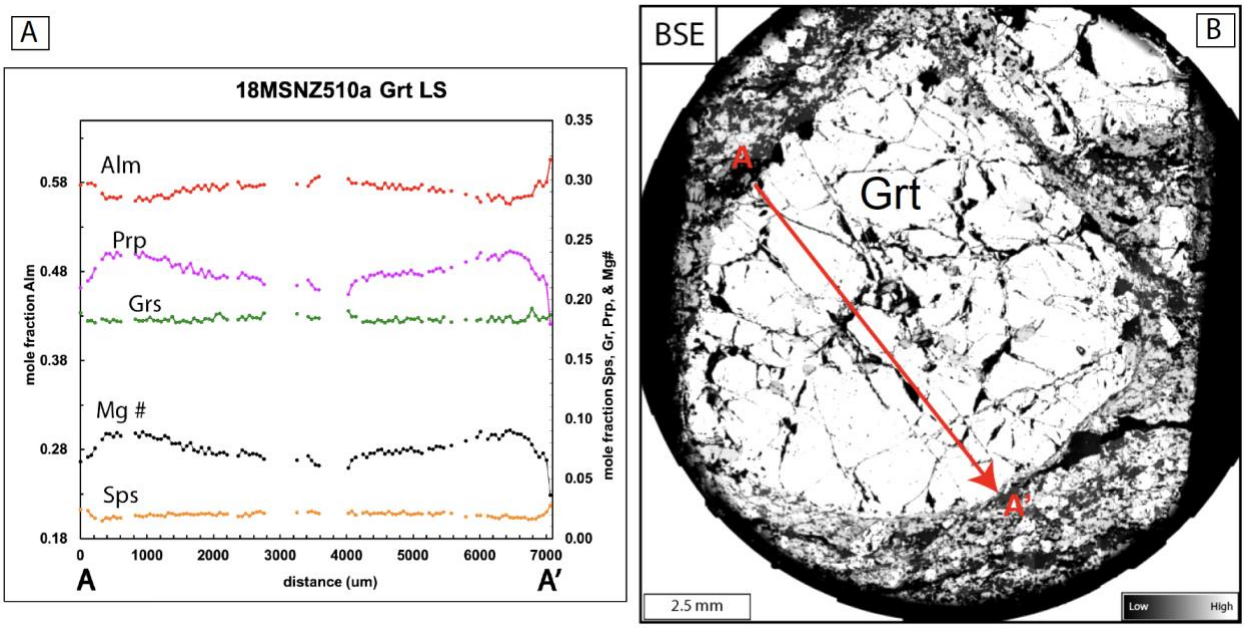

Figure 12. Garnet composition and zoning in sample 18MSNZ510a, Milford Sound, New Zealand. (A) BSE map showing the line where 75 analyses were collected on garnet. (B) Garnet end members versus distance along the line shown in (A).

15NZ51

Kα X-ray maps for sample 15NZ51 indicate that garnet is weakly zoned with no evidence for modification near the rims (Fig. 13). Manganese is higher in the core and decreases approaching the rim. Magnesium, Fe, and Ca show no little to no zoning present in these Kα X-ray maps, However, in these maps we see the numerous inclusions that are included in these garnets. I Infer the garnet overgrew the foliation defined by hornblende, pyroxene, and biotite. The curved helicitic nature of these inclusions indicates possible rotation of the garnet and syn- to post-deformational growth. Local amphibole and biotite rimming garnet could have resulted from an influx of water at high T after or near the end of garnet growth. The very weak zoning in garnet is tentatively interpreted to result from growth with little or no change in P, T, and available growth constituents (Mn, Mg, Fe, and Ca) as inferred for garnet in Pembroke Granulite (Stowell et al., 2010). However, high temperature modification cannot be ruled out.

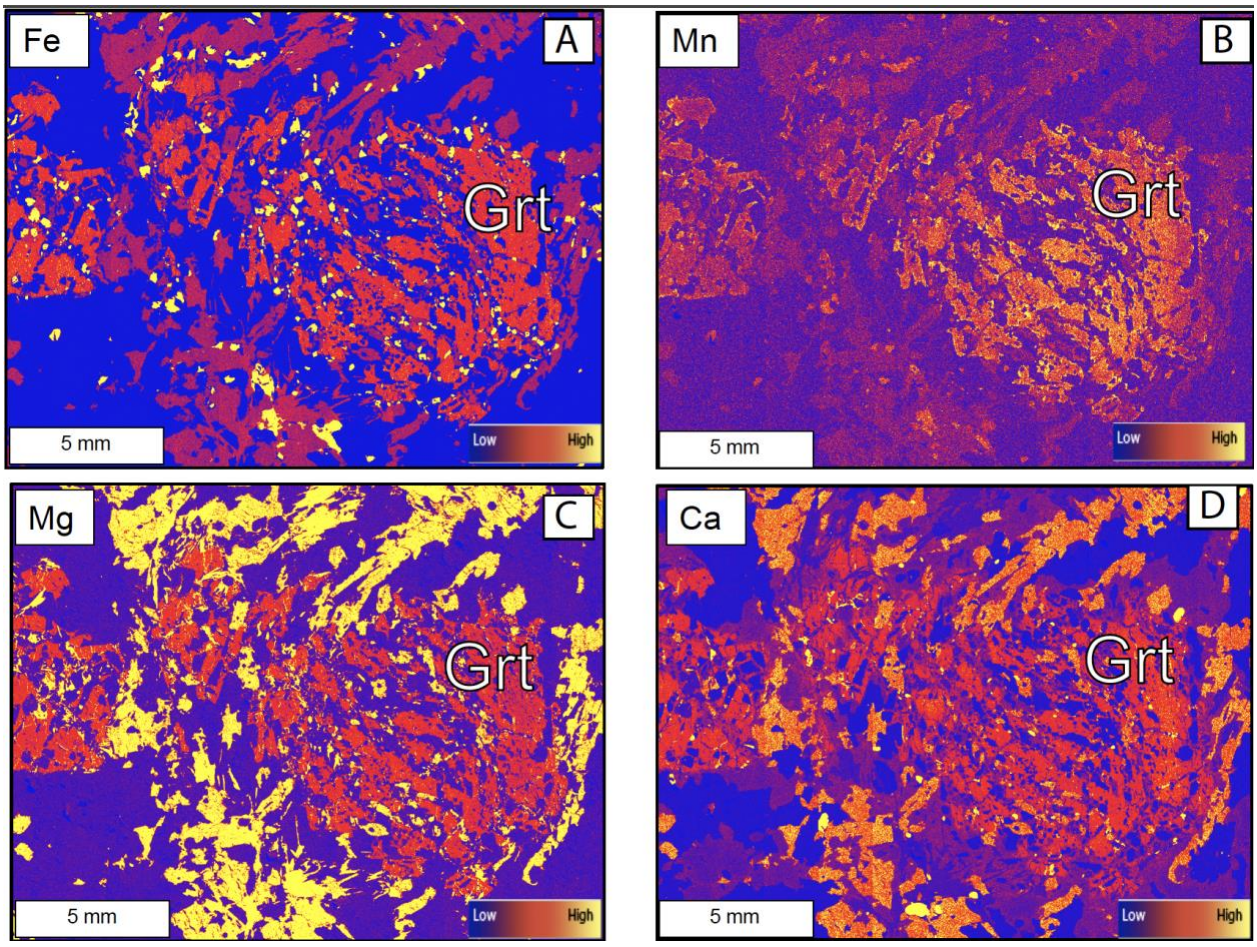

Figure 13. Compositional zoning in garnet from sample 15NZ51. A-D. Iron, Mn, Mg, and Ca Kα X-ray maps. Higher concentrations are shown in lighter warmer colors (red) and lower concentrations in darker cooler colors (purple).

05NZ12

Garnet in sample 05NZ12 has little or no compositional zoning (Fig. 14). The composition versus distance plot (Fig. 14), shows no significant change in any of the garnet end members. The near inclusion free garnet grains, which are directly associated with leucosome veins are tentatively interpreted to have grown without significant compositional zoning (e.g., Stowell et al., 2010). This very limited compositional variation in garnet from this sample is similar to that in 15NZ51; however, the grains lack the helicitic structures seen in that sample. Although garnet from this sample and 15NZ51 may preserve growth compositions, high temperature modification cannot be ruled out.

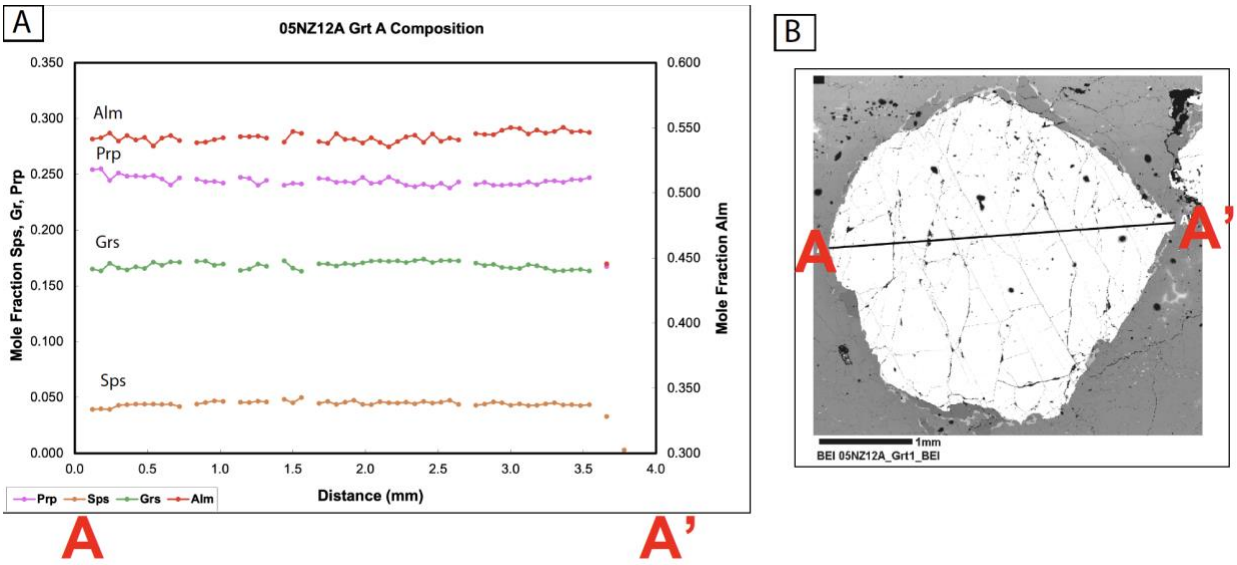

Figure 14. Garnet compositional zoning in sample 05NZ12, Milford Sound. (A) Mole fractions vs distance. (B) Back scattered electron (BSE) image showing the line where the 50 analyses in (A) were collected.

15NZ63

Garnet from sample 15NZ63 has significant zoning in Mn and Ca and lesser zoning in Mg and Fe (Fig. 15). Although the line of quantitative analyses only extends from rim to core (Fig. 16A), the X-ray maps confirm that the zoning is generally concentric. In the Ca Kα X-ray map, the low Ca core and high Ca rims are distinct and these are generally the inverse of Mn zoning which has higher concentration in the core decreasing toward the rim. However, the small increase of Mn within 1 mm of the rim is largely offset by a decrease in Mg. In general, the Mg and Fe concentrations are fairly constant from core to rim.

The high Mn cores mole fraction spessartine 0.1, lower Mn rims, mole fraction spessartine 0.04-0.08, and the uptick of Mn at the outermost garnet rims, mole fraction spessartine 0.08 (Figs. 15, 16) are common features in garnet from metasedimentary rocks from Fiordland (Bradshaw, 1989). I interpret this zoning to indicate preservation of growth zoning in the interiors of grains with partial modification after growth. Anhedral garnet grains and the high Mn rims likely result from resorption of garnet at high temperature and back diffusion of Mn into the garnet (Kohn and Spear, 2000). The high Mn cores are tentatively interpreted as relict growth zoning, but the anhedral nature of the grains and high Mn rims are interpreted to indicate significant resorption and diffusional modification after growth.

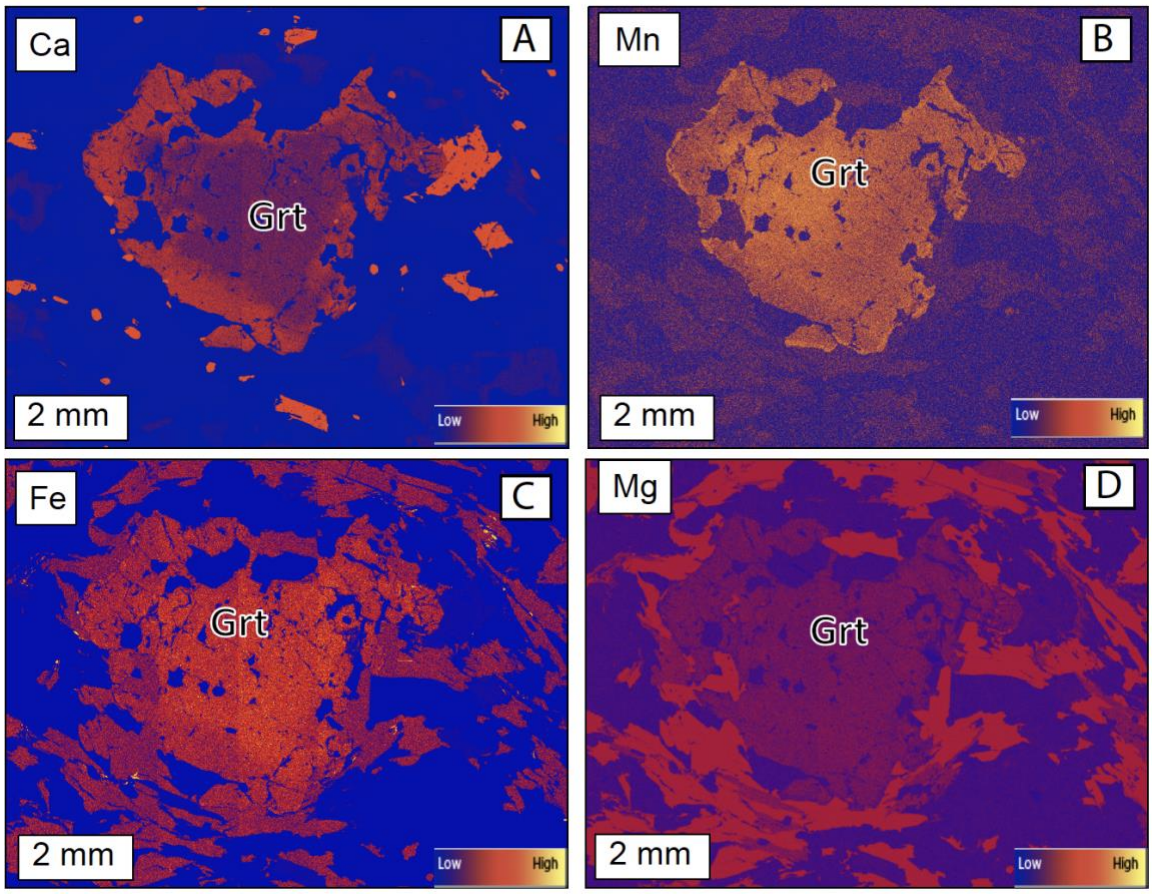

Figure 15. Garnet zoning maps from sample 15NZ63. A-D. Calcium, Mn, and Fe, and Mg Kα X-ray maps. Higher concentrations are shown in lighter warmer colors (red) and lower concentrations in darker cooler colors (purple).

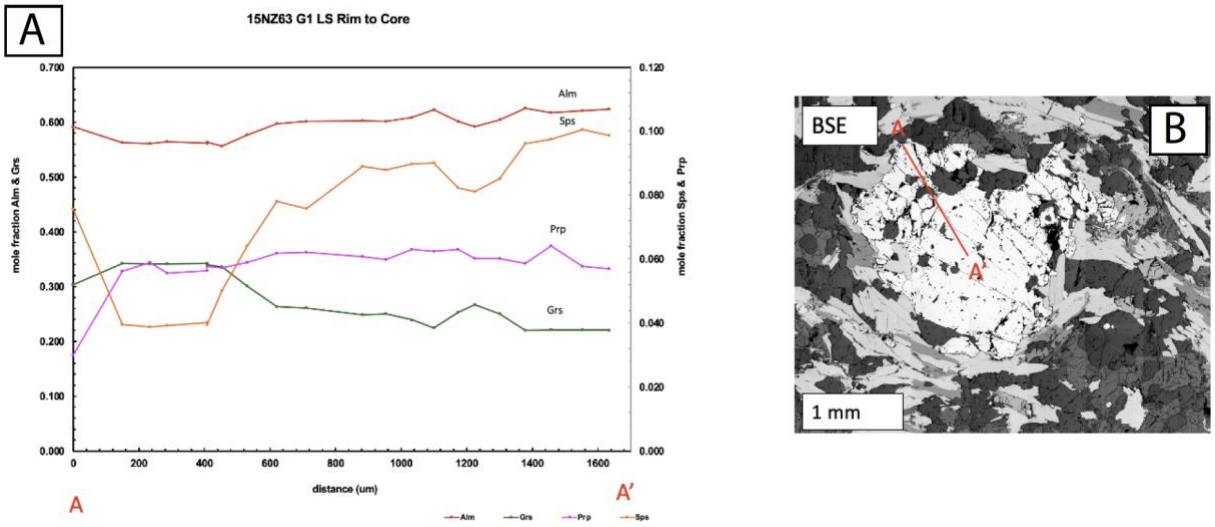

Figure 16. Compositional zoning in garnet from sample 15NZ63. (A)Mole fraction vs distance plot. (B) Back scattered electron (BSE) map showing where the 20 analyses in (A) were obtained.

Garnet Sm-Nd Ages

Samarium and Nd isotopic ratios and the resulting isochron ages are presented in Table 3. The garnet Sm-Nd isochrons for samples along the Milford Sound transect are presented graphically: 18MSNZ511b (Fig. 16), 18MSNZ510a (Fig. 17), 15NZ51 (Fig.18), 05NZ12 (Fig. 19), and 15NZ63 (Fig. 20 - 25). No useful age was obtained for sample 18MSNZ511b. The useful ages are: 18MSNZ510a: 99.2 ± 6.5 Ma; 15NZ51: 92.5 ± 5.1 Ma; 05NZ12: 121.8 ± 1.5Ma; 15NZ63: 94- 147 Ma. Based on these ages and additional ages from Stowell and others (2010), we tentatively interpret metamorphic events at >135, 126-122, and 106-88 Ma.

Table 3. Sm and Nd isotope data for metamorphic rocks along the Milford Transect, New Zealand.

Sample	Sm ppm	Nd ppm	$^{147}Sm/^{144}Nd$	2 σ	$^{143}Nd/^{144}Nd$	**2 σ combined**		Age (Ma)	MSWD
18MSNZ511b								n.a.	n.a
WR	7.816924	44.351362	0.106539	0.000724	0.512012	0.000008			
Mtx	6.890106	39.085378	0.106560	0.000716	0.512018	0.000008			
GX	4.441303	19.298246	0.139115	0.000935	0.512016	0.000011			
G1	5.228658	24.578615	0.128592	0.000827	0.512009	0.000008			
G2	3.437547	14.951510	0.138977	0.000918	0.511997	0.000015			
GX1	3.087570	11.536611	0.161778	0.001063	0.512022	0.000007			
GX2	3.056039	11.329874	0.163048	0.001038	0.512030	0.000009			
GX3	3.596512	14.279015	0.152253	0.000949	0.512019	0.000008			
G1-75	3.328219	12.519990	0.160700	0.001100	0.511982	0.000007			
G2-75	2.487631	8.519944	0.176493	0.001169	0.511990	0.000007			
G1-45	5.020196	23.071801	0.131528	0.000861	0.511983	0.000010			
G2-45	3.764701	16.044833	0.141832	0.000819	0.511997	0.000007			
GX<45	13.415300	70.856755	0.114446	0.001243	0.512003	0.000007			
18MSNZ510a									
WR	1.944429	8.936054	0.131549	0.000928	0.512601	0.000010		99.2±6.5	4.50
Mtx	2.558512	9.894686	0.156324	0.001100	0.512600	0.000009	core	98.4±3.1	0.00
GX	1.697706	1.204150	0.852453	0.006030	0.513066	0.000012	rim	97.4±3.7	0.00
GR1	1.884407	1.624695	0.701265	0.004991	0.512976	0.000009			
GC2	1.870116	1.259221	0.897963	0.006362	0.513095	0.000011			
GR2	0.002699	0.003863	0.908840	0.006420	0.513080	0.000015			
15NZ51									
WR-1	2.558590	7.404441	0.208925	0.001472	0.513008	0.000012		92.2±5.1	0.32
WR-2	5.590375	17.768529	0.190227	0.001320	0.512998	0.000008			
Mtx	4.662560	16.949095	0.166325	0.001153	0.512985	0.000008			
GXC	0.231067	0.849526	0.164453	0.001177	0.512987	0.000007			
GC	*0.562782*	*0.004023*	*0.562782*	*0.004023*	*0.513166*	*0.000013*			
GR2	1.154236	0.876811	0.795990	0.005705	0.513368	0.000021			
05NZ12									
WR-1	2.408113	10.157813	0.143330	0.001013	0.512780	0.000008		121.8±1.5	1.60
WR-2	0.144475	1.068652	0.081735	0.000623	0.512722	0.000016			
Mtx	0.259050	2.097455	0.074669	0.000547	0.512708	0.000011			
G3	2.134231	1.237455	1.042904	0.007247	0.513494	0.000014			
G4	2.218868	1.303604	1.029241	0.007190	0.513481	0.000012			
G5	1.849118	1.075622	1.039529	0.007304	0.513485	0.000008			
GR	1.515932	0.980687	0.934700	0.006555	0.513397	0.000014			
15NZ63									
WR	5.423220	22.574540	0.145229	0.000995	0.512352	0.000007		119.0±8.1	46.00
Mtx	2.505167	10.413026	0.145437	0.001030	0.512351	0.000007			
GX1a	2.495687	3.325912	0.453648	0.003222	0.512590	0.000010			
GX1b	4.468988	8.987591	0.300604	0.001990	0.512484	0.000008			
GX2a	1.333133	3.085795	0.261175	0.002062	0.512447	0.000010			
GX2b	2.927982	1.783536	0.992607	0.007193	0.513086	0.000008			
GX3	3.665276	3.501146	0.632923	0.004376	0.512734	0.000008			
Grt 1	1.406559	1.422391	0.597837	0.004087	0.512630	0.000011			
Grt 2	4.442204	6.917131	0.388251	0.002593	0.512587	0.000008			
Grt 3	4.723172	4.827903	0.591462	0.004236	0.512703	0.000014			
Grt 4	3.183298	1.034175	1.861376	0.013217	0.513674	0.000014			
Grt 5	3.993097	4.662779	0.517741	0.003429	0.512661	0.000009			

*Grt= garnet; WR= whole rock; Mtx= whole rock minus garnet
* Ages in bold include all data for sample.
* Excluded aliquots are indicated in italics
* Jndi 143Nd/144Nd 2σ average= 0.512117±13 ppm
* BHVO-1 143Nd/144Nd and 147Sm/144Nd 2σ = 0.512960±9 ppm and 0.1500±0.0004
* 15NZ63 is 'split' into different ages due to different age populations

18MSNZ511b

Whole rock (WR), matrix = rock minus garnet (MTX), and 11 aliquots of garnet were analyzed for sample 18MSNZ511b. Multiple sieve size fractions ranging from 75 µm to <45 µm and variable leaching times were used on the garnet aliquots. The garnet Nd concentrations from isotope dilution were ≥8 ppm and the $^{147}Sm/^{144}Nd$ ratios were ≤0.1765 on all of these aliquots. The high concentration of REE (Table 3) and low $^{147}Sm/^{144}Nd$ ratios are interpreted to indicate incomplete removal of inclusions from the garnet. The most likely culprits are the numerous apatite and allanite inclusions that were observed in the garnet. The results are problematic and the Sm-Nd garnet errorchron has a negative slope (Fig. 17). However, if garnet aliquots that have a higher $^{143}Nd/^{144}Nd$ and $^{147}Sm/^{144}Nd$ isotopic ratio than the WR and MTX, the age for 18MSNZ511b is 23 ± 21 Ma (N= 6/13; MSWD = 0.99). Therefore, the oldest possible garnet age is ca. 44 Ma for this rock.

The poor linear fit may result from at least 3 scenarios which are compatible with the high Nd in garnet, lower $^{143}Nd/^{144}Nd$ in garnet than in whole rocks.

1) The scatter in Nd isotope ratios result from inclusions that were never fully removed from the garnet aliquots in spite of multiple leaching combinations. This is likely because the garnet grains contain numerous < 0.1 mm apatite and allanite crystals, and garnet aliquots have very low Sm/Nd ratios.
2) Isotopic disequilibrium during growth or later partial modification of the garnet and/or matrix minerals. The seven garnet aliquots with $^{143}Nd/^{144}Nd$ less than in the whole rock could reflect partial modification of garnet which is not in equilibrium with the whole rock.

3) Mixing of young and old aliquots of garnet which caused low $^{143}Nd/^{144}Nd$ in garnet aliquots and whole rocks containing garnet.

I interpret that all of these are likely based on the high Nd concentrations found in garnet due to unremoved high REE inclusions and the complex garnet zoning observed that indicates partial modification of garnet after growth.

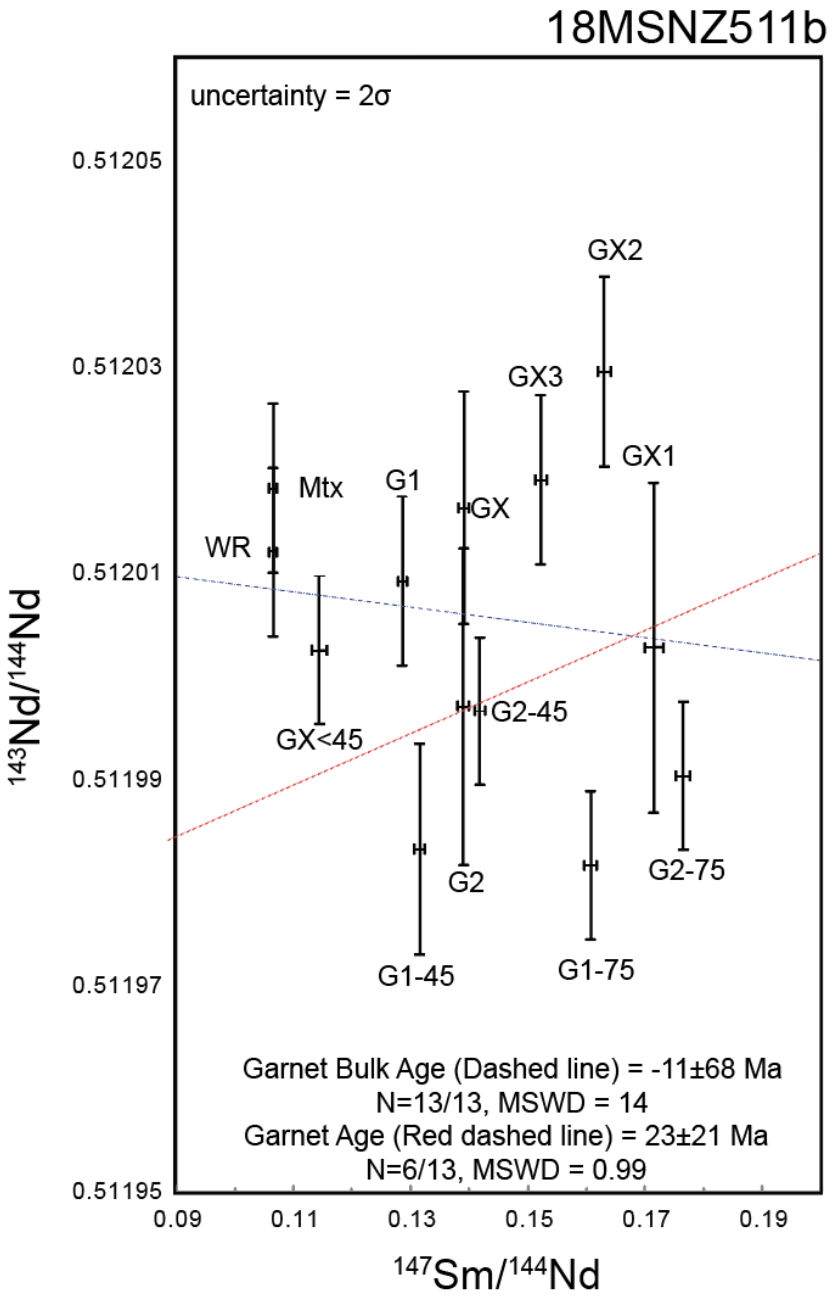

Figure 17. Sm–Nd isotope plot for sample 18MSNZ511 from the St. Anne Gneiss, Milford Sound, New Zealand. The scatter and negative slope on this errorchron precludes any age determination. The red dashed line shows the oldest possible age, when looking at garnet aliquots that have higher $^{143}Nd/^{144}Nd$ and $^{147}Sm/^{144}Nd$ isotope ratios than the WR and MTX.

18MSNZ510a

Six rock and garnet aliquots (WR, MTX, GX, GR1, GC2, GR2) were analyzed from sample 18MSNZ510a. Unlike sample 18NZ511b, the garnet have Sm and Nd concentrations < 2 ppm and the $^{147}Sm/^{144}Nd$ ratios are between 0.70 and 0.91. The resulting six point isochron is 99.2 ±6.5 Ma mean squared weighted deviation (MSWD) = 4.5. The high MSWD indicates that this isochron may include more than one age population; therefore, two point isochrons were used to calculate garnet core and rim ages. Garnet core 2 aliquot was plotted with the WR and garnet rim 2 aliquot was plotted with the MTX to obtain single garnet grain ages of 98.4±3.1 (MSWD = 3.1) and 97.4±3.7 Ma (MSWD = 3.7) (Fig. 18), respectively. Although the core and rim ages overlap within uncertainty, they show a logical progression from core to rim. These results are compatible with garnet growth in < 8 m.y. and as little as ca. 1 m.y. Perhaps most importantly garnet growth in this part of the Anita Shear Zone must have occurred between 101 and 93 Ma.

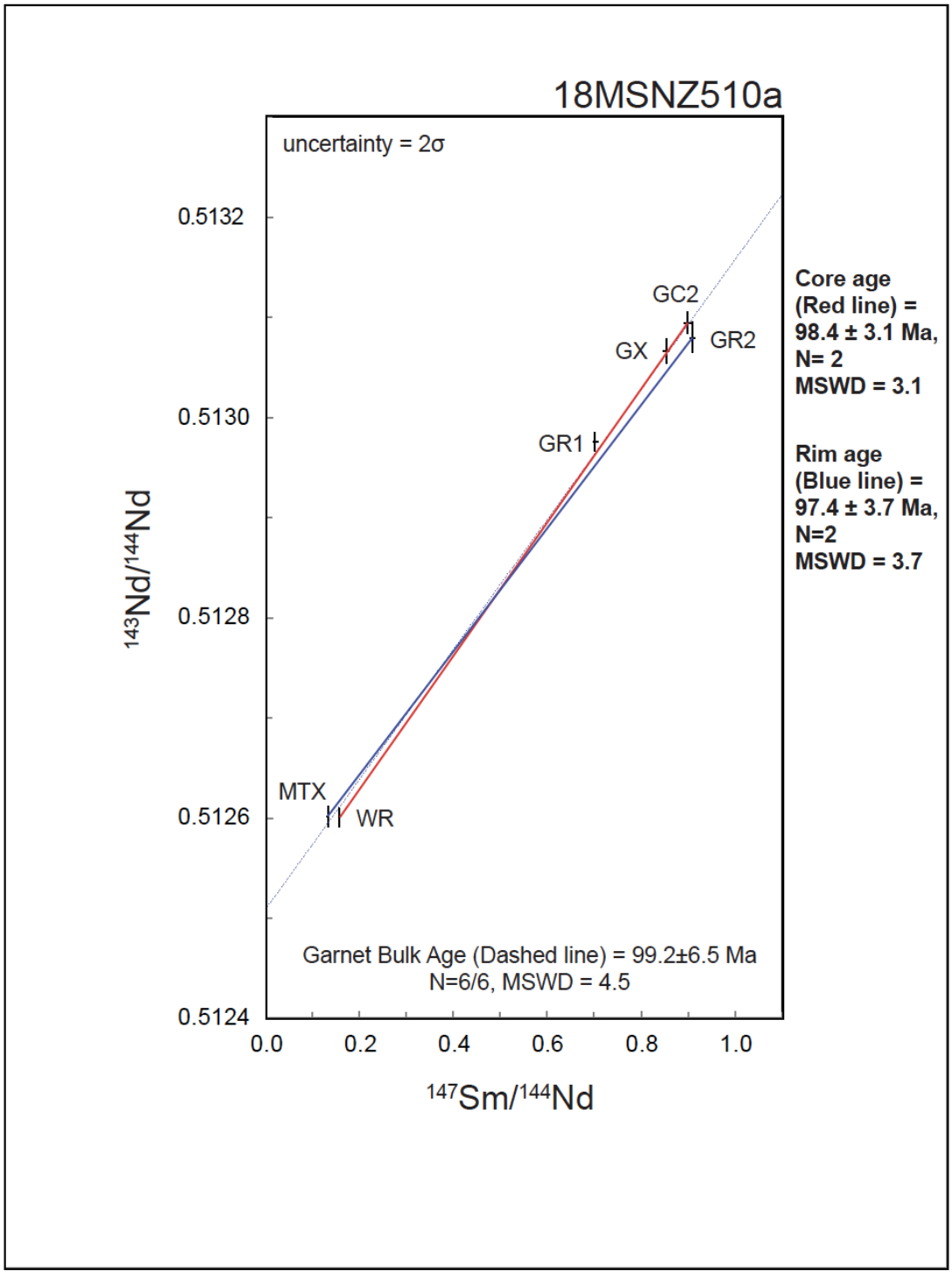

Figure 18. Garnet Sm-Nd isochron for 18MSNZ510, Thurso Gneiss, Milford Sound, New Zealand. The six aliquot isochron yields an age of 99.2±6.5 Ma (MSWD = 6.5). Individual core and rim aliquots of a single grain yield 98.4±3.1 (MSWD = 3.1) (Red line) and 97.4±3.7 Ma (MSWD = 3.7) (blue line) respectively.

15NZ51

WR, MTX, two garnet cores, and one garnet rim were analyzed from sample 15NZ51. All garnet aliquots were hand picked to make sure garnet was as clean as possible. The garnet have Sm and Nd concentrations < 2 ppm and the $^{147}Sm/^{144}Nd$ ratios are between 0.1 and 0.8. One garnet core had an extremely low Nd concentration < 0.005 was disregarded for age calculations. The resulting 5-point isochron age for this sample is 92.2±5.1 Ma (MSWD = 0.32) (Fig. 19). Considering the uncertainties, samples 18MSNZ510 and 15NZ51 are indistinguishable and indicate widespread garnet growth in rocks exposed along the western end of Milford Sound.

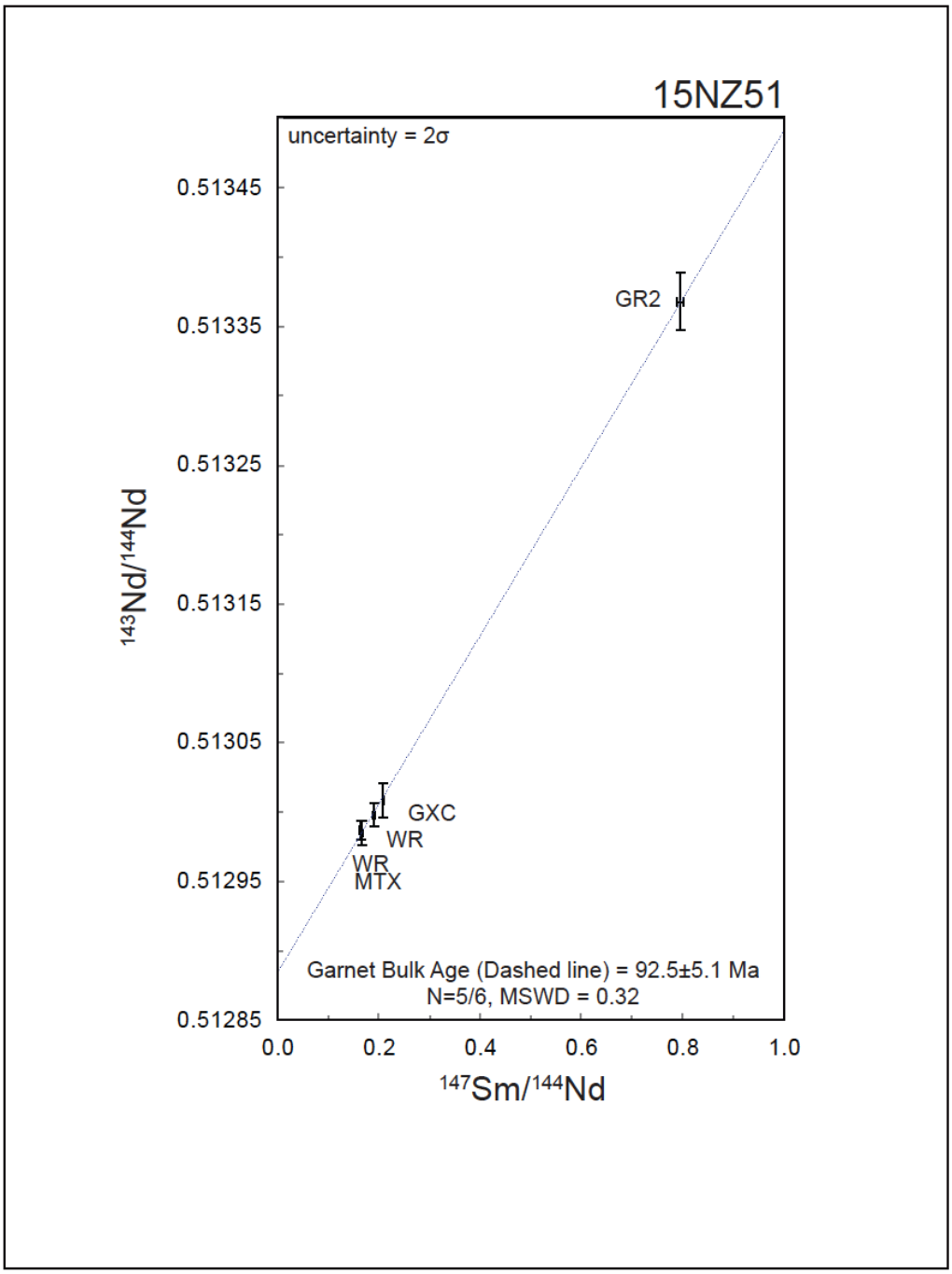

Figure 19. Garnet Sm-Nd isochron for 15NZ51 from the Milford Gneiss, Milford Sound, New Zealand. Five of the six aliquots yield an age of 92.2±5.1 Ma (MSWD = 5.1).

05NZ12

A Sm-Nd age was presented for sample 05NZ12 in Stowell and others (2010); however, the reported age was ca. 10 m.y. younger than other garnet ages reported for the Pembroke Granulite. I report a total of seven new aliquots from this sample (Table 3). These aliquots consisted of MTX from the leucosome, WR from the garnet reaction zone, WR leucosome with garnet, and 3 garnet aliquots from the vein selvage. The garnet Nd concentrations from isotope dilution were 1 ppm and the $^{147}Sm/^{144}Nd$ ratios were 0.9 – 1 on all of these aliquots. The seven aliquots yield an age of 121.8±1.5 Ma with an MSWD of 0.32 (Fig. 20). No points were excluded for this isochron age calculation. This result is indistinguishable from the 122-126 Ma ages for the majority of garnet in the Pembroke Granulite (Stowell et al., 2010).

The precision of this age allows several conclusions: 1) The inclusion of leucosome and garnet reaction zone aliquots indicates that they were in equilibrium with each other, 2) The previous age of ca. 109 Ma (Stowell et al. 2010) published for this sample is likely erroneous. I tentatively attribute this inadequate cleanliness of garnet aliquots, 3) The new high precision age for this sample is indistinguishable from previously determined ages for diorite gneiss from the Pembroke Granulite (Stowell et al. 2010) confirming that metamorphism of these rocks substantially predates that of rocks exposed to the west in the Milford Gneiss and Anita Shear Zone, and south in the WFO (Stowell, et al., 2014).

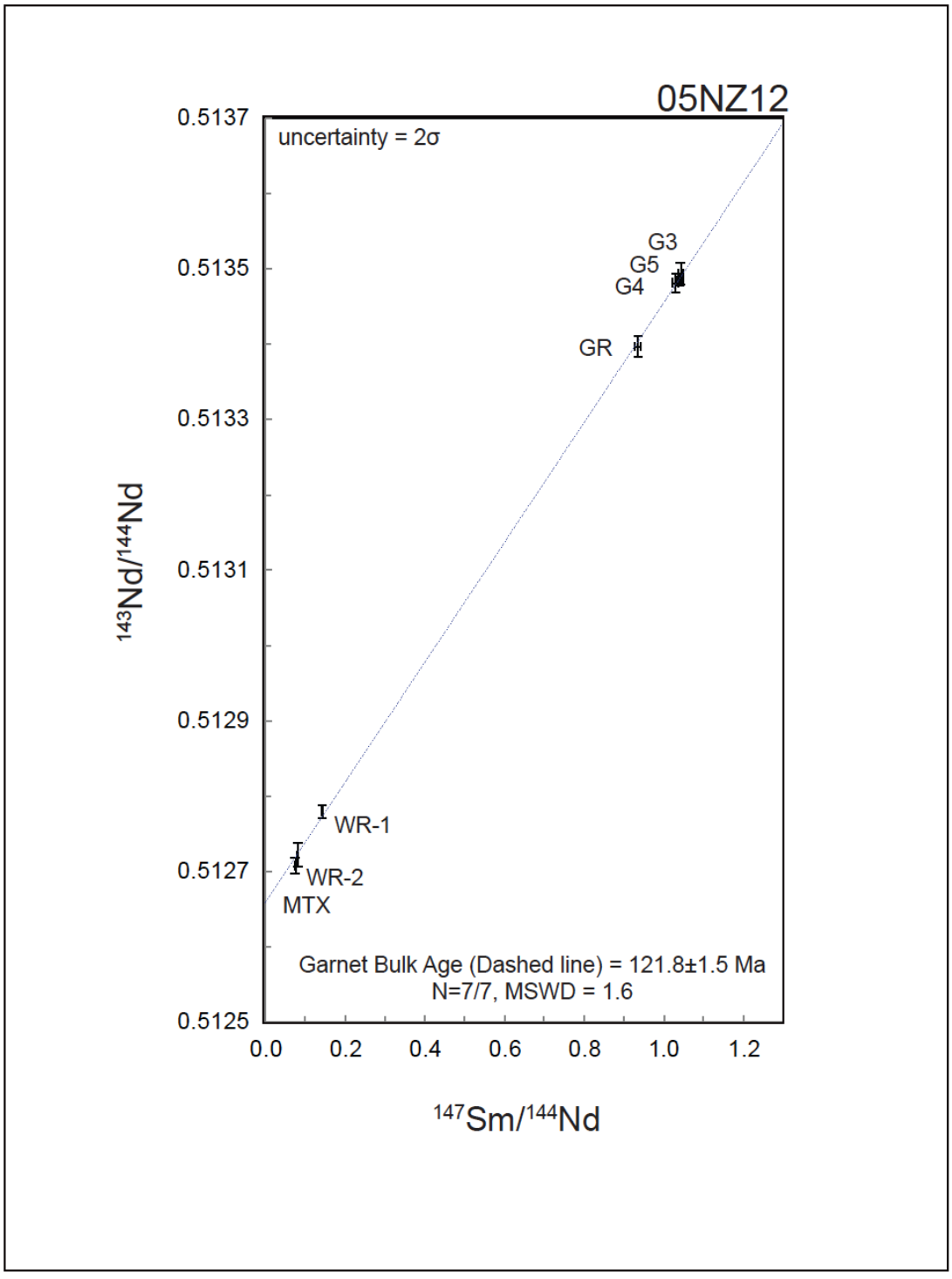

Figure 20. Garnet Sm-Nd isochron for 05NZ12 from the Pembroke Granulite, Pembroke Valley, New Zealand. Seven of the 7 aliquots yield an age of 121.8±1.5 Ma MSWD = 0.32.

15NZ63

Whole Rock, MTX, and 10 garnet aliquots were analyzed from 15NZ63 from Camp Oven Creek in the Arthur River Complex, near the east end of Milford Sound.[1] The garnet Nd concentrations from isotope dilution were 1.03 to 8.99 ppm and the $^{147}Sm/^{144}Nd$ ratios were 0.1 – 1.8 on all of these aliquots. In spite of several garnet aliquots with high Nd, the large range in concentrations precluded objective elimination of aliquots in age calculations. This sample yields an age of 119.2±8.1 Ma for all aliquots (Fig. 21); however, the MSWD of 46 indicates multiple age populations. A probability density plot (Fig. 22) was compiled based on 3-point isochron ages of WR, MTX and each aliquot of garnet (Table 5). This plot indicates four age populations of ca. 94, 118, 130, and 147 Ma. The corresponding aliquots were grouped together and used to calculate isochrons for each age group (Fig. 23). Two age populations are well-defined at 132.0±2.0 Ma (MSWD=1.4, N=6) and 118.3±1.5 Ma (MSWD=0.53, N=6). The remaining two populations are less well-defined with essentially two point isochrons (MTX~WR) and MSWD far from 1.0.

We conclude that there were multiple garnet growth events in the Arthur River Complex at the east end of the Milford Transect. The ca. 132 and 118 Ma age populations are robust and correlate with zircon ages in the Arthur River Complex orthogneisses and the intrusion of WFO plutons south of the Arthur River Complex (Hollis et al. 2004; Schwartz et al. 2017). However, ca. 118 Ma garnet growth is significantly younger than most, but not all of the published U-Pb zircon ages (125 to 112 Ma) from the Worsely Pluton (e.g., Decker et al. 2017) which is the northernmost WFO pluton.

[1] Sm- Nd isotope data collected by James Yelverton in the UA RadIs laboratory

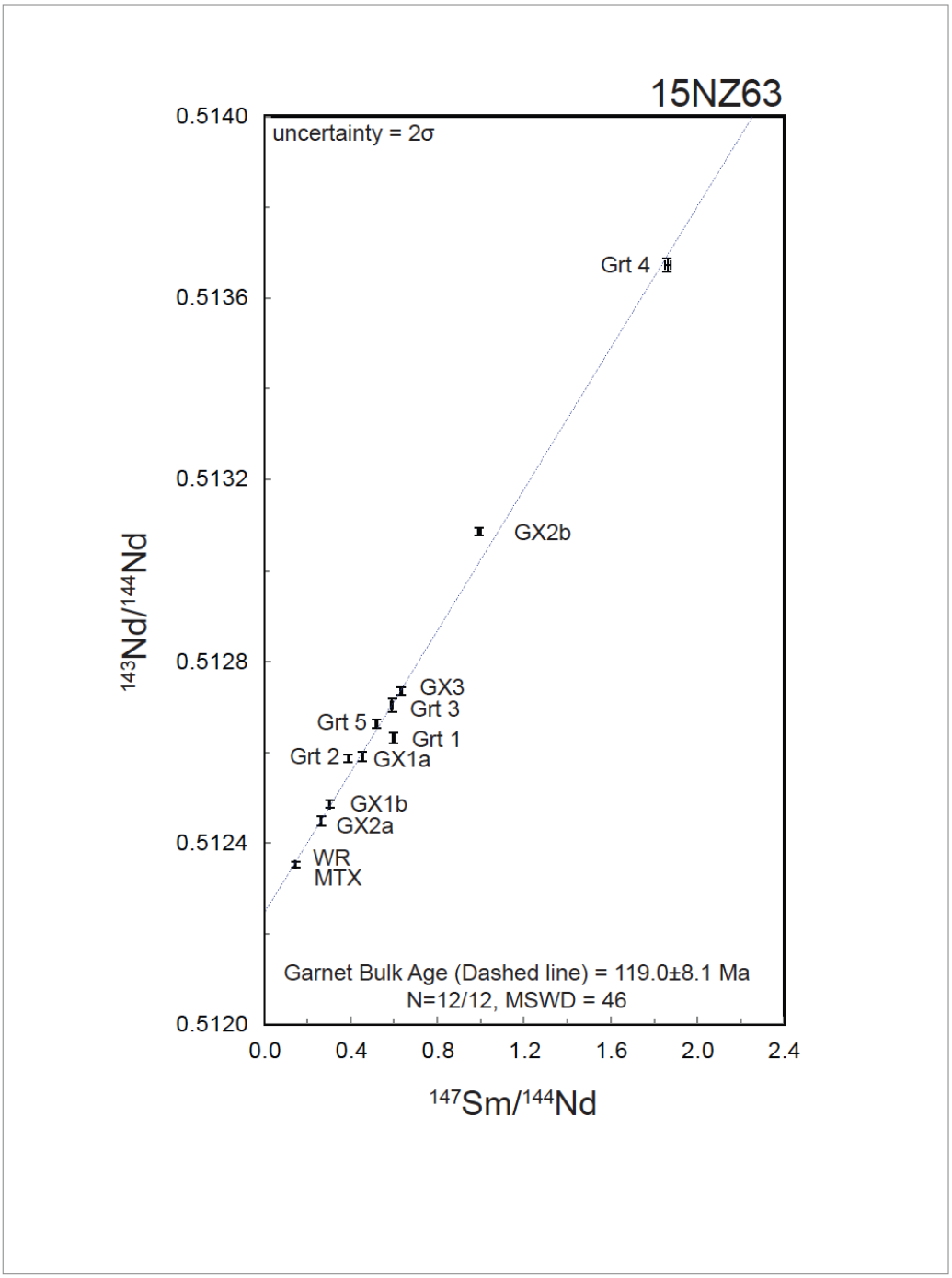

Figure 21. Sm-Nd data and "isochron" for 15NZ63 from the Arthur River Complex at Camp Oven Creek. The Sm-Nd isochron for 12/12 aliquots yields an age of 119.8±8.1 Ma. The MSWD of 46 and large age uncertainty indicate multiple age populations.

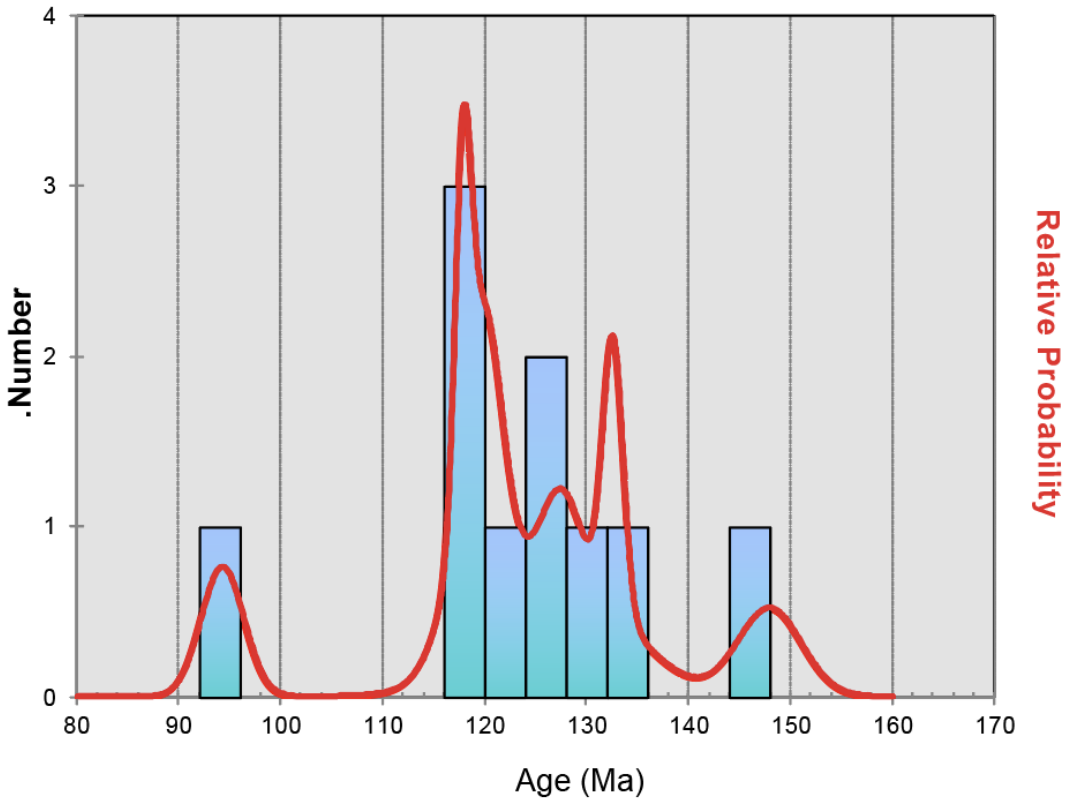

Figure 22. Probability density plot for garnet Sm-Nd ages in 15NZ63 from the Arthur River Complex at Camp Oven Creek. X- axis is age and the Y- axis shows number of aliquots at that age and their relative probability. Results indicate 4 age populations at ca. 94, 118, 130, and 147 Ma.

Table 4. Garnet Sm-Nd ages and uncertainties for each of 10 garnet aliquots for 15NZ63

Aliquot	Weight (g)	$[Sm]_{ppm}$	$[Nd]_{ppm}$	$^{147}Sm/^{144}Nd$	2 SE	$^{143}Nd/^{144}Nd$	2 SE ISOPLOT	Age (Ma) 3 points	MSWD	Age group
WR	0.099123	5.423220	22.574540	0.145229	0.000995	0.512352	0.000007	**118.5±5.7**	0.025	118
MTX	0.097752	2.505167	10.413026	0.145437	0.001030	0.512351	0.000007			
GX1a	0.020487	2.495687	3.325912	0.453648	0.003222	0.512590	0.000010			
WR	0.099123	5.423220	22.574540	0.145229	0.000995	0.512352	0.000007	**130.8±9.5**	0.026	130
MTX	0.097752	2.505167	10.413026	0.145437	0.001030	0.512351	0.000007			
GX1b	0.026672	4.468988	8.987591	0.300604	0.001990	0.512484	0.000008			
WR	0.099123	5.423220	22.574540	0.145229	0.000995	0.512352	0.000007	**127±15**	0.026	130
MTX	0.097752	2.505167	10.413026	0.145437	0.001030	0.512351	0.000007			
GX2a	0.390080	1.333133	3.085795	0.261175	0.002062	0.512447	0.000010			
WR	0.099123	5.423220	22.574540	0.145229	0.000995	0.512352	0.000007	**132.5±2**	0.027	130
MTX	0.097752	2.505167	10.413026	0.145437	0.001030	0.512351	0.000007			
GX2b	0.031055	2.927982	1.783536	0.992607	0.007193	0.513086	0.000008			
WR	0.099123	5.423220	22.574540	0.145229	0.000995	0.512352	0.000007	**119.9±3.2**	0.026	118
MTX	0.097752	2.505167	10.413026	0.145437	0.001030	0.512351	0.000007			
GX3	0.065860	3.665276	3.501146	0.632923	0.004376	0.512734	0.000008			
WR	0.099123	5.423220	22.574540	0.145229	0.000995	0.512352	0.000007	**94.2±4.2**	0.024	94
MTX	0.097752	2.505167	10.413026	0.145437	0.001030	0.512351	0.000007			
Grt 1	0.017872	1.406559	1.422391	0.597837	0.004087	0.512630	0.000011			
WR	0.099123	5.423220	22.574540	0.145229	0.000995	0.512352	0.000007	**147.9±6.2**	0.028	147
MTX	0.097752	2.505167	10.413026	0.145437	0.001030	0.512351	0.000007			
Grt 2	0.030975	4.442204	6.917131	0.388251	0.002593	0.512587	0.000008			
WR	0.099123	5.423220	22.574540	0.145229	0.000995	0.512352	0.000007	**120.5±5.2**	0.026	118
MTX	0.097752	2.505167	10.413026	0.145437	0.001030	0.512351	0.000007			
Grt 3	0.052232	4.723172	4.827903	0.591462	0.004236	0.512703	0.000014			
WR	0.099123	5.423220	22.574540	0.145229	0.000995	0.512352	0.000007	**117.8±1.6**	0.025	118
MTX	0.097752	2.505167	10.413026	0.145437	0.001030	0.512351	0.000007			
Grt 4	0.032642	3.183298	1.034175	1.861376	0.013217	0.513674	0.000014			
WR	0.099123	5.423220	22.574540	0.145229	0.000995	0.512352	0.000007	**127.2±4.4**	0.026	130
MTX	0.097752	2.505167	10.413026	0.145437	0.001030	0.512351	0.000007			
Grt 5	0.037215	3.993097	4.662779	0.517741	0.003429	0.512661	0.000009			

These ages are grouped 4 populations based on probability density (Fig. 21): 94 Ma- purple, 118 Ma- blue, 130 Ma- green, and 147 Ma- orange.

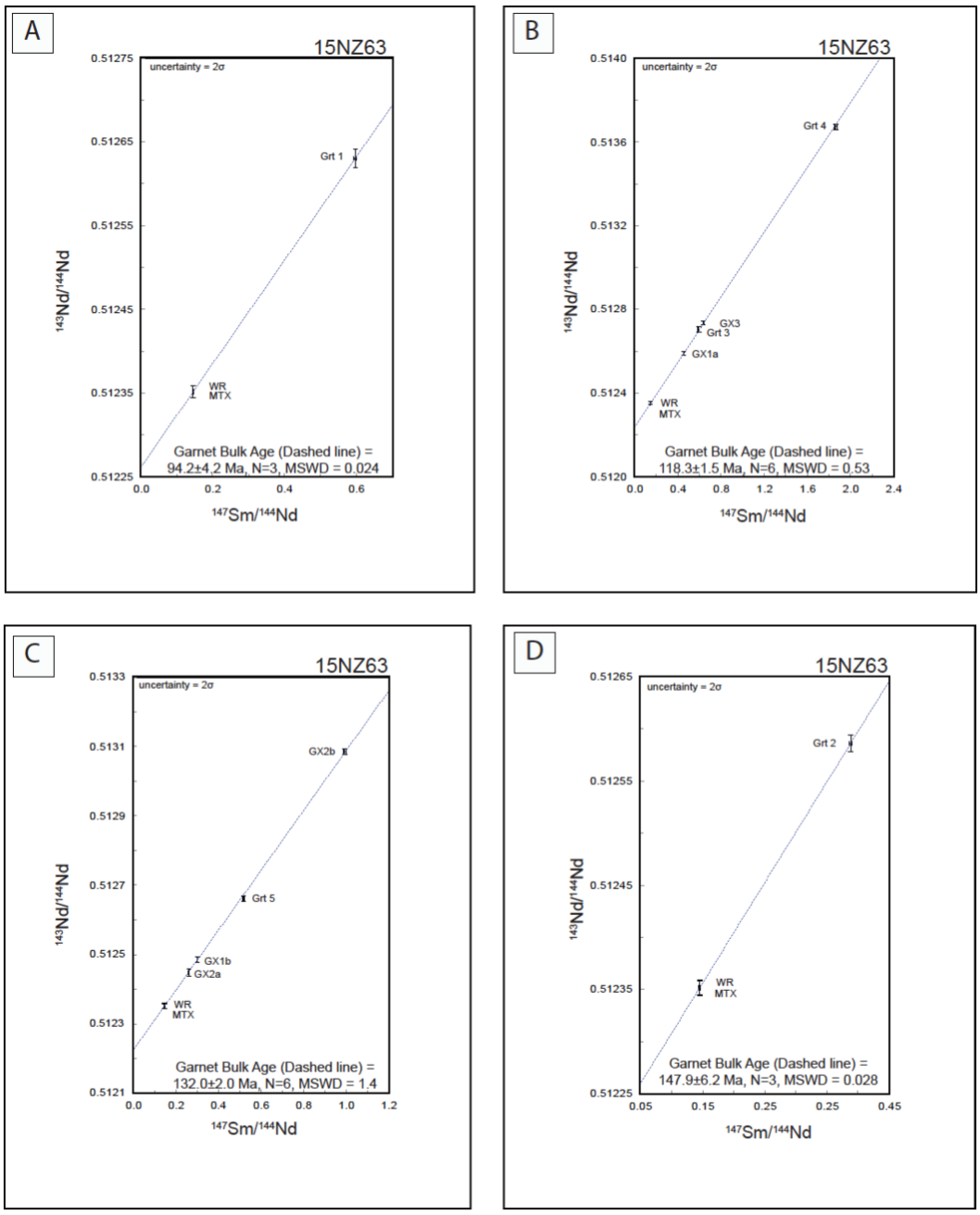

Figure 23. Garnet Sm-Nd isochrons for four age populations from 15NZ63 from the Arthur River Complex, Camp Oven Creek, New Zealand. (A) Garnet Sm-Nd isochron for 3/12 aliquots that yields an age of 94.2±4.2 Ma (MSWD = 0.024). (B) Garnet Sm-Nd isochron for 6/12 aliquots that yields an age of 118.3±1.5 Ma (MSWD = 0.53). (C) Garnet Sm-Nd isochron for 6/12 aliquots that yields an age of 132.0±2.0 Ma (MSWD = 1.4). (D) Garnet Sm-Nd isochron for 3/12 aliquots that yields an age of 147.9±6.2 Ma (MSWD = 0.028).

Metamorphic P-T Estimates

MAD and Thermobarometry

MAD were constructed for samples 18MSNZ511b, 18MSNZ510a,15NZ51, 05NZ12, and 15NZ63. Isopleths for the observed garnet compositions provide useful P-T estimates for sample 18MSNZ511b. Additional P-T estimates were obtained for samples 18MSNZ511b and 18MSNZ510a using thermobarometry. The garnet, biotite, muscovite, plagioclase, and hornblende compositions used for P-T estimates are listed in Table 5.

Table 5. Mineral compositions used for P-T estimates from thermobarometry and MAD along the Milford Transect.

Representative garnet comporitions

	18MSNZ511b		18MSNZ510a		15NZ51	05NZ12		15NZ63	
	Core average	Rim average	Core average	Rim Average	n.d.	Core average	Rim average	Core average	Rim average
Wt. % oxides									
SiO2	37.86	37.48	37.89	38.02	n.d.	37.77	40.33	38.46	37.68
Al2O3	22.07	21.64	21.58	21.71	n.d.	21.52	22.11	21.30	21.14
FeO	28.57	27.63	26.27	25.96	n.d.	24.83	21.14	27.06	26.29
MgO	5.54	4.78	5.68	5.91	n.d.	6.28	5.19	1.49	1.15
MnO	0.42	0.45	0.95	0.86	n.d.	2.02	1.48	3.30	2.57
CaO	5.02	6.69	6.55	6.53	n.d.	6.00	8.27	9.81	11.17
TiO2	0.02	0.60	0.07	0.07	n.d.	n.d	n.d	0.04	0.05
Cr2O3	0.14	0.29	0.20	0.21	n.d.	n.d	n.d	n.d	n.d
Total	99.64	99.56	99.18	99.27	n.d.	98.42	98.51	101.47	100.06
Cations per 12 oxygen									
Si	2.96	2.97	2.99	2.99	n.d.	2.99	3.10	3.02	3.00
Ti	0.04	0.04	0.00	0.00	n.d.	n.d.	n.d.	0.00	0.00
Al	2.03	2.02	2.00	2.01	n.d.	2.00	2.01	1.97	1.98
Fe2+	1.87	1.83	1.73	1.71	n.d.	1.64	1.38	1.78	1.75
Mg	0.65	0.56	0.67	0.69	n.d.	0.74	0.60	0.17	0.17
Mn	0.03	0.03	0.06	0.06	n.d.	0.13	0.10	0.22	0.14
Ca	0.42	0.57	0.55	0.55	n.d.	0.51	0.69	0.83	0.95
Fe/(Fe+Mg)	0.74	0.77	0.72	0.71	n.d.	0.69	0.70	0.91	0.91
Mole fractions									
Pyrope	0.22	0.19	0.22	0.23	n.d.	0.24	0.20	0.06	0.05
Almandine	0.63	0.61	0.57	0.57	n.d.	0.54	0.45	0.59	0.58
Spessartine	0.01	0.01	0.02	0.02	n.d.	0.04	0.03	0.07	0.06
Grossular	0.14	0.19	0.18	0.18	n.d.	0.17	0.31	0.28	0.32

Representative plagioclase compositions

	18MSNZ511b	18MSNZ510a	15NZ51	05NZ12	15NZ63
Wt. % oxides					
SiO2	60.40	n.d.	n.d.	n.d.	n.d.
Al2O3	25.47	n.d.	n.d.	n.d.	n.d.
FeO	0.08	n.d.	n.d.	n.d.	n.d.
MgO	0.00	n.d.	n.d.	n.d.	n.d.
CaO	6.03	n.d.	n.d.	n.d.	n.d.
Na2O	7.57	n.d.	n.d.	n.d.	n.d.
K2O	0.08	n.d.	n.d.	n.d.	n.d.
MnO	0.01	n.d.	n.d.	n.d.	n.d.
TiO2	0.00	n.d.	n.d.	n.d.	n.d.
Cr2O3	0.38	n.d.	n.d.	n.d.	n.d.
Total	100.03	n.d.	n.d.	n.d.	n.d.
Cations per 8 oxygen					
Si	2.69	n.d.	n.d.	n.d.	n.d.
Al	1.34	n.d.	n.d.	n.d.	n.d.
Fe3+	0.00	n.d.	n.d.	n.d.	n.d.
Ca	0.29	n.d.	n.d.	n.d.	n.d.
Na	0.65	n.d.	n.d.	n.d.	n.d.
K	0.00	n.d.	n.d.	n.d.	n.d.
Total cations	4.97	n.d.	n.d.	n.d.	n.d.
Mole fractions					
Ab	0.69	n.d.	n.d.	n.d.	n.d.
An	0.30	n.d.	n.d.	n.d.	n.d.
Or	0.00	n.d.	n.d.	n.d.	n.d.

Table 5. Mineral compositions used for P-T estimates from thermobarometry and MAD along the Milford Transect. (cont.)

Representative muscovite compositions

	18MSNZ511b	18MSNZ510a	15NZ51	05NZ12	15NZ63
Wt. % oxides					
SiO2	45.69	n.d.	n.d.	n.d.	n.d.
Al2O3	36.24	n.d.	n.d.	n.d.	n.d.
FeO	1.25	n.d.	n.d.	n.d.	n.d.
MgO	1.46	n.d.	n.d.	n.d.	n.d.
CaO	0.01	n.d.	n.d.	n.d.	n.d.
Na2O	0.96	n.d.	n.d.	n.d.	n.d.
K2O	9.21	n.d.	n.d.	n.d.	n.d.
MnO	0.00	n.d.	n.d.	n.d.	n.d.
TiO2	0.72	n.d.	n.d.	n.d.	n.d.
Cr2O3	0.00	n.d.	n.d.	n.d.	n.d.
Total	95.54	n.d.	n.d.	n.d.	n.d.
Cations per 22 oxygen					
Si	6.03	n.d.	n.d.	n.d.	n.d.
Ti	0.07	n.d.	n.d.	n.d.	n.d.
Al	5.64	n.d.	n.d.	n.d.	n.d.
Fe2+	0.14	n.d.	n.d.	n.d.	n.d.
Mn	0.00	n.d.	n.d.	n.d.	n.d.
Mg	0.29	n.d.	n.d.	n.d.	n.d.
Na	0.25	n.d.	n.d.	n.d.	n.d.
K	1.55	n.d.	n.d.	n.d.	n.d.
H	2.00	n.d.	n.d.	n.d.	n.d.
Site fractions					
Mg#	0.67	n.d.	n.d.	n.d.	n.d.
Al(IV)	1.97	n.d.	n.d.	n.d.	n.d.
Al(VI)	3.68	n.d.	n.d.	n.d.	n.d.
Fe #	0.33	n.d.	n.d.	n.d.	n.d.

Representative biotite compositions

	18MSNZ511b	18MSNZ510a	15NZ51	05NZ12	15NZ63
Wt. % oxides					
SiO2	37.18	n.d.	n.d.	n.d.	n.d.
Al2O3	19.92	n.d.	n.d.	n.d.	n.d.
FeO	13.95	n.d.	n.d.	n.d.	n.d.
MgO	13.30	n.d.	n.d.	n.d.	n.d.
CaO	0.00	n.d.	n.d.	n.d.	n.d.
Na2O	0.23	n.d.	n.d.	n.d.	n.d.
K2O	8.90	n.d.	n.d.	n.d.	n.d.
MnO	0.02	n.d.	n.d.	n.d.	n.d.
TiO2	1.30	n.d.	n.d.	n.d.	n.d.
Cr2O3	0.00	n.d.	n.d.	n.d.	n.d.
Total	94.80	n.d.	n.d.	n.d.	n.d.
Cations per 22 oxygen					
Si	5.49	n.d.	n.d.	n.d.	n.d.
Ti	0.14	n.d.	n.d.	n.d.	n.d.
Al	3.47	n.d.	n.d.	n.d.	n.d.
Fe2+	1.72	n.d.	n.d.	n.d.	n.d.
Mn	0.00	n.d.	n.d.	n.d.	n.d.
Mg	2.93	n.d.	n.d.	n.d.	n.d.
Na	0.06	n.d.	n.d.	n.d.	n.d.
K	1.68	n.d.	n.d.	n.d.	n.d.
H	2.00	n.d.	n.d.	n.d.	n.d.
Site fractions					
Mg#	0.63	n.d.	n.d.	n.d.	n.d.
Al(IV)	2.51	n.d.	n.d.	n.d.	n.d.
Al(VI)	0.96	n.d.	n.d.	n.d.	n.d.
Fe #	0.37	n.d.	n.d.	n.d.	n.d.

Representative hornblende compositions

	18MSNZ511b	18MSNZ510a	15NZ51	05NZ12	15NZ63
Wt.% oxide					
SiO2	n.d.	43.68	n.d.	n.d.	n.d.
TiO2	n.d.	1.12	n.d.	n.d.	n.d.
Al2O3	n.d.	13.16	n.d.	n.d.	n.d.
FeO	n.d.	14.44	n.d.	n.d.	n.d.
MnO	n.d.	0.05	n.d.	n.d.	n.d.
MgO	n.d.	11.44	n.d.	n.d.	n.d.
CaO	n.d.	10.79	n.d.	n.d.	n.d.
Na2O	n.d.	1.81	n.d.	n.d.	n.d.
K2O	n.d.	1.03	n.d.	n.d.	n.d.
H2O	n.d.	2.12	n.d.	n.d.	n.d.
Total	n.d.	97.87	n.d.	n.d.	n.d.
Cations per 23 oxygen					
Si	n.d.	6.46	n.d.	n.d.	n.d.
Ti	n.d.	0.12	n.d.	n.d.	n.d.
Al	n.d.	2.30	n.d.	n.d.	n.d.
Fe2+	n.d.	1.79	n.d.	n.d.	n.d.
Mn	n.d.	0.01	n.d.	n.d.	n.d.
Mg	n.d.	2.52	n.d.	n.d.	n.d.
Ca	n.d.	1.71	n.d.	n.d.	n.d.
Na	n.d.	0.52	n.d.	n.d.	n.d.
K	n.d.	0.19	n.d.	n.d.	n.d.
H	n.d.	2.00	n.d.	n.d.	n.d.
Site fractions					
Mg#	n.d.	0.59	n.d.	n.d.	n.d.
Al(IV)	n.d.	1.54	n.d.	n.d.	n.d.
Al(VI)	n.d.	0.76	n.d.	n.d.	n.d.
Fe #	n.d.	0.41	n.d.	n.d.	n.d.

n.d= not determined

18MSNZ511b

18MSNZ511b has a peak metamorphic mineral assemblage of plagioclase, garnet, biotite, quartz, kyanite, and rutile based on the observed mineral textures (Table 2). The predicted stability field for this assemblage is highlighted in yellow on the T-H_2O and P-T MAD (Figs. 23, 24). In the T vs H_2O MAD at constant P= 12 kbar, the peak mineral assemblage plots at 650- 675 °C (Fig. 24). The H_2O in line (blue line) requires an H content of 10 for water saturation at 500 °C. Therefore, this sample was modeled with water saturation at H=10 (Fig. 24) in order to produce the observed minerals and water saturation below the solidus. Peak metamorphic P-T conditions are estimated at approximately 650- 700°C and 7-11.5 kbar, based on the peak mineral assemblage on the P vs. T MAD (Fig. 25). This field borders to the solidus on the low temperatures side. Garnet core isopleths (blue field) intersect at ca. 650 -700 °C and 7- 10 kbar within the peak mineral assemblage field (Fig. 25). Garnet-biotite- plagioclase-muscovite thermobarometry (purple field) using mineral rim compositions was used to calculate 680 ± 50°C @ 10.5 ± 1 kbar (Fig. 25). This garnet rim estimate overlaps with the peak metamorphic mineral assemblage field at 625 – 675°C and 9.5- 11 kbar (Fig. 25). Garnet modes (black dashed lines) are subvertical and increase with temperature, but at a relatively constant pressure. I interpret garnet growth to have occurred at constant temperature ca. 675 °C and with a slight increase in pressure ca. 7 kbar to 11 kbar. I infer that, the innermost garnet core preserves initial garnet growth and this was followed by a near isothermal increase in pressure. Rutile exsolution needles found in the rims of garnets (Fig. 3), and increases of Ca at garnet rims further support this change in pressure.

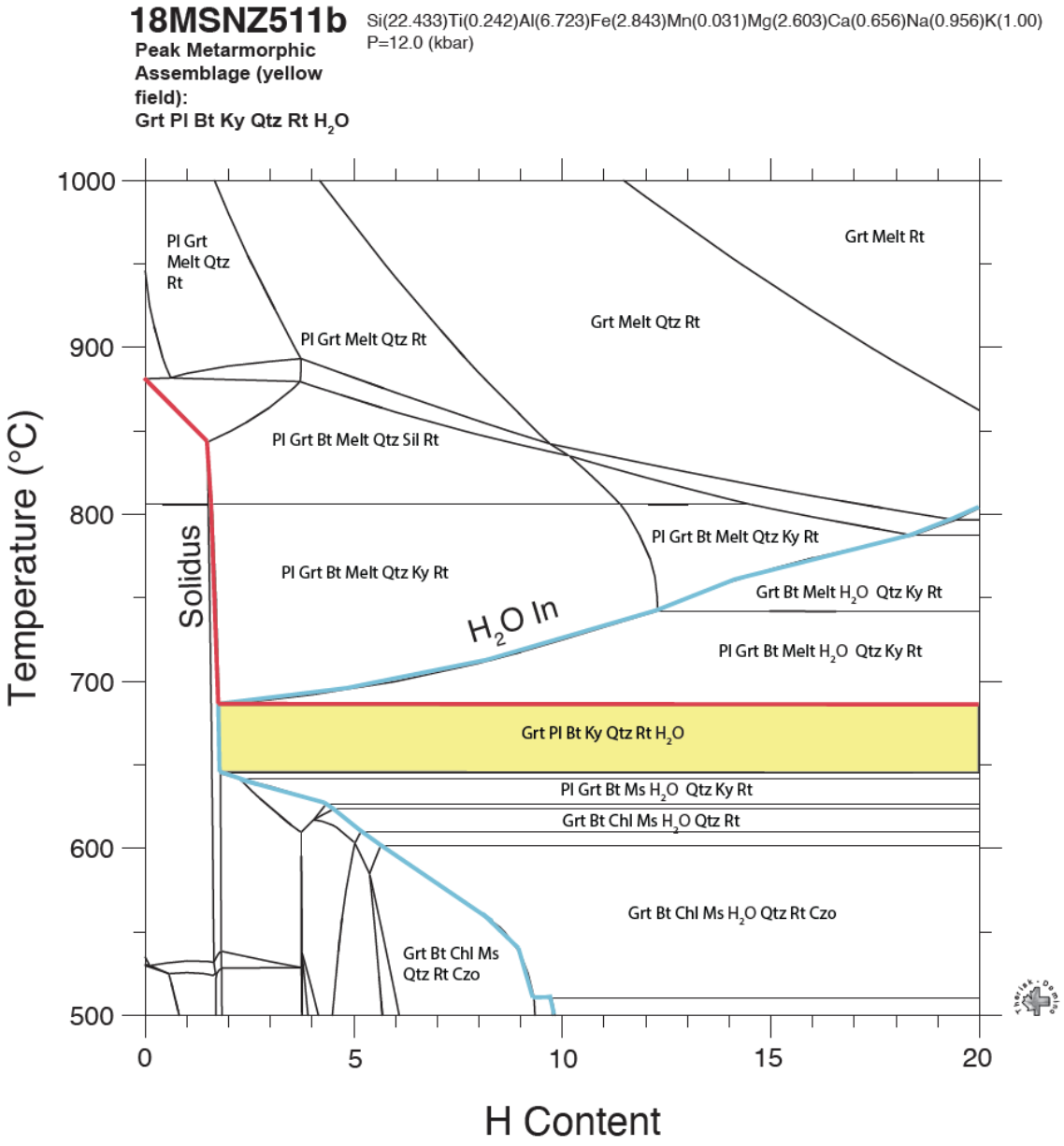

Figure 24. T -H_2O MAD for estimating water content in 18MSNZ511b from the St. Anne Gneiss, Milford Sound, New Zealand. The bold blue line indicates the boundary of water saturation on the right of the line and an absence of free water on the left of the line and melt is predicted at T above the solidus shown in red. The highlighted yellow field indicates the P-T range for the peak metamorphic assemblage.

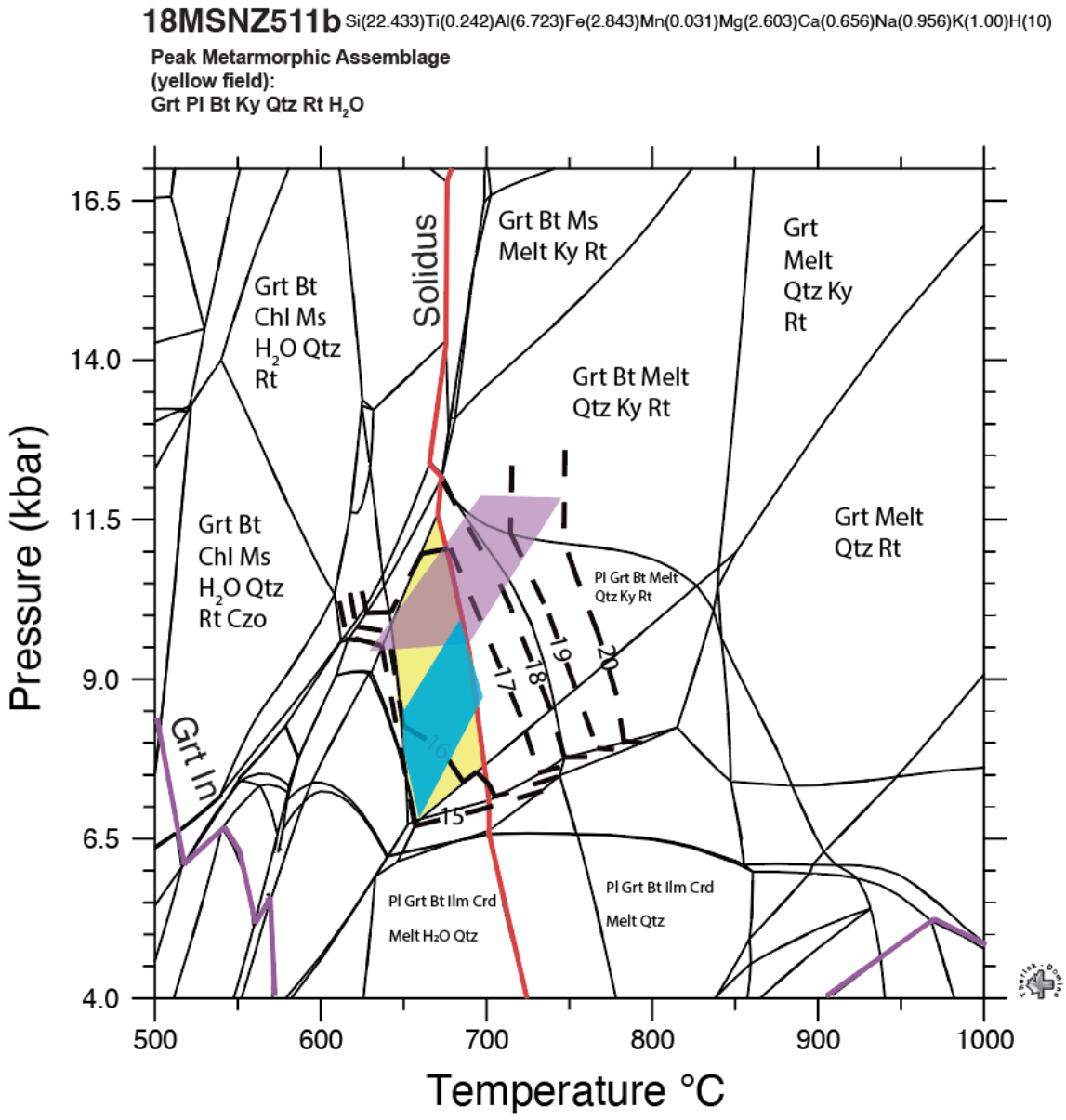

Figure 25. P - T MAD for sample 18MSNZ511b from the St. Anne Gneiss, Milford Sound, New Zealand.. Garnet is predicted to be stable at P and T above the *Garnet in* line shown in purple and melt is predicted at T above the solidus shown in red. Garnet mode lines are shown as black dashed lines. The observed peak metamorphic minerals are predicted to be stable in the yellow field at 650- 700°C and 7-11.5 kbar. Garnet core isopleths intersections are shown in the blue field at 7-10 kbar and 650- 700 °C . Garnet rim thermobarometry estimates are shown in the purple field at ca. 680 °C and 11 kbar.

18MSNZ510a

18MSNZ510a has a peak metamorphic mineral assemblage of garnet, biotite, hornblende, titanite, plagioclase, rutile, clinozoisite, and quartz based on mineral relationships and textures (Table 2). The predicted stability field for this assemblage is highlighted in yellow on the T-H_2O and P-T MAD (Figs. 26, 27). In the T vs H_2O MAD at constant P= 9 kbar, the peak mineral assemblage plots at 550- 575 °C (Fig. 26). The H_2O in line (blue line) requires an H content of 7 for water saturation at 500 °C. (Fig. 26). Therefore, this sample was modeled with water saturation at H=7 (Fig. 27) in order to produce the observed minerals and water saturation below the solidus. Peak metamorphic P-T conditions are estimated at approximately 525- 625°C and 7.5-12 kbar, based on the peak mineral assemblage on the P vs. T MAD (Fig. 27). Iron-Mg exchange thermometry for hornblende inclusions near the garnet rim indicate temperatures of 600 ± 50°C, where the peak metamorphic mineral assemblage plots within this estimate. Garnet rim thermometry estimates overlap with the peak metamorphism field at 550 – 625°C and 8 – 12 kbar (Fig. 26). Garnet modes (black dashed lines) are subvertical and increase with temperature, and with slight increases in pressure. Based on these fields, I interpret garnet growth to have occurred at constant temperature ca. 600 °C and with an increase in pressure ca. 8 kbar to 12 kbar. I infer that the core of this garnet preserves growth zoning, and, therefore, we can interpret peak metamorphism occurring at 525 – 625° C and 8 – 12 kbar at 99 Ma.

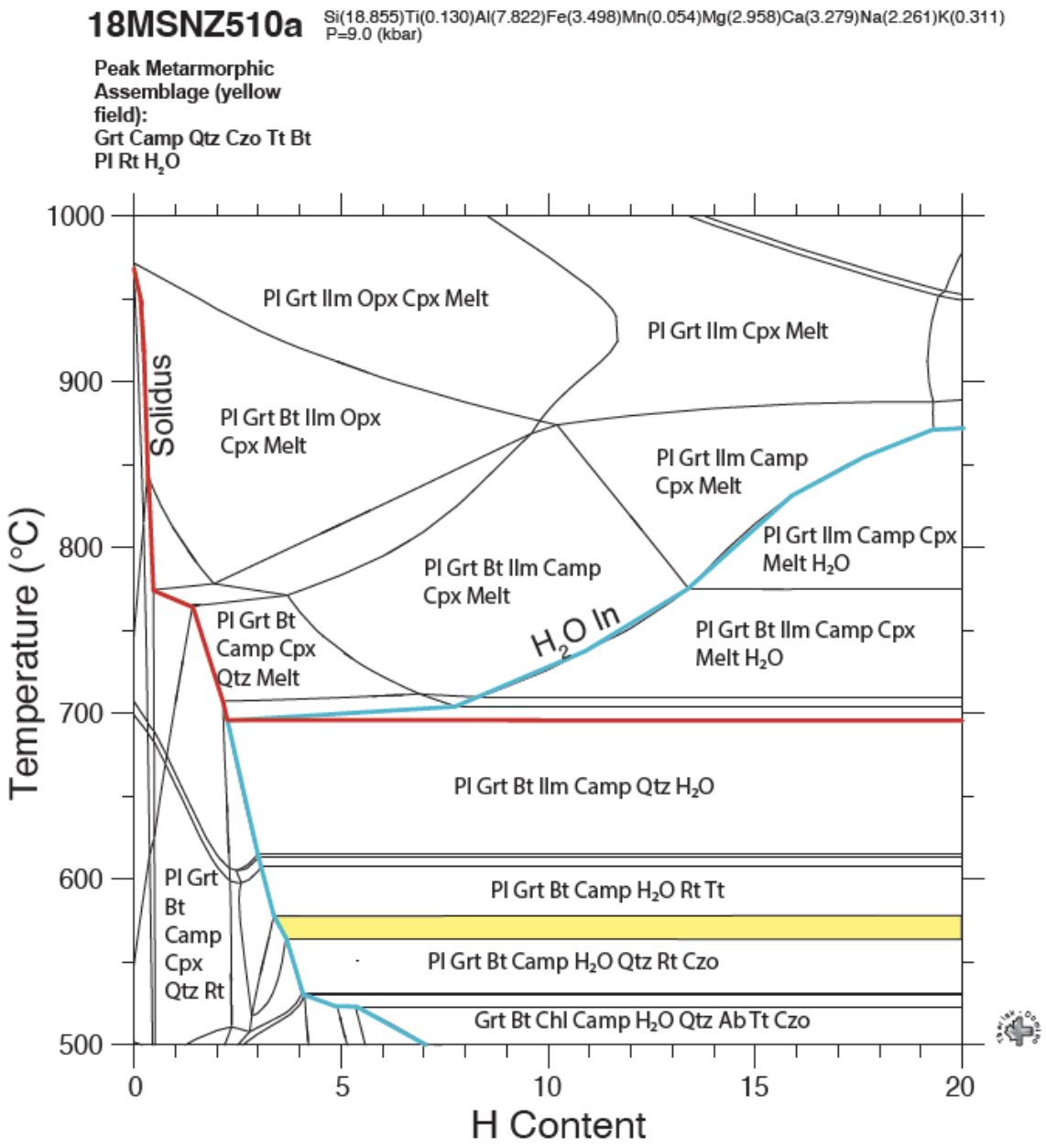

Figure 26. T- H_2O MAD for estimating water content in 18MSNZ510a from the Thurso Gneiss, Milford Sound, New Zealand. The bold blue line indicates the boundary of water saturation on the right of the line and an absence of free water on the left of the line and melt is predicted at T above the solidus shown in red. The highlighted yellow field indicates the P-T range for the peak metamorphic assemblage.

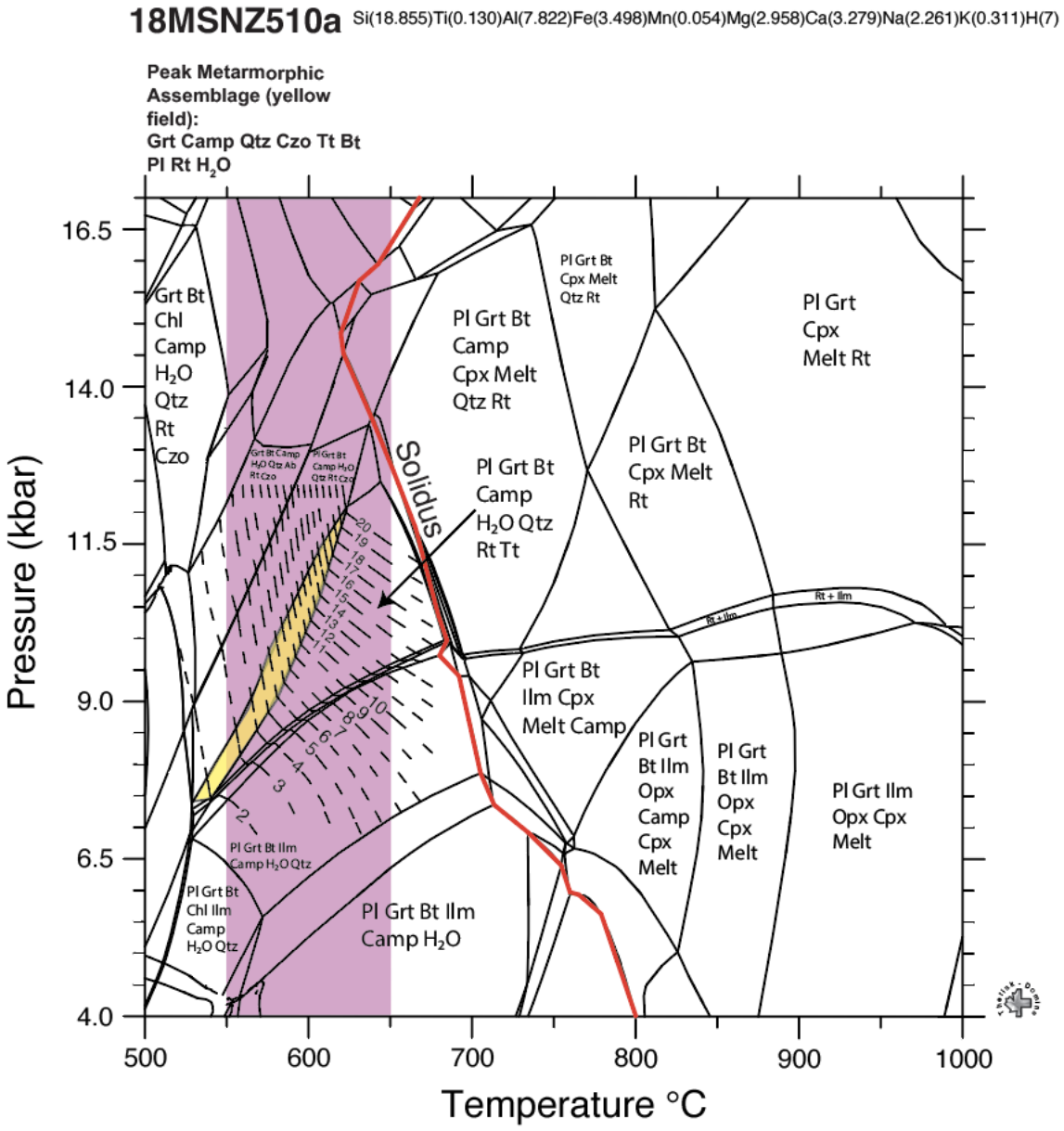

Figure 27. P- T MAD for sample 18MSNZ510a from the Thurso Gneiss, Milford Sound, New Zealand. Garnet is predicted to be stable over the entire P and T range and melt is predicted at T above the solidus shown in red. Garnet mode lines are shown as black dashed lines. The observed peak metamorphic minerals are predicted to be stable in the yellow field at 525- 625°C and 7.5-12 kbar. Garnet rim thermobarometry estimates are shown in the purple field at ca. 550 -650 °C.

15NZ51

Sample 15NZ51 has a peak metamorphic mineral assemblage of garnet, biotite, plagioclase, hornblende, rutile, quartz, and clinopyroxene based on mineral relationships and textures (Table 2). The predicted stability field for this assemblage is highlighted in yellow on the MAD (Figs. 28, 29). In the T vs H_2O MAD at constant P= 12 kbar, the peak mineral assemblage plots at 610- 650°C (Fig. 28). The H_2O in line (blue line) requires an H content of 6.5 for water saturation at 500 °C. (Fig. 28). Therefore, this sample was modeled with water saturation at H=7 (Fig. 28) in order to produce the observed minerals and water saturation below the solidus. The peak metamorphic conditions are estimated as 625 – 675°C and 10.5 – 11 kbar based on the predicted location of the peak mineral assemblage on the P vs. T MAD. This field lies along the solidus at ca. 650°C (Fig. 29). Garnet modes (black dashed lines) are subhorizontal and increase with pressure, and with slight increases in temperature. Garnet in this sample show growth zoning and therefore, we can assume peak metamorphism occurred under P – T conditions of 625 – 675°C and 10.5 – 11 kbar at ca. 93 Ma. We can tentatively interpret peak metamorphism occurring at 625 – 675° C and 10.5 – 11 kbar at ca. 93 Ma since growth zoning is preserved in this sample.

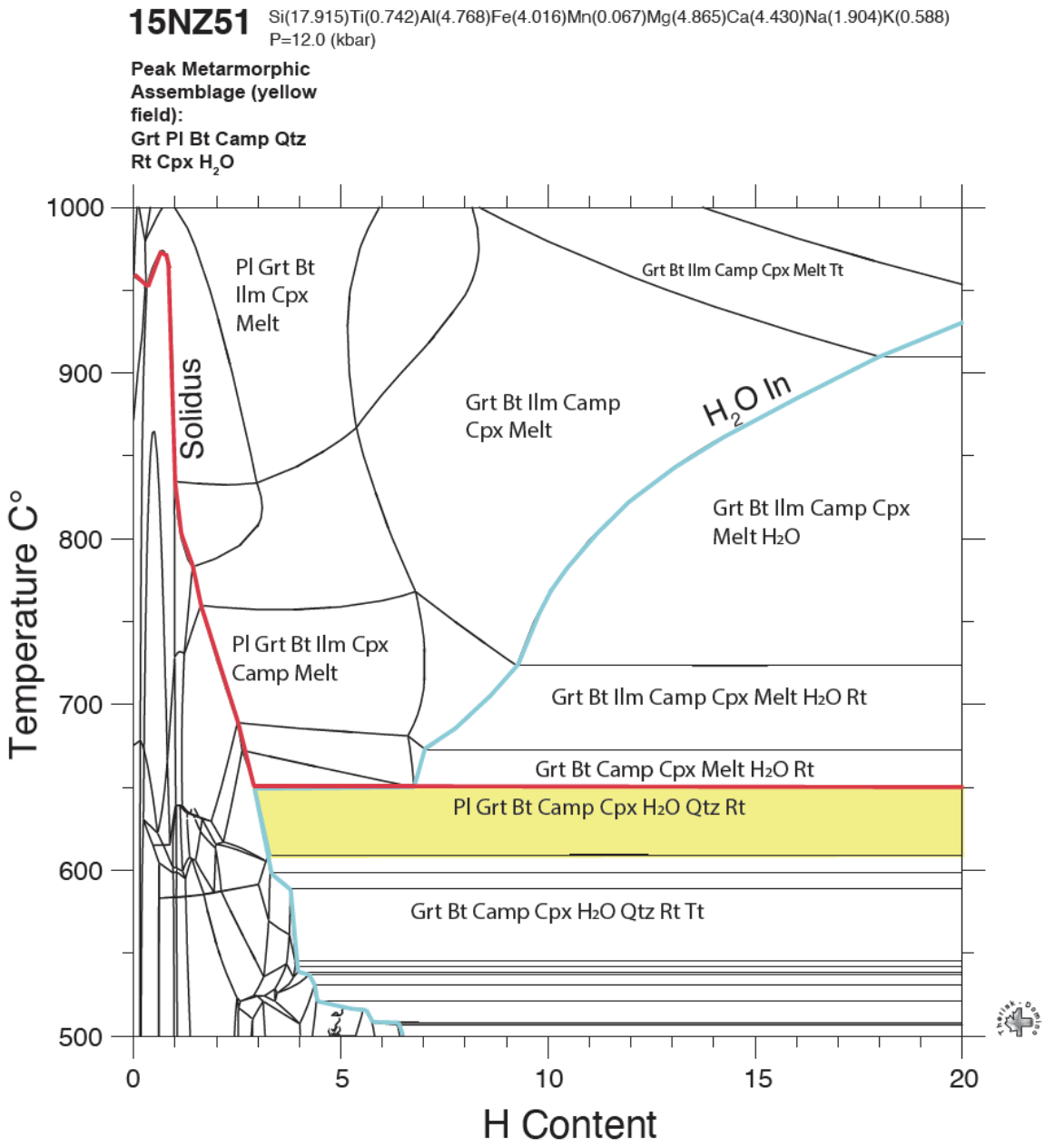

Figure 28. T-H_2O MAD for estimating water content in sample 15NZ51, Milford Gneiss, Milford Sound, New Zealand. The bold blue line indicates the boundary of water saturation on the right of the line and an absence of free water on the left of the line and melt is predicted at T above the solidus shown in red. The highlighted yellow field indicates the P-T range for the peak metamorphic assemblage.

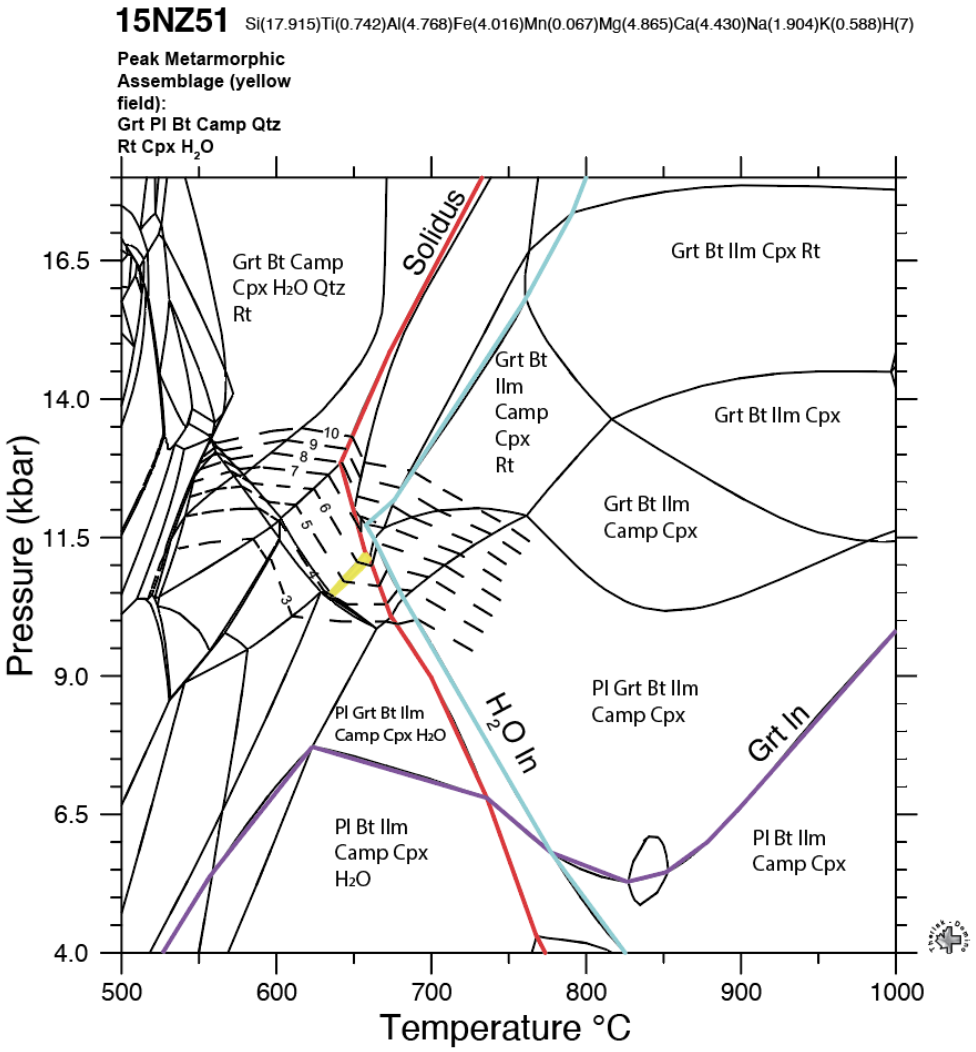

Figure 29. P-T MAD for sample 15NZ51, Milford Sound, New Zealand. Garnet is predicted to be stable above the garnet in line (bold purple line) and melt is predicted at T above the solidus shown in red. H_2O is present at lower temperatures below the H_2O in line (blue line). The observed peak metamorphic minerals are predicted to be stable in the yellow field at 625 – 675°C and 10.5 – 11 kbar. Garnet mode lines are shown as black dashed lines.

05NZ12

05NZ12 has a peak metamorphic mineral assemblage of plagioclase, garnet, hornblende, biotite, clinopyroxene, quartz, rutile based on mineral relationships and textures (Table 2). In addition, I infer that melt was in equilibrium with these minerals, based on the vein of trondhjemite and leucocratic matrix around the garnet clinopyroxene aggregates in the garnet reaction zone. The host rock WR composition was used for calculating T vs. H_2O and P-T MAD. The inferred peak phase assemblage is highlighted in yellow in both of the MAD (Figs. 30, 31). The T vs. H_2O MAD at a constant pressure of 12 kbar (Fig. 30) was used to infer a water content during metamorphism. In this MAD, the peak mineral assemblage, which includes clinoamphibole, plots at 675 725 °C (Fig. 30). Because this rock is a granulite gneiss derived from an igneous protolith it was likely undersaturated with respect to water. Therefore, a water content of H=2, just sufficient to stabilize amphibole, was used for construction of the P-T MAD. The peak metamorphic conditions are estimated as 640 – 725°C and 10.5 – 16 kbar based on the predicted location of the peak mineral assemblage on the P vs. T MAD. This field lies along the solidus at ca. 650°C (Fig. 31). Garnet modes (black dashed lines) are subhorizontal and increase with pressure, and with slight increases in temperature. So, we infer an increase in pressure after initial garnet growth at ca. 122 Ma to support garnet growth conditions. Peak metamorphism temperatures of ca. 650 °C are similar to 18MSNZ511b, 18MSNZ510a, 15NZ51, discussed previously, but pressures are significantly higher in 05NZ12. P-T results for this sample are very similar to the results of Stowell et al. (2010) who reported 650- 825 °C and 10 - 16 kbar.

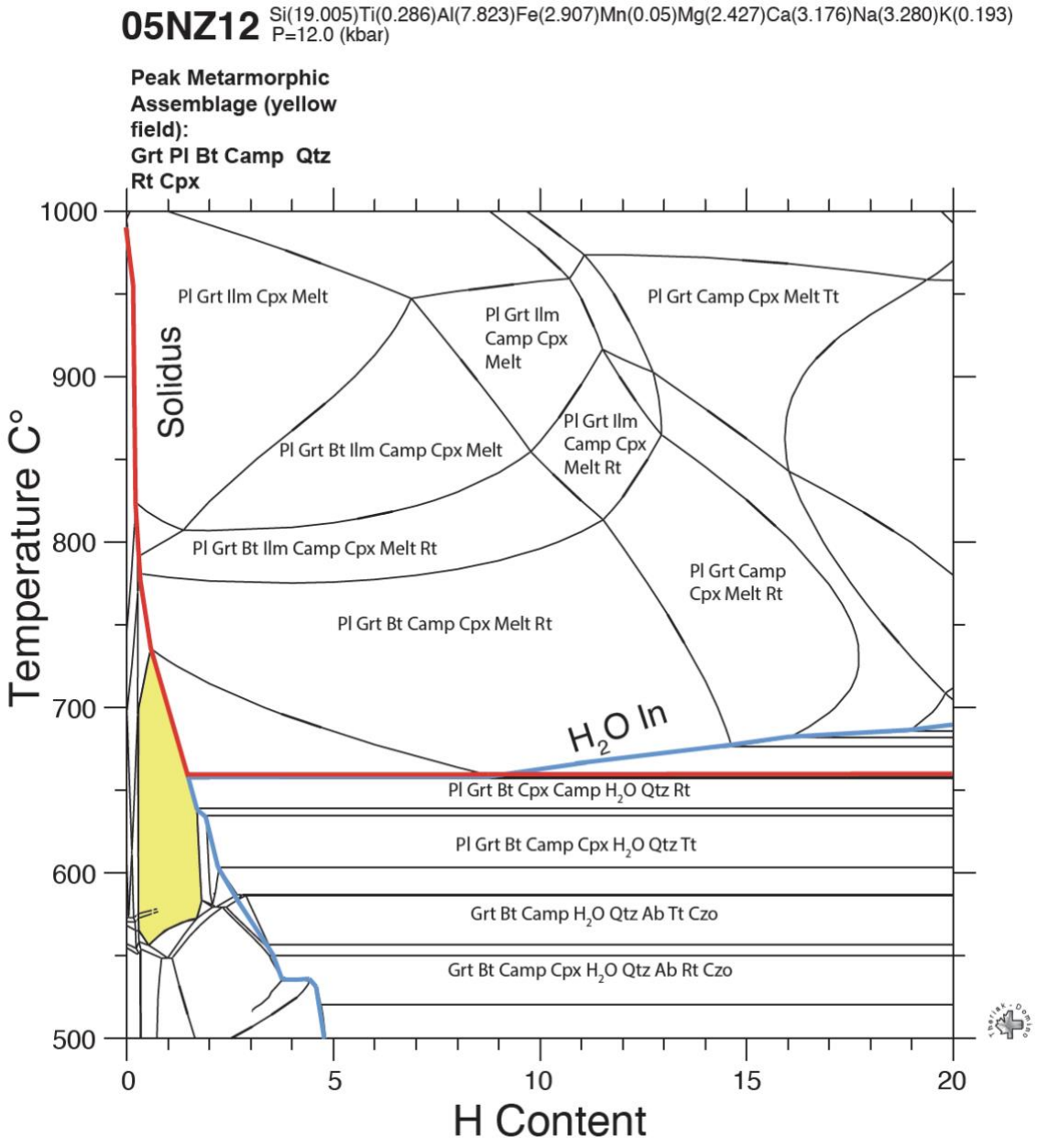

Figure 30. T-H_2O MAD for estimating water content in sample 05NZ12, Pembroke Granulite, New Zealand. The bold blue line indicates the boundary of water saturation on the right of the line and an absence of free water on the left of the line melt is predicted at T above the solidus shown in red. The highlighted yellow field indicates the P-T range for the peak metamorphic assemblage.

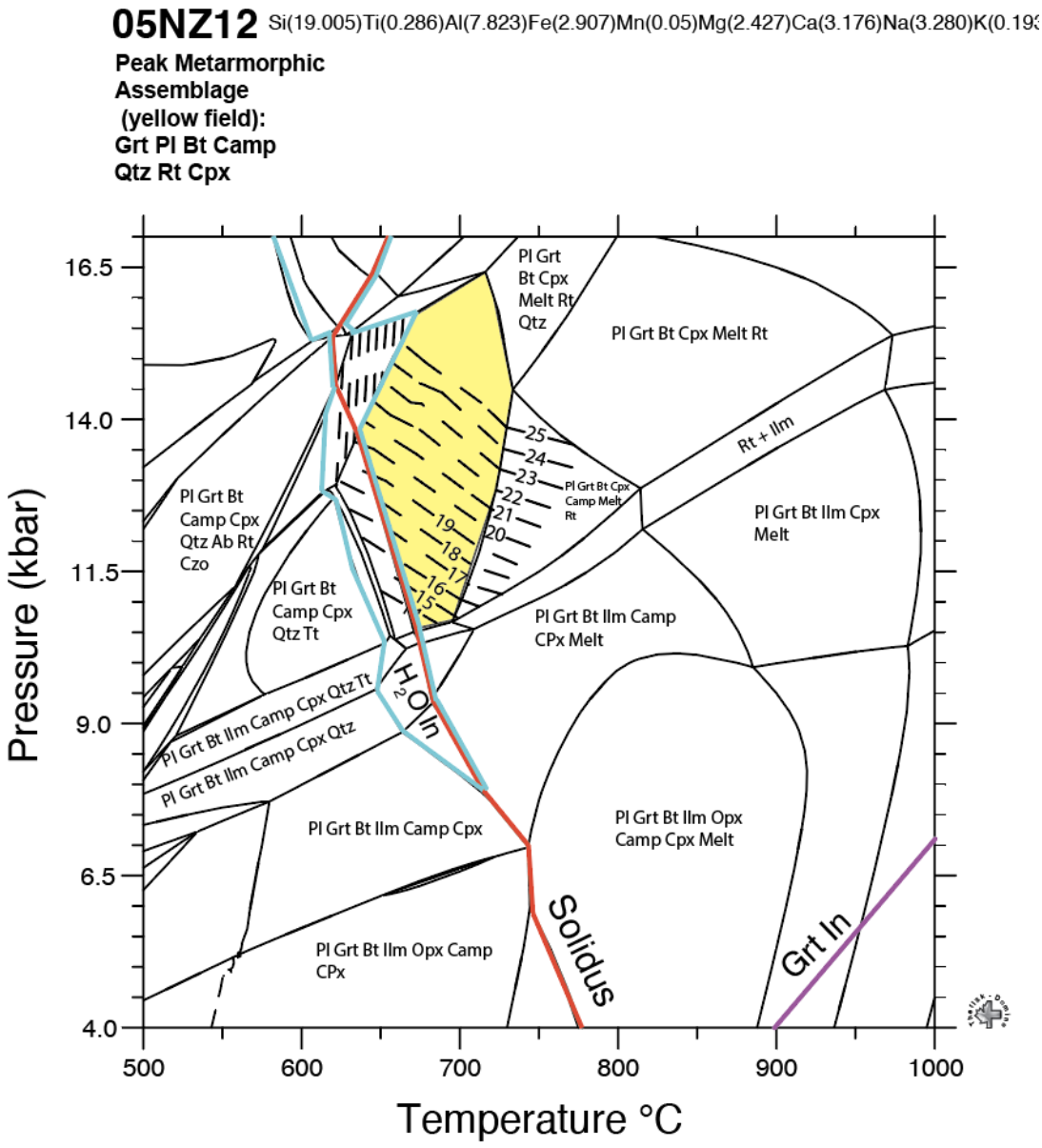

Figure 31. P-T MAD for sample 05NZ12, Pembroke Granulite, New Zealand. Garnet is predicted to be stable above P and T of the garnet in line (bold purple line) and melt is predicted at T above the solidus shown in red. H_2O is present at in the fields between the H_2O in lines (blue line).The observed peak metamorphic minerals are predicted to be stable in the yellow field at 625 – 675°C and 10.5 – 11 kbar. Garnet mode lines are shown as black dashed lines.

15NZ63

15NZ63 has a peak metamorphic mineral assemblage of plagioclase, garnet, biotite, clinozoisite, rutile, and quartz based on mineral relationships and textures (Table 2). The predicted stability field for this assemblage is highlighted in yellow on the MAD (Figs. 32, 33). In the T vs H_2O MAD at constant P= 12 kbar, the peak mineral assemblage plots at 575- 625°C (Fig. 32). The H_2O in line (blue line) requires an H content of 2.5 at 500°C. and therefore, this sample was modeled with water saturation at H=3 (Fig. 32), which is sufficient to stabilize biotite below the solidus. Note that the horizontal phase boundaries below 700°C in Figure 32 indicate that H content has no effect on the predicted mineral stability. The peak metamorphic conditions are estimated as 525 – 625°C and 8.5 – 13.5 kbar based on the predicted location of the peak mineral assemblage on the P vs. T MAD. This field lies along the solidus at ca. 625°C, which in addition to the greater amounts of plagioclase and quartz together in the matrix could indicate possible melt in this sample. (Fig. 33). Garnet modes (black dashed lines) are vertical and increase with temperature in the peak field. This sample preserves growth zoning, so we can infer a decrease in pressure and temperature after initial garnet growth in this sample at ca. 119 Ma.

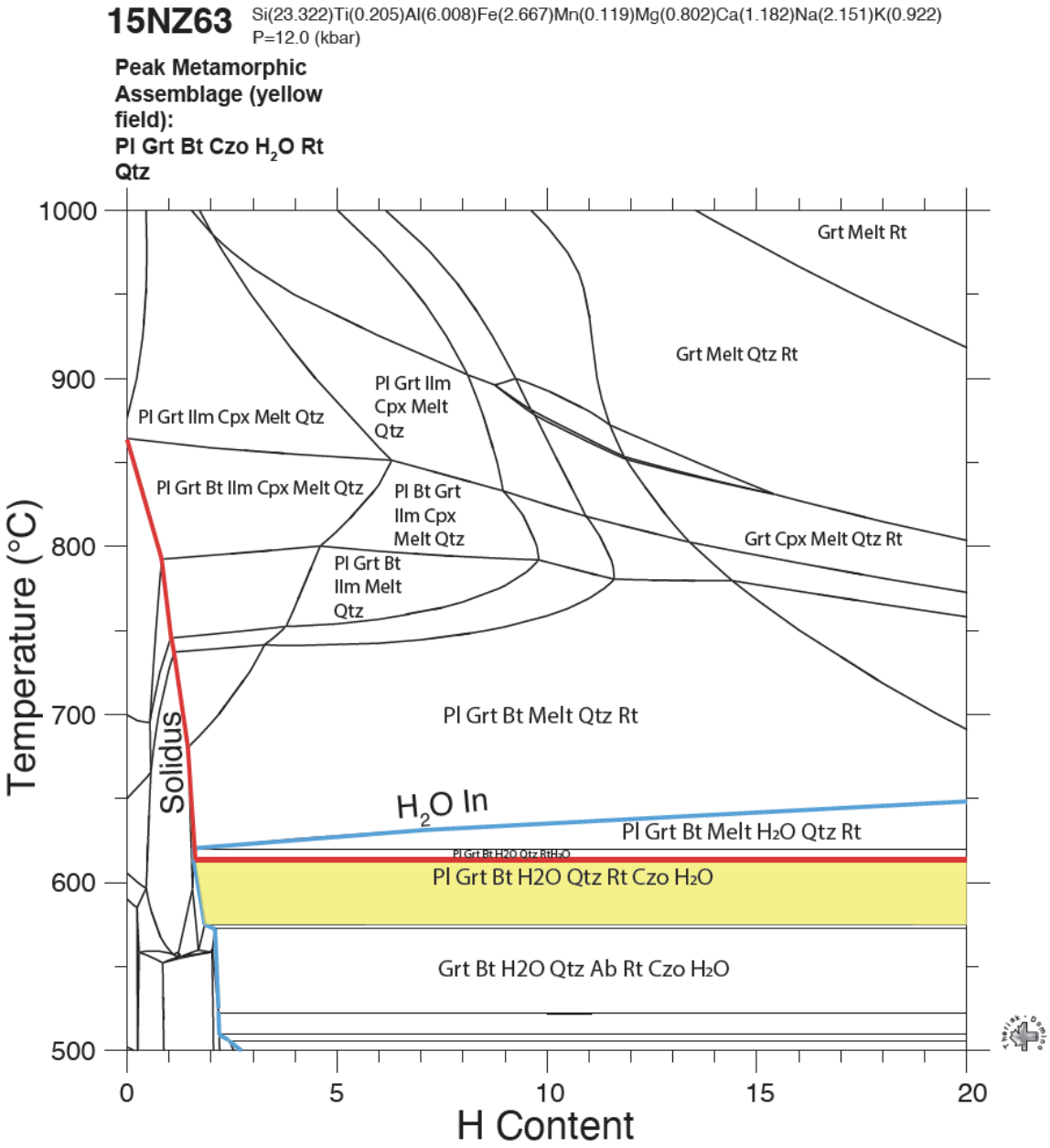

Figure 32. T-H_2O MAD for estimating water content in sample 15NZ63 from the Arthur River Complex, Camp Oven Creek, New Zealand. Bold blue line indicates where water is found on the right of the line and where water is absent on the left of the line melt is predicted at T above the solidus shown in red. Highlighted yellow field indicates the P-T range for the peak metamorphic assemblage.

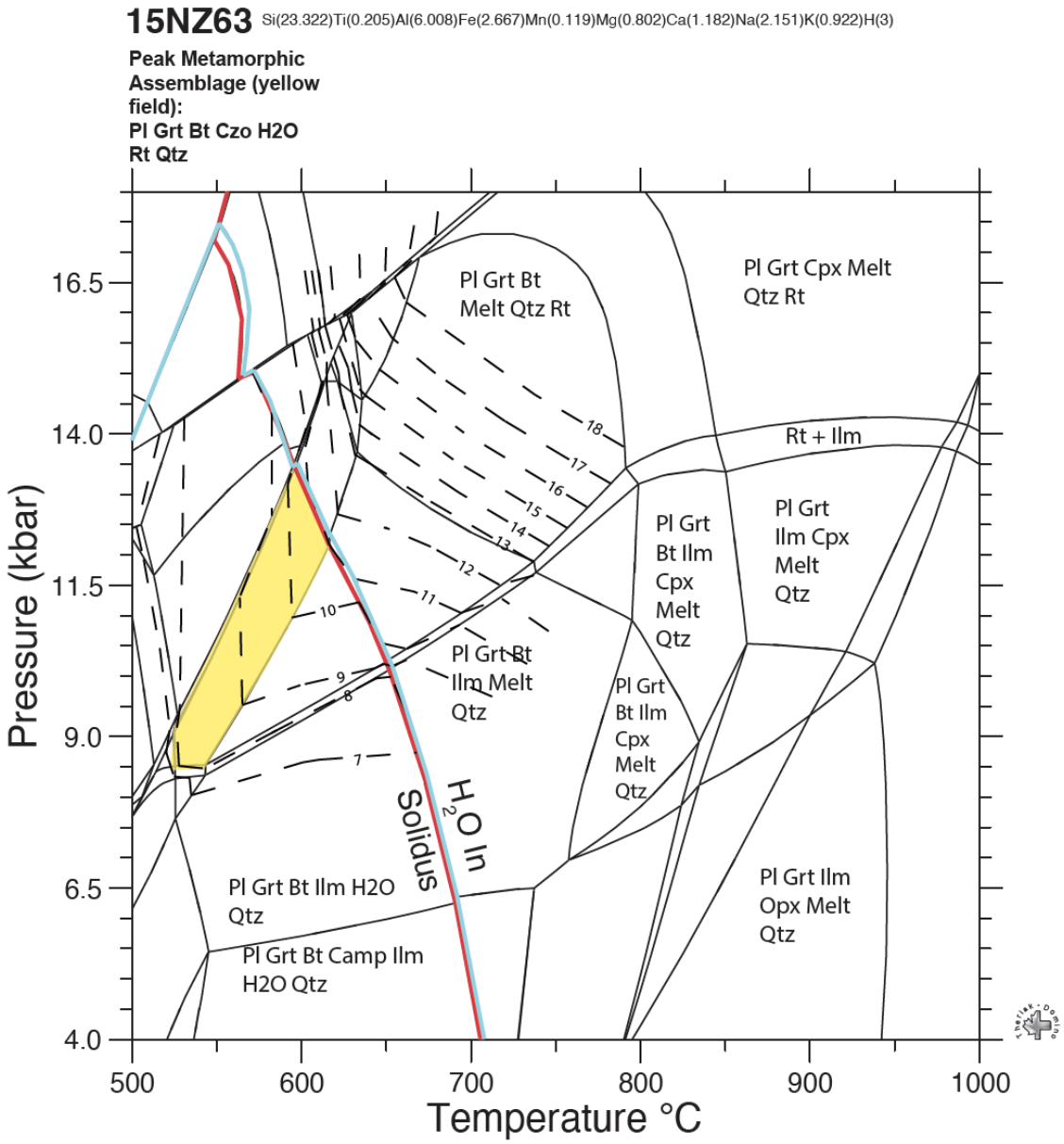

Figure 33. P- T MAD for sample 15NZ63 from the Arthur River Complex, Camp Oven Creek, New Zealand. Garnet is predicted to be stable at all P and T and melt is predicted at T above the solidus shown in red. H_2O is present at lower temperatures below the H_2O in line (blue line). The observed peak metamorphic minerals are predicted to be stable in the yellow field at 525 – 625°C and 8.5 – 13.5 kbar. Garnet mode lines are shown as black dashed lines and bold blue line is the H_2O in line.

DISCUSSION

Samples in this study are divided into three groups for discussion. First, samples 18MSNZ511b, 18MSNZ510a, and 15NZ51 within and adjacent to the Anita Shear Zone are grouped based on their location to the shear zone and similar garnet growth ages. Although these samples were at similar crustal conditions and depth, right lateral strike slip motion resulting from the Alpine Fault could have significantly displaced these samples. Therefore, 18MSNZ510a and 15NZ51 may not have been adjacent to each other prior to possible displacement. Next, 05NZ12 from the Pembroke Granulite is discussed separately based on its distinct textures and P-T history. Finally, 15NZ63 from the Camp Oven Creek Paragneiss in the Arthur River Complex, is also discussed separately based on the isotopic complexity and likely protracted thermal history. P-T estimates and timing of metamorphism for all samples along Milford Sounds are shown in Fig. 34.

Anita Shear Zone and adjacent rocks

Pressure estimates for samples 18MSNZ511b and 18MSMZ510a overlap between 9.5 and 11 kbar, with no overlap in the temperature estimates of 650 – 700 °C and 525- 625 °C, respectively. These results and the new garnet Sm-Nd ages are used with published data to construct a tentative model for the Anita Shear Zone. The ages and P-T results presented here, and in Klepeis et al., (1999) and Czertowicz et al. (2016) are linked by their estimates for P-T conditions during evolution of the steep subvertical mylonitic fabric. Figure 35 is a P-T MAD which includes data from Klepeis et al., 1999 deformation events (D2 and D3), Czertowicz et al., 2016 stages of metamorphism and counterclockwise P-T-t path (Stage I, Stage II, and Stage III),

titanite ages from Simon (2017), and our new P-T-t data for 18MSNZ511b, 18MSNZ510a, and 15NZ51.

Our new estimates for garnet growth (18MSNZ510a) and modification (18MSNZ511b) in the Anita Shear Zone, nearby (15NZ51), combined with published data allow reconstruction of two P-T-t paths for rocks in the shear zone along the Milford transect. The garnet Sm-Nd ages indicate that initial garnet growth in many of the rocks west of Pembroke was likely ca. 98 Ma (18MSNZ510a). However, I interpret that garnet was locally modified at high temperature between 23 and 44 Ma (18MSNZ511b). This interpretation is based on the complex Sm and Nd isotope results and the U-Pb ages presented by Simon (2017) which indicate that titanite growth extended from 9 to 19 Ma.

Samples 18MSNZ510a and 18MSNZ511b within the Anita Shear Zone are interpreted to be metasediments; therefore, the P-T paths begin at the surface with sedimentation. Clearly, these sediments were buried via crustal thickening and heated to mid- or upper-amphibolite facies. Although early mineral assemblages (e.g., sillimanite) were not identified in samples 18MSNZ510a and 18MSNZ511b, the samples reported in Klepeis and others (1999) and Czertowicz and others (2016) indicate early sillimanite zone high temperature metamorphism. These observations and the garnet core P-T estimates for 18MSNZ511 indicate that some or all of the Anita Shear Zone rocks followed a counterclockwise P-T-t path. However, the minerals associated with subhorizontal versus subvertical fabrics (Klepeis et al., 1999) and the significantly different temperatures estimated for the samples described here, indicate that rocks from the Anita Shear Zone likely experienced somewhat variable P-T-t paths.

The westernmost sample from near St. Anne Point (18MSNZ511b) contains garnet with numerous rutile inclusions concentrated in mantle areas. These arrays of rutile needles (Fig. 3)

likely indicate ‘exsolution’ and re-equilibration events that occurred during decrease in temperature (e.g., Ackerson et al. 2017) and possibly pressure. The complex zoning found in this sample with multiple spikes in major elements further supports that this sample underwent a complex thermal and barometric history. Titanite ages from Simon (2017) are 9- 19 Ma and record temperatures of ca. 690 °C, which overlap with temperatures recorded in 18MSNZ511b. Our new garnet Sm-Nd age indicates that the oldest garnet in this sample is ca. 44 Ma younger than garnet in 18MSNZ510a 2 km to the east.

Further east in the Anita Shear Zone, 18MSNZ510a lacks the dense mantles of rutile inclusions in 18MSNZ511b and garnet may never have experienced the high temperatures estimated for 18MSNZ511b. However, sparse rutile inclusions in garnet from 18MSNZ510a (Fig. 4) may indicate changes in pressure and temperature. In addition, garnet zoning in 18MSNZ510a indicates modification after growth and contains weak major element zoning. Therefore, initial garnet growth zoning could have been reset ca. 98 Ma. Zircon U-Pb ages from Czertowicz and others (2016) are 104 Ma and have P-T estimates that are between the boundaries of Stage II and Stage III metamorphic events (Fig 35), which overlap with 18MSNZ510a.

The P-T estimates of 10.5 – 11 kbar and 625 – 675 °C for sample 15NZ51 from the Milford Gneiss are similar to estimates for samples from the Anita Shear Zone. Sample 15NZ51 garnet preserves weak major element zoning and has evidence for syn-post deformational growth, which can indicate little or no change in pressure and temperature conditions. Our new 93 Ma garnet ages for the 15NZ51 further defines growth < 100 Ma west of the Pembroke Granulite.

Compositional modification after garnet growth is prominent throughout samples in the Anita Shear Zone which is interpreted to indicate that these rocks remained hot for an extended time before exhumation occurred. Figure 35 demonstrates the complexity of P-T-t paths for different rocks that are all within the Anita Shear Zone. The P-T-t path for sample 18MSNZ511b on the west, peaked at <10 kbar, lower pressure than rocks to the east, and shows final garnet equilibration ca. 23- 44 Ma. Whereas, the P-T-t path for sample 18MSNZ510a on the east peaked at ~10.2 kbar and equilibrated ca. 98 Ma. Both of the new P-T paths differ only slightly from those of Czertowicz and others (2016) (Fig. 35); however, unlike those in Czertowicz and others (2016) there is no known plutonic heat source for the Milford rocks. The two Milford Sound rocks (18MSNZ511b and 18MSNZ510a) could have both have reached temperatures sufficient for intracrystalline diffusion of major elements in garnet and similar P-T paths. But, the apparent ca. 50 m.y. age difference in garnet requires that 18MSNZ511b experienced much later REE isotope re-equilibration than 18MSNZ510a. Alternately, sample 18MSNZ510a may not have reached the higher apparent temperatures indicated for 18MSNZ511b.

Pembroke Granulite

New P-T estimates of 11- 16 kbar and 640 – 725 °C for sample 05NZ12 are distinctly higher than those for adjacent rocks to the west and east. Previous work in the Pembroke Granulite from Stowell et al., 2010 estimated peak temperature of garnet growth > 680 °C and 11-14 kbar which is consistent with what we determined in 05NZ12. However, 05NZ12 may have peaked at a lower temperature for garnet growth. Garnet growth in 05NZ12 is 122±2 Ma, which is significantly older than all other samples in this study, but confirms that there are no young garnet (109 Ma) in the Pembroke Granulite. This age also coincides with timing of the

Cretaceous high-T and P event in the Western Province of Fiordland at 126-110 Ma (Bradshaw, 1989; Gibson and Ireland, 1995; Brown, 1996; Klepeis et al., 2003).

Arthur River Complex

15NZ63 P-T estimates of 8.5 – 13.5 kbar and 525 – 625 ° C are to those at the western end of the Milford Transect in the Anita Shear Zone; however, the garnet growth in the Camp Oven Creek Paragneiss in the Arthur River Complex was likely polyphase with growth at ca. 94, 118, 132, and 147 Ma. 94 Ma age corresponds with the age seen in 18MSNZ510a and 15NZ51 and the garnet age of 118 is similar to those seen to the south in WFO. Zircon U- Pb ages in the Arthur River Complex show bimodal peaks at 357 and 134 Ma. Therefore, the 134 Ma Zircon peak could correspond to the garnet age of 132 Ma within uncertainty. 15NZ68, a garnet age ca. 20 km south of Milford Sound and the Arthur River Complex in the Darran Complex, is ca. 102 Ma (Yelverton, unpublished), which further defines garnet growth in Milford Sound ca. 100 Ma. Based on the 30 m.y. garnet age difference between samples 15NZ51 and 05NZ12, ~ 4 km apart, and the higher pressure estimates of 11-16 kbar for 05NZ12, I tentatively infer a fault separating the young (<100 Ma) medium pressure (9.5-11 kbar) metamorphism along the eastern Milford Transect and the considerably older (122 to 126 Ma) Pembroke Granulite metamorphism at higher pressure (>11 kbar). If there is not a fault between the Pembroke Granulite and Milford Gneiss, it is possible that shear zones are acting as major boundaries with multiple offsets and different timing of metamorphism.

Polyphase Metamorphism

The multiple metamorphic events and variable peak metamorphic conditions described for the Milford Sound rocks indicates the possibility that all or most of the rocks experienced polyphase metamorphism. Numerous authors have addressed this question for some of these

rocks (e.g., Klepeis et al. 1999; Clarke et al. 2000; Tulloch et al. 2009; Stowell et al. 2010); however, this is the first opportunity to use garnet ages across the region. Rocks from the Arthur River Complex preserve the best evidence for the complex metamorphic history and the earliest events inferred for these rocks may have extended spatially along the entire transect. Rocks in the Anita Shear Zone show complex garnet zoning that could reflect diffusion and re-equilibration of older garnets > 100 Ma. In this case, garnets include zoning from older metamorphic events. However, if my tentative interpretation is correct that growth zoning is preserved in garnet from the Milford Gneiss west of Pembroke, then all of the rocks west of the Pembroke Granulite, including the Anita Shear Zone may not have been affected by > 100 Ma older metamorphic events. Rocks in the Pembroke Granulite and Camp Oven Creek Paragneiss in the Arthur River Complex reflect considerably older metamorphic events than rocks to the west (ca. 122-126 Ma). Both the Pembroke and Arthur River Complex rocks to the east underwent high temperature metamorphism and were affected by diffusion and re-equilibration. All of these rocks likely experienced polyphase metamorphism that may have begun as early as ca. 134 Ma (e.g., Tulloch et al., 2010).

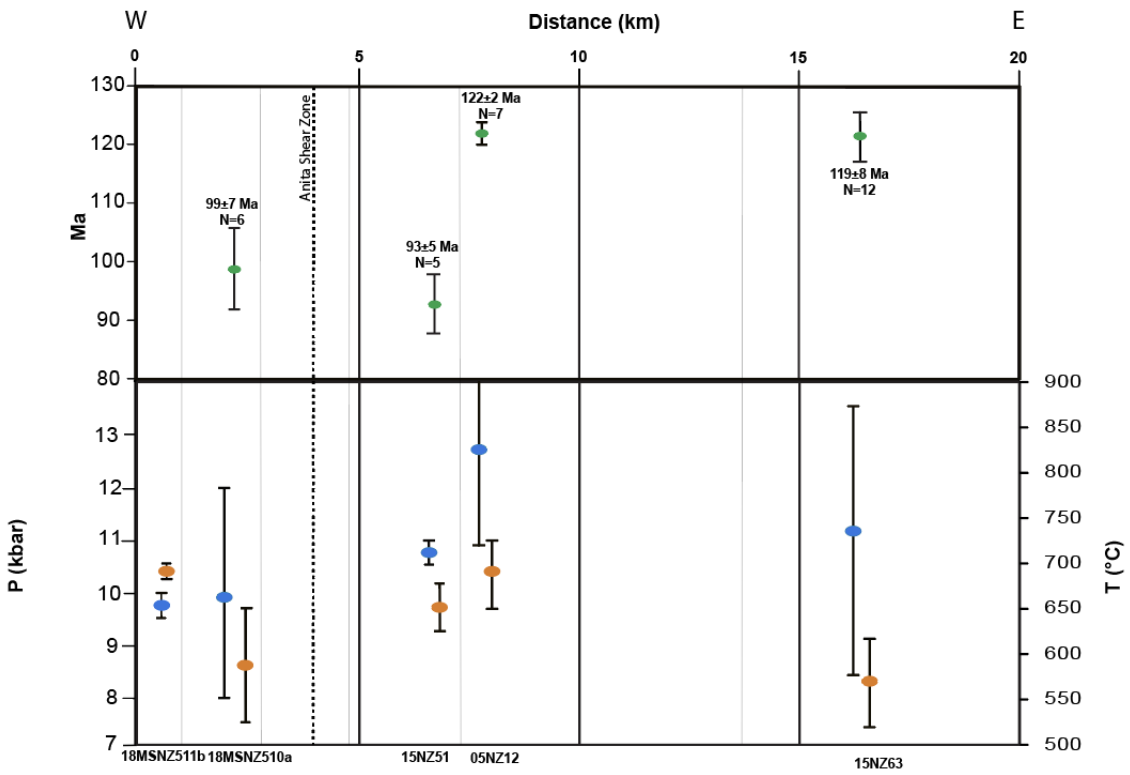

Milford Sound Transect

Figure 34. Milford transect cross section W-E with ages for all samples based on location on top (green) and corresponding P-T estimates (Blue- pressure and orange- temperature) on bottom. P-T estimates for 18MSNZ511b were from the overlap of the peak metamorphic assemblage field from the P-T MAD and rim thermobarometry and no age provided; 18MSNZ510a estimates are from the overlap of the peak metamorphic assemblage field from the P-T MAD and rim thermometry and the average garnet Sm- Nd age; 15NZ51 estimates are from the peak metamorphic assemblage field from the P-T MAD and garnet Sm-Nd age; 05NZ12 estimates are from the peak metamorphic assemblage field from the P-T MAD and the garnet Sm- Nd age; 15NZ63 are from the peak metamorphic assemblage field from the P-T MAD and the average garnet Sm-Nd age.

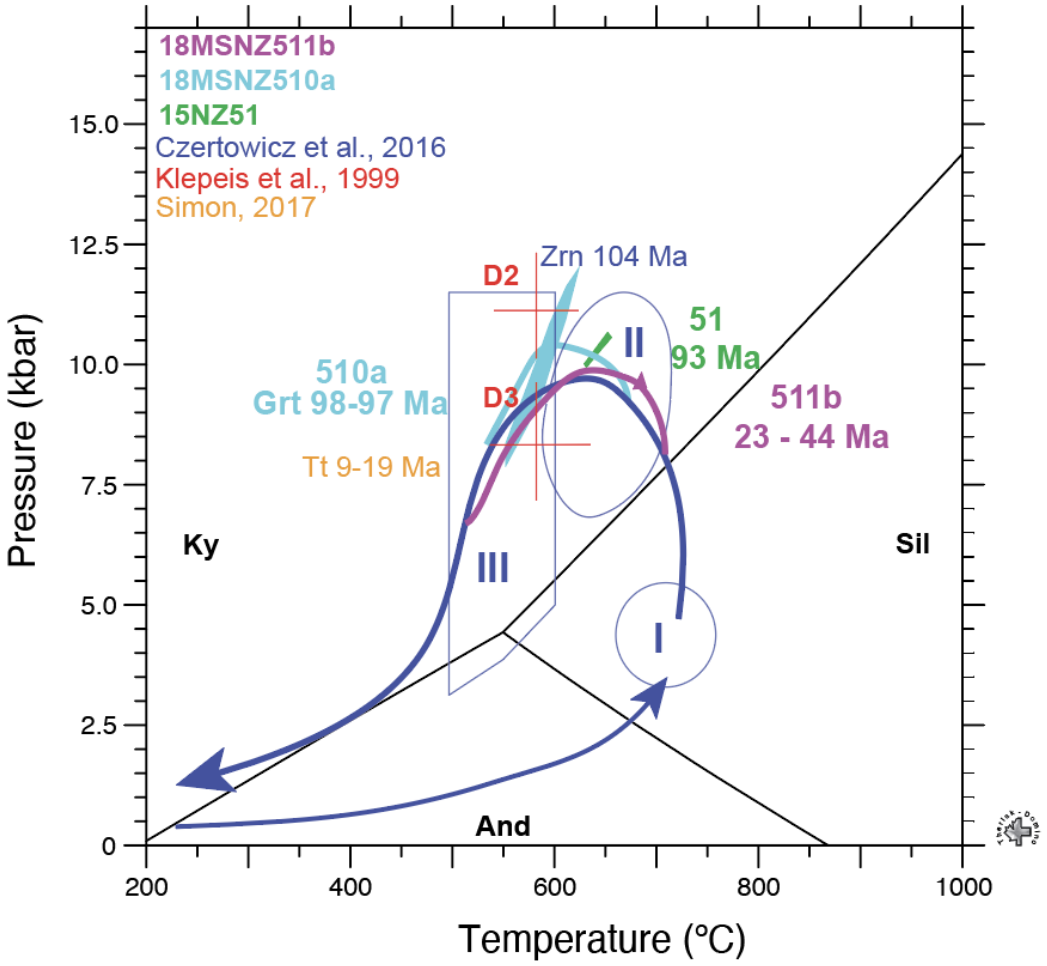

Figure 35. Comparison of P-T-t paths for different rocks in the Anita Shear Zone, Fiordland New Zealand. We include data (18MSNZ511b, 18MSNZ510a, and 15NZ51) and interpretations from Czertowicz et al. (2016); Klepeis et al. (1999); and Simon, (2017).

CONCLUSIONS

Milford Transect

Thermobarometry and P-T MAD estimates along the 20 km Milford Transect indicate variations in the peak pressures of metamorphism, with lower pressures on the west and higher pressures on the east. Samples from the Anita Shear Zone (18MSNZ511b; 18MSNZ510a) and Milford Gneiss (15NZ51), have mid pressure estimates of < 11 kbar. Samples from the Pembroke Granulite (05NZ12) and Camp Oven Creek Paragneiss in the Arthur River Complex (15NZ63) have significantly higher pressure estimates > 11 kbar. Therefore, there is a sharp break in pressure between the Milford Gneiss and Pembroke Granulite; however, there are no significant variations in temperature estimates.

The garnet Sm-Nd ages along the Milford Transect (Fig. 34), indicate significant breaks in the timing of metamorphism from west to east. On the west, ages are < 100 Ma with ca. 99 (18MSNZ510a) and 93 Ma (15NZ51) indicating garnet growth in the Anita Shear Zone occurred ca. 99 Ma and in adjacent rocks ca. 93 Ma. Further east, 122-126 Ma ages (e.g., 05NZ12) may be restricted to the Pembroke Granulite. At the east end of the Milford Transect, mixed ages (15NZ63) exemplified by 132 and 118 Ma garnet growth are restricted to the Arthur River Complex. These garnet ages provide evidence for the is a general decrease in age west to east along the Milford transect, but is a sharp break between the Milford Gneiss and Pembroke Granulite of > 100 Ma and < 100 Ma.

Based on the 30 m.y. garnet age difference between samples 15NZ51 and 05NZ12, which are ~ 4 km apart, and the higher pressure estimates of 11-16 kbar for 05NZ12, I speculate that

there may be a fault separating the young medium pressure metamorphic rocks along the eastern Milford Transect and the considerably older Pembroke Granulite rocks which experienced higher pressure. However, more detailed pressure estimates and additional geochronology are needed to confirm this hypothesis.

In conclusion, this study determined P-T-t paths in the Anita Shear Zone, that the 90-100 Ma thermal event extends east as far as sample 15NZ51, that the youngest garnet in the Pembroke Granulite is likely ca. 122 Ma and the young 109 Ma age in these rocks was erroneous, and metamorphism in the Arthur River Complex near Camp Oven Creek (15NZ63) was complex, and garnet retains evidence for multiple stages of growth.

REFERENCES

Ackerson, M.R., Watson, E.B., Tailby, N.D., Spear, F.S., 2017. Experimental investigation into the substitution mechanisms and solubility of Ti in garnet. American Mineralogist, v. 102, p. 158- 172

Allibone, A., Jongens, R., Turnbull, I.M., Milan, L.A., Daczko, N.R., DePaolo, M.C., Tulloch, A.J., 2009. Plutonic rocks of western Fiordland, New Zealand: field relations, geochemistry, correlation and nomenclature. New Zealand Journal of Geology and Geophysics v. 52, p. 379–415.

Anczkiewicz, R., Thirwall, M.F., 2003: Improving Precision of Sm-Nd Garnet Dating By H_2SO_4 Leaching: A Simple Solution to the Phosphate Inclusion Problem, Geological Society of London, v. 220, p. 83-91.

Barnes, P.M., Sutherland, R., Delteil, J., 2005: Strike- slip structure and sedimentary basins of the southern Alpine Fault, Fiordland, New Zealand, GSA Bulletin, v. 117 (3-4), p. 411-435

Baxter, E.F., and Scherer, E.E., 2013: Garnet Geochronology: Timekeeper of Tectonometamorphic Processes: ELEMENTS, v. 9, p. 433-438.

Blattner, P., 1991,"The North Fiordland transcurrent convergence."*New Zealand Journal of Geology and Geophysics* v. 34, p. 533-542.

Bradshaw, J.Y., 1989, Origin and metamorphic history of an early Cretaceous polybaric granulite terrain, Fiordland, southwest New Zealand: Contributions to Mineralogy and Petrology, v. 103, p. 346-360.

Brown, E.H., 1996, High-pressure metamorphism caused by magma loading in Fiordland, New Zealand: Journal of Metamorphic Geology, v. 14, p. 441-452.

Claypool, A.L., Klepeis, K. A., Dockrill, B., Clarke, G. L., Zwingmann, H., Tulloch, A., 2002, Structure and kinematics of oblique continental convergence in northern Fiordland, New Zealand, Tectonophysics, v. 359, p. 329-358.

Czertowicz, T. A., Scott, J. M., Waight, T. E.,Palin, J.M., Van der Meer, Q. H. A., Le Roux, P., Münker, S. Piazolo, C., 2016: The Anita Peridotite, New Zealand: Ultra-depletion and Subtle Enrichment in Sub-arc Mantle, *Journal of Petrology*, v. 57, no. 4, p. 717–750

Daczko, N.R., Clarke, G.L., & Klepeis, K.A., 2001, Transformation of two-pyroxene hornblende granulite to garnet granulite involving simultaneous melting and fracturing of the lower crust, Fiordland, New Zealand: Journal of Metamorphic Geology, v. 19, p. 549-562.

de Capitani C. and Petrakakis K., 2010: The computation of equilibrium assemblage diagrams with Theriak/Domino software: American Mineralogist v. 95 p. 1006-1016.

Diener, J.F.A., and Powell, R., 2012: Revised Activity- Composition Models for Clinopyroxene and Amphibole, Journal of Metamorphic Petrology, v. 30, p. 131-142.

Ferry, J.M., and Spear, F.S., 1978: Experimental Calibration of the Partitioning of Fe and Mg Between Biotite and Garnet. *Contributions to Mineralogy and Petrology*,v. 66, p.113-117.

Gaina C, Muller D.R., Royer J.Y., Stock J., Hardebeck J., Symonds P., 1998: The Tectonic History of the Tasman Sea - a Puzzle With 13 Pieces. *Journal of Geophysical Research-Solid Earth* v.103, p. 12413-33.

Ghent, E.D. and Stout, M.Z. 1981;Metamorphism at the base of the Samail ophiolite, southeastern Oman Mountains. Journal of Geophysical Research v.86, p. 0148-0227.

Gibson, G.M. & Ireland, T.R. 1995, Granulite formation during continental extension in Fiordland: Nature, v. 375, p. 479-482.

Hill, E.J., 1995a: A deep crustal shear zone in western Fiordland, New Zealand, American Geophysical Union, Tectonics v. 14, no. 5, p. 1172- 1181.

Hill, E.J., 1995b: The Anita Shear Zone: A major, middle Cretaceous tectonic boundary in northwestern Fiordland, New Zealand Journal of Geology and Geophysics, v. 38:1, p. 93-103.

Hodges, K.V., Crowley, P.D., 1985; Error estimation and empirical geothermobarometry for pelitic systems. American Mineralogist, v.70 (7-8), p. 702–709.

Holland, T. J. B. and Powell, R. 1998, An internally consistent thermodynamic data set for phases of petrological interest: Journal of Metamorphic Geology, v. 16, p.309-343.

Holland, T. J. B. and Powell, R. 2003: Activity- Composition Relations For Phases in Petrological Calculations: An Asymmetric Multicomponent Formulation, *Contributions to Mineral Petrology*, v. 145, p. 492-501.

Hollis, J.A., Clarke, G.L., Klepeis, K.A., Daczko, N.R., and Ireland, T.R., 2004, The regional significance of Cretaceous magmatism and metamorphism in Fiordland, New Zealand, from U Pb zircon geochronology: Journal of Metamorphic Geology, v. 22, p. 607-627.

Kimbrough, D.L., Tulloch, A.J., Coombs, D.S., Landis, C.A., Johnston, M.R., Mattinson, J.M., 1994:Uranium-lead zircon ages from the Median Tectonic Zone, New Zealand, New Zealand Journal of Geology and Geophysics, v. 37:4, p. 393-419.

Klepeis, K.A., Clarke, G.L., and Rushmer, T., 2003, Magma transport and coupling between deformation and magmatism in the continental lithosphere: GSA Today, v. 13: 1, p. 4-11.

Klepeis, K. A., Daczko, N. R., Clarke, G. L., 1999: Kinematic vorticity and tectonic significance of superposed mylonites in a major lower crustal shear zone, northern Fiordland, New Zealand, Journal of Structural Geology, v. 21, p. 1385-1405.

Klepeis, K. A., Schwartz, J. J., Stowell, H., Tulloch, A., 2016, Gneiss domes, vertical and horizontal mass transfer, and initiation of extension in the hot lower-crustal root of a continental arc, Fiordland, New Zealand, GSA Publications.

Klepeis, K.A., Webb, L.E., Blatchford, H.J., Jongens, R., Turnbull, R.E., Schwartz, J.J., 2019: The Age and Origin of Miocene- Pliocene Fault Reactivations in the Upper Plate of an Incipient Subduction Zone, Puysegur Margin, New Zealand, AGU, Tectonics, v. 38, p. 3237-3260

Kohn, M.J., and Spear, F., 2000, Retrograde net transfer reaction insurance for pressure temperature estimates: Geology Boulder, v. 28, Issue 12, p. 1127-1130.

Li., C., Li, X., Li, Q., Guo, J., Li, X., Yang, Y., 2012: Rapid and precise determination of Sr and Nd isotopic ratios in geological samples from the same filament loading by thermal ionization mass spectrometry employing a single-step separation scheme, Analytica Chimica Acta., v. 727, p. 54- 60.

Ludwig, K.R., 2008, A geochronological toolkit for Microsoft Excel: Berkeley Geochronology Center Special Publication v. 4, p. 1-77.

Mortimer, N., 2008: "Zealandia." ASEG Extended Abstracts 2006.1: 1-4.

Mortimer, N., Campbell, H.J., Tulloch, A.J., Kink, P.R., Stagpoole, V.M., Wood, R.A., Rattenbury, M.S., Sutherland, S., Adams, J.A., Seton, M., 2017, Zealandia: Earth's Hidden Continent, GSA Today, v. 27.

Mortimer, N., Tulloch, A.J., Spark, R.N, Walker, N.W., Ladley, E., Allibone, A., and Kimbrough, D.L., 1999, Overview of the Median Batholith New Zealand: a new interpretation of the geology of the Median Tectonic Zone: Journal of African Earth Science, v. 29, p. 257-268.

Norris, R.J., and Toy, V.G., 2014: Continental transforms: A view from the Alpine Fault, Journal of Structural Geology, v. 64, p.3-31,

Kretz, R. (1983) Symbole for Rock Forming Minerals. American Mineralogist, v. 68, p. 277-279.

Raczek, I., Jochum, K.P., Hofmann, A.W., 2003: Neodymium and Strontium Isotope Data for USGS Reference Materials BCR-1, BCR-2, BHVO-1, BHVO-2, AGV-1, AGV-2, GSP-1, GSP-2 and Eight MPI-DING Reference Glasses. Geostand. Newsl. v. 27 p. 173.

Ravna, E.K. (2000) Distribution of Fe2+ and Mg between coexisting garnet and hornblende in synthetic and natural systems: an empirical calibration of the garnet-hornblende Fe-Mg geothermometer. Lithos, v.53, no. 3–4, p.265–277.

Schwartz, J.J., Klepeis, K., Sadorski, J.F., Stowell, H.H., Tulloch, A., and Coble, M., 2017, The tempo of continental arc construction in the Mesozoic Median Batholith, Fiordland, New Zealand: Lithosphere, v. 8, p. 116-140.

Shaw, D.M., 1958: Geochemistry Of Pelitic Rocks. Part III: Major Elements and General Geochemistry. GSA Bulletin, v. 67 (7), p. 919–934.

Simon, I. J., 2017: Direct Dating of Exhumational Fabrics in the Anita Shear Zone, Fiordland, New Zealand, Undergraduate Senior Thesis, California State University, Northridge

Stowell, H.H., Odom Parker, K., Gatewood, M.P., Tulloch, A., Koenig, A., 2014: Temporal links between pluton emplacement, garnet granulite metamorphism, partial melting, and extensional collapse in the lower crust of a Cretaceous magmatic arc, Fiordland New Zealand, *Journal of Metamorphic Geology*, v. 32, p. 151-175.

Stowell, H.H., Schwartz, J., Klepeis, K., Hout, C., Tulloch, A., Koenig, A., 2017: Sm-Nd garnet ages for granulite and eclogite in the Breaksea Orthogneiss and widespread granulite facies metamorphism of the lower crust, Fiordland magmatic arc, *Lithosphere*. v. 9; no 6; p. 953- 975.

Stowell, H.H., Taylor, D.L., Tinkham, D.K., Goldberg, S.A. and Ouderkirk, K.A., 2001, Contact metamorphic P-T-t Paths from Sm-Nd Garnet Ages, Phase Equilibria Modeling, and Thermobarometry: Garnet Ledge, Southeastern Alaska: Journal of Metamorphic Geology, v. 19, p. 645-660.

Stowell, H.H., Tulloch, A., Zuluaga, C.A., Koenig, A., 2010: Timing and duration of garnet granulite metamorphism in magmatic arc crust, Fiordland, New Zealand: *Chemical Geology*, v. 273, p. 91-110.

Sutherland, R., 1999: Cenozoic bending of New Zealand basement terranes and Alpine Fault displacement: A brief review, New Zealand Journal of Geology and Geophysics, v. 42:2, p. 295-301

Tanaka, T., Togashi, S., Kamioka, H., Amakawa, H., Kagami, H., Hamamoto, T., Yuhara, M.,Orihashi, Y., Yoneda, S., Shimizu, H., Kunimaru, T., Takahashi, K., Yanagi, T., Nakano, T., Fujimaki, H., Shinjo, R., Asahara, Y., Tanimizu, M., Dragusanu, C., 2000.: JNdi-1: a neodymium isotopic reference in consistency with LaJolla neodymium. Chem. Geol. v. 168, p. 279–281.

Tinkham, D.K., Zuluaga, C.A., Stowell. H.H., 2001: Metapelite phase equilibria modeling in MnNCKFMASH: The effect of variable Al_2O_3 and MgO/(MgO+FeO) on mineral stability, *Geologic Materials Research,* v 3., n.1, p. 2.

Tulloch, A.J., Ramezani, J., Mortimer, N., Mortensen, J., van den Bogaard, P., and Maas, R., 2009, Cretaceous felsic volcanism in New Zealand and Lord Howe Rise (Zealandia) as a precursor to final Gondwana breakup, in Ring, U., and Wernicke, B., eds., Extending a Continent: Architecture, Rheology and Heat Budget: Geological Society of London Special Publication v. 321, p. 89–118.

Tulloch, A.J., Ireland, T.R., Kimbrough, D., Griffin, W.L., Ramezani, J., 2010, Autochthonous inheritance of zircon through Cretaceous partial melting of Carboniferous plutons: the Arthur River Complex, Fiordland, New Zealand, Contrib Mineral Petrol

Turnbull, I.M., Allibone, A.H., Jongens, R., and (compilers). 2010, GNS Science, Lower Hutt, New Zealand, Institute of Geological and Nuclear Sciences, geological map 17, scale 1:250 000, 1 sheet.

White, R.W., Powell, R. & Holland T.J.B., 2007. Progress relating to calculation of partial melting equilibria for metapelites. Journal of Metamorphic Geology, 25, 511–527.

Wood, B.L., 1972. Metamorphosed ultramafites and associated formations near Milford Sound, New Zealand. New Zealand Journal of Geology and Geophysics v. 15, p. 88-127.

APPENDIX A: Complete Mineral Compositions: WDS points

18MSNZ511b Line Numbers	SiO2	Al2O3	FeO	MnO	TiO2	Cr2O3	CaO	MgO	Na2O	K2O	NOTES	Totals
Plagioclase												
943	59.193153	26.519974	0.099638	0.022893	0.016589	1.669739	6.944274	0	7.141834	0.051226	Start LS1	101.65932
944	59.868042	25.564949	0.091265	0.009228	0.004322	0.09342	6.24419	0	7.472862	0.090487		99.438765
952	61.070965	24.860727	0.07256	0	0.008027	0	5.315094	0	7.901528	0.118271		99.347172
953	61.363922	24.916878	0.033353	0	0	0	5.478033	0.007608	7.853866	0.094076		99.747736
954	61.764877	25.025347	0	0	0.000618	0	5.566622	0.000366	8.136296	0.092121		100.586247
955	61.532574	25.323706	0.098003	0	0	2.069655	5.694342	0	8.01209	0.080962		102.811332
956	61.142059	25.355217	0.073106	0.010829	0.007349	0	5.98263	0	7.710359	0.102332		100.383881
957	58.767658	25.817768	0.10404	0	0	0	6.693587	0.007835	6.629778	0.051953	End LS1	98.072619
958	58.791355	26.610794	0.179238	0.012588	0	0	7.248387	0	6.996667	0.039222		99.878251
959	60.533619	24.718687	0.035852	0.003148	0	0	5.121501	0.007291	7.842149	0.093843		98.35609
968	60.277401	25.097601	0.045858	0	0	0	4.98484	0.008696	8.271354	0.142865	Start LS2	98.828615
969	60.45174	24.439287	0.019591	0	0.007067	1.695154	4.893401	0	8.276175	0.142761		99.925176
970	60.752853	24.468847	0.04046	0.007209	0	0	5.110529	0	8.179728	0.121587		98.681213
971	60.663807	24.872801	0.0743	0.020004	0	0	5.204433	0	7.924869	0.142236		98.90245
972	61.229309	25.263515	0	0.005621	0	0.862786	5.482647	0	7.943455	0.116616		100.903949
973	60.813465	24.930502	0	0	0	0	5.647717	0.002761	7.899449	0.104488	End LS2	99.398382
Biotite												
976	38.692108	20.381161	10.429696	0	1.055187	0	0	15.421902	0.313218	8.786141		95.079413
977	38.93401	21.000265	10.229637	0.033016	1.034368	0.523529	0	15.615856	0.334674	8.810081		96.515436
978	38.447945	20.800142	10.132603	0.014418	1.198974	0	0	15.6417	0.311938	8.775599		95.323319
979	38.473042	20.594616	10.423223	0.044416	1.123982	0.052184	0	15.336969	0.343649	8.838584		95.230665
981	38.721252	20.424276	10.47558	0.006194	1.116972	0	0.021419	16.118406	0.37797	8.837548		96.099617
982	37.650528	20.63155	11.805107	0.041709	1.143147	0	0.057552	14.289177	0.334044	8.502372		94.455186
984	36.50375	19.580046	11.499015	0.024938	1.190804	0.749415	0.061233	14.879016	0.363687	8.452622		93.304526
985	36.98336	20.098217	14.333081	0.022657	1.179289	1.124931	0.009498	12.931133	0.316431	8.747972		95.746569
986	37.285179	19.906992	14.283281	0.038025	1.305132	0	0.014108	13.418305	0.247617	8.866996		95.365635
987	37.560452	19.67149	13.774889	0.013874	1.351689	0	0.04492	13.295633	0.299063	8.412515		94.424525
995	36.483036	19.551422	14.578799	0.03122	1.394221	0	0	13.178657	0.187948	8.984393		94.389696
996	37.274876	20.12361	13.367893	0.049119	1.336908	0	0	12.986176	0.255913	8.641706		94.036201
997	37.189114	19.903793	14.137009	0.012554	1.328247	0	0.011525	13.394167	0.223914	8.93455		95.134873
1001	37.604797	19.822289	13.8049	0.00705	1.282824	0	0	13.475332	0.279377	8.998217		95.274786
1002	37.41843	20.084929	13.74393	0	1.274967	0	0	13.424611	0.195879	8.990869		95.133615
1003	37.122177	20.041843	14.047554	0.039665	1.188851	0	0.001034	13.323517	0.211564	8.843085		94.81929
Muscovite												
988	46.853794	35.088741	1.222	0	0.685974	0	0.022059	1.755235	0.831106	9.477227		95.936136
989	46.983124	35.728493	1.233986	0	0.774269	0	0.015948	1.766223	0.946989	9.201058		96.65009
990	47.313755	34.653564	1.349673	0	0.805405	0	0	1.876918	0.888248	9.461694		96.349257
991	47.513321	35.068481	1.240568	0	0.846086	0	0	1.736302	0.913305	9.598581		96.916644
992	49.001163	38.324879	1.255873	0.00961	0.58354	0	0.026257	1.548896	0.897068	8.293387		99.940673
993	46.261169	35.81237	1.153125	0	0.735348	0	0.006491	1.509257	1.057259	9.178712		95.713731
994	46.337948	36.205414	1.122403	0	0.690875	0	0	1.453006	1.013291	9.387397		96.210334
999	45.868961	34.803963	1.296126	0	0.771384	0	0.04469	1.901389	0.840306	9.113379		94.640198
1000	46.068455	34.649513	1.283101	0	0.800345	0	0	1.867136	0.850781	9.501356		95.020687
1004	42.984596	36.293259	1.350944	0	0.687449	0	0	1.203447	1.010761	8.987464		92.51792
1005	45.830212	37.066555	1.168449	0.006268	0.647545	0	0	1.219883	1.055451	9.395696		96.390059
1006	47.70842	38.411232	1.129415	0.001574	0.670383	0	0.015279	1.084894	1.053977	9.073302		99.148476
Garnet												
1007	37.325275	21.83201	27.632298	0.453488	0.054424	0	7.058566	4.660362	0	0		99.016423
1008	37.174541	21.530317	27.251293	0.468202	0.030718	0.154415	7.098592	4.89809	0.072595	0		98.678763
1009	37.694592	21.866682	26.889479	0.364712	0.059355	0	7.040673	5.132633	0	0		99.048126
1010	37.828579	21.873138	26.803747	0.273074	0.016717	0	7.184154	5.285089	0	0		99.264498
1011	37.841785	21.657242	27.174156	0.330778	0.045371	0	6.893298	5.285345	0.011747	0		99.239722
1012	38.186127	21.807089	27.865534	0.402777	0.023964	0	6.274292	5.331859	0	0		99.891642
1013	37.595879	21.661764	28.631878	0.44667	0	0	6.743278	4.576268	0	0		99.655737
1014	37.199577	21.460291	28.818245	0.859079	0.035065	0	6.921513	3.854274	0	0		99.148044
1015	35.544964	20.920525	27.42128	0.33209	5.570113	1.75362	5.877561	4.680239	0	0		102.100392
1017	38.617447	23.940691	28.934788	0.462682	0.01284	0	3.49996	5.420794	0	0		100.889202
1018	37.523258	21.493633	30.343798	0.46477	0.02749	0	3.038476	5.906294	0.033651	0		98.83137
1019	38.124813	21.966997	28.242729	0.455025	0.008172	0.564295	5.450571	5.658689	0	0		100.471291
1020	36.867706	21.532391	28.866943	0.374965	0	0.252992	4.979376	5.635691	0	0		98.510064
1021	38.252575	21.8473	27.423567	0.360408	0.026702	0.42698	6.496986	5.214156	0.028886	0		100.07756
1022	37.854347	21.575451	27.862387	0.690474	0.022383	0	6.219177	4.173013	0.017509	0		98.414741
1024	38.295685	21.819801	27.597374	0.269545	0.151723	0.528268	6.248892	5.279108	0.0198	0		100.210196

18MSNZ510a

Line Numbers	SiO2	Al2O3	FeO	MnO	TiO2	Cr2O3	CaO	MgO	Na2O	K2O	NOTES	Totals
Plagioclase												
2698	61.703384	24.393116	0.084608	0	0	0.616416	4.842161	0	8.967662	0.048257	100.655602	
2699	60.513706	25.031212	0.068732	0.006598	0	0	5.640201	0	8.601622	0.064918	99.927002	
2701	59.980598	24.748436	0.007079	0	0.005584	0	5.595396	0.010725	8.484498	0.046395	98.878716	
2702	59.263588	25.647165	0.008516	0	0	0	6.433613	0	7.873335	0.033357	99.259567	
2703	60.341606	24.968359	0.005482	0	0	0	5.482522	0	8.493455	0.057633	99.349052	
2704	60.737637	24.658258	0.228946	0.014338	0.02593	0	5.39222	0	8.465009	0.05865	99.580994	
2705	60.626926	24.893419	0.193406	0	0	0	5.506861	0	8.561445	0.099006	99.881073	
2706	60.373943	24.544096	0.157988	0.012524	0.002884	0	5.506192	0	8.524283	0.07826	99.200188	
Hornblende												
2678	43.772835	13.218495	14.588885	0.046255	1.092236	0.185466	10.869778	11.405538	1.783876	1.000999	97.964371	
2679	43.605862	13.455531	14.361383	0.045003	1.034458	0.176367	10.80697	11.220099	1.745322	1.054852	97.505959	
2680	43.715458	13.607465	14.420059	0.052391	1.045842	0.767631	10.780297	11.264356	1.754389	1.07043	98.478317	
2681	43.098194	13.253793	14.622099	0.055819	1.113158	0	10.830168	11.354176	1.716375	1.109171	97.152954	
2682	42.840828	13.426211	14.755451	0.052826	1.261984	0	10.755582	11.102092	1.750019	1.06738	97.012383	
2683	43.250271	13.682815	14.623765	0.085004	1.125886	1.915841	10.875612	11.24058	1.838986	1.046571	99.685333	
2684	44.148228	12.647906	14.464324	0.051529	1.0999	0	10.701509	11.816481	1.915537	1.014206	97.859627	
2685	44.288094	12.569901	13.925099	0.019532	1.150918	0.176925	10.667051	11.701759	1.897179	0.963208	97.359665	
2686	44.393559	12.598372	14.192181	0.034317	1.111315	0	10.787026	11.835967	1.880799	0.961435	97.794968	
2690	41.479431	15.553017	16.10878	0.065564	0.950252	1.187486	10.861199	9.881282	1.750303	0.829246	98.66655	
2691	41.529087	15.685929	15.887241	0.081091	1.057458	0.687439	10.724626	9.907193	1.8292	1.021934	98.311188	
2692	41.985439	15.461584	15.494184	0.079286	0.985637	0	10.947551	9.949308	1.779318	0.852804	97.53511	
2693	42.591583	15.438125	14.943024	0.088626	0.964769	0	10.887273	10.039328	1.467997	0.829233	97.249954	
2694	42.470661	15.638705	15.082592	0.099369	0.981864	0	11.152783	9.904747	1.518386	0.815299	97.664413	
2697	42.600094	15.786458	14.576446	0.01188	0.906987	0	11.030279	10.105886	1.634645	0.933831	97.58651	
Garnet												
2707	38.502853	21.818319	26.954481	1.01309	0.035181	0	6.708572	5.662996	0	0	100.695488	
2708	38.340462	21.602961	27.018938	0.87938	0.032058	0	6.557374	5.712397	0	0	100.143555	
2709	38.047478	21.578785	27.176529	1.011009	0.027411	0	6.552081	5.437071	0	0	99.830368	
2710	38.051632	21.700447	26.844007	0.867546	0.045514	0.849714	6.583235	5.69502	0	0	100.637115	
2711	37.936485	21.483212	26.724981	0.953628	0.00855	1.979254	6.817762	5.61203	0	0	101.515907	
2548	37.78183	21.688238	26.410849	1.106162	0.052912	0	6.73855	5.384634	0	0	99.163177	
2549	37.252163	23.685625	25.380693	1.007494	0.082453	0	6.214579	6.098041	0	0	99.721039	
2550	37.879028	21.756954	26.529541	1.055627	0.051162	0	6.506556	5.544008	0	0	99.322876	
2551	38.225658	21.743231	26.81612	0.882898	0.028759	0	6.587369	5.675183	0	0	99.959213	
2552	38.161694	21.659264	26.577398	0.772765	0.044796	0	6.490671	5.840293	0	0	99.546875	
2554	38.362309	21.792686	26.166101	0.670614	0.099488	0	6.610456	6.042422	0	0	99.74408	
2555	37.672081	21.481358	25.84672	0.782024	0.031389	0	6.560117	6.155841	0	0	98.529526	
2556	38.232563	21.752832	26.092995	0.754022	0.083411	0	6.547641	6.196187	0	0	99.659653	
2557	38.177593	21.624958	26.046265	0.844945	0.0695	0	6.595778	6.094241	0	0	99.453278	
2558	38.246185	21.790009	26.061569	0.780341	0.064176	0	6.575283	6.229559	0	0	99.747116	
2559	38.118401	21.788885	25.668283	0.779633	0.040279	0.299735	6.440876	6.039979	0	0	99.176071	
2563	38.435863	21.809422	25.839186	0.873	0.059606	0	6.606543	6.167603	0	0	99.791229	
2564	38.11734	21.653299	25.875643	0.850542	0.053237	0	6.515275	6.05537	0	0	99.120689	
2565	37.996765	21.725719	25.716581	0.827502	0.110343	0	6.521806	6.169196	0	0	99.067909	
2566	38.056171	21.805452	25.734091	0.849376	0.064137	2.187744	6.533782	6.070613	0	0	101.301376	
2567	38.157337	21.649416	25.644341	0.933255	0.032901	0	6.614188	6.052466	0	0	99.083908	
2568	38.121948	21.802273	26.039602	0.883994	0.105048	0	6.568352	6.058893	0	0	99.580109	
2569	38.377766	21.671022	25.918442	0.866519	0.049363	0	6.522586	5.988048	0	0	99.393738	
2570	38.24197	21.699675	26.1784	0.879973	0.111816	0	6.543161	6.055432	0	0	99.710434	
2571	38.278564	21.764673	25.530952	0.835225	0.108492	0	6.49655	6.000992	0	0	99.015442	
2572	38.243568	21.668173	25.795385	0.974094	0.112733	0	6.522522	6.004972	0	0	99.321442	
2573	38.141472	21.693699	25.882973	0.936799	0.067293	0	6.621908	6.032915	0	0	99.177055	
2574	38.235645	21.754787	26.286234	0.893341	0.069651	0	6.504045	5.928519	0	0	99.672211	
2575	38.147507	21.656452	26.263487	0.900494	0.097175	0.438513	6.518247	5.939645	0	0	99.961525	
2576	37.887821	21.522718	26.247866	0.932157	0.08707	0	6.504473	5.713789	0	0	98.895889	
2662	38.136925	21.682732	25.791454	0.756102	0.070316	0	6.564263	5.961228	0	0	98.96302	
2663	38.371071	21.757856	25.986065	0.859439	0.061834	0	6.537123	6.136169	0	0	99.709557	
2664	38.122242	21.665079	25.03838	0.864513	0.069204	0.74799	6.486561	6.031056	0	0	99.025032	
2665	38.111404	21.742334	25.513512	0.793034	0.045204	2.117486	6.65692	6.186977	0	0	101.16687	
2666	38.16124	21.698063	25.784931	0.781698	0.057834	0.031755	6.478855	6.163951	0	0	99.158318	
2667	38.182201	21.633024	26.134722	0.800934	0.064118	0.608166	6.539824	6.213857	0	0	100.17642	
2668	37.885914	21.807531	25.864482	0.780595	0.039565	0	6.524131	6.134941	0	0	99.039154	
2669	38.060455	21.810226	25.885527	0.803665	0.074375	0	6.527346	6.046413	0	0	99.208008	
2670	38.070164	21.621061	25.764816	0.716214	0.07399	0	6.609881	5.957395	0	0	98.813522	
2671	35.666836	20.179174	24.107372	0.68638	0.090519	0	6.398902	5.399552	0	0	92.528732	
2672	37.756882	21.744009	25.827724	0.724476	0.047081	0	6.5114	5.572083	0	0	98.183655	
2673	38.073463	21.703735	26.4688	0.837038	0.078023	1.971177	6.489389	5.539938	0	0	101.161568	
2674	38.033268	21.479801	26.170401	0.882173	0.051832	0	6.554898	5.597133	0	0	98.769501	
2675	37.886513	21.660181	26.248718	0.98618	0.086461	0	6.492108	5.396605	0	0	98.756775	
2676	37.785404	21.448238	27.213511	1.228247	0.059558	0	6.564637	4.525836	0	0	98.825424	
2577	38.09853	21.681749	26.205093	0.942774	0.046846	0	6.501648	5.831176	0	0	99.307816	
2579	38.150242	21.579124	26.205593	1.097635	0.070462	0	6.57834	5.698476	0	0	99.179878	
2580	37.926487	21.852629	26.726091	0.928234	0.111082	0	6.593194	5.757899	0	0	99.895615	
2581	38.247711	21.585875	26.382124	0.951243	0.053915	0	6.511788	5.817935	0	0	99.550598	
2582	38.01059	21.544195	26.732052	0.932631	0.040252	0	6.649227	5.686863	0	0	99.59581	
2583	38.106007	21.4837	26.280918	0.968449	0.082226	0	6.600658	5.776369	0	0	99.298325	
2584	37.866657	21.581638	26.658691	0.911672	0.061718	0	6.563458	5.68117	0	0	99.324997	
2585	37.832851	21.555744	26.407309	0.872913	0.047497	0	6.719676	5.598484	0	0	99.034485	
2586	38.06818	21.543407	26.106543	0.985204	0.034222	0	6.704331	5.593959	0	0	99.035851	
2587	37.799854	21.518845	26.244011	0.903583	0.031154	0	6.57674	5.633434	0	0	98.707626	
2588	37.850712	21.553282	26.686674	0.937833	0.027022	0.714303	6.588839	5.65492	0	0	100.01358	
2591	37.86174	21.35593	26.437754	0.834118	0.099827	0	6.507847	5.562265	0	0	98.659592	
2592	37.624302	21.342112	25.929972	0.832054	0.068798	0	6.543715	5.636176	0	0	97.977135	
2593	37.619137	21.551401	26.389091	0.939572	0.053594	0	6.541487	5.663057	0	0	98.757347	
2594	37.659603	21.491144	26.198067	0.84619	0.102403	0	6.610232	5.549469	0	0	98.457108	
2595	37.729603	21.475248	26.091864	0.954013	0.090738	0.170531	6.528228	5.563519	0	0	98.603729	
2596	37.671936	21.472969	26.181196	0.989767	0.094289	0	6.550892	5.559573	0	0	98.52063	
2597	37.248802	21.483671	26.064592	1.00185	0.034252	0	6.481322	5.484516	0	0	97.798996	
2598	37.065063	21.121246	25.699545	0.924831	0.09139	2.040932	6.541497	5.310491	0	0	98.794998	
2607	38.017292	21.60531	26.080694	0.969269	0.031792	0	6.611537	5.357653	0	0	98.673553	
2608	36.972305	22.383606	26.235147	1.027945	0.028558	0	6.366974	5.688344	0	0	98.702881	
2609	36.850689	21.579763	25.853802	0.870326	0.00901	0	6.455134	5.917075	0	0	97.535797	
2610	37.54385	21.386692	26.364162	1.004156	0.078843	0.013608	6.624694	5.548449	0	0	98.5646	
2611	37.928432	21.537897	26.676685	1.024876	0.063842	0	6.559894	5.467874	0	0	99.259506	
2612	38.344959	21.758865	26.578424	0.98296	0.043532	0	6.545959	5.319774	0	0	99.574478	
2613	38.149597	21.675604	26.944687	0.94408	0.004687	0.383256	6.606863	5.369703	0	0	100.078476	
2621	38.03302	21.538359	26.609062	0.956787	0.052654	0	6.769597	5.225139	0	0	99.184616	
2622	37.902599	21.411169	26.599613	1.032378	0.032676	0	6.6532	5.462627	0	0	99.094254	
2623	38.104458	21.542969	26.576956	0.879832	0.049963	0	6.640375	5.550898	0	0	99.345444	
2625	37.628854	21.649055	26.496014	0.964903	0.050961	1.631596	6.474897	5.621685	0	0	100.517776	
2626	38.132618	21.597925	26.544127	1.000464	0.019747	0	6.483305	5.539292	0	0	99.317482	
2627	37.89571	21.651363	26.43648	0.907429	0.032815	0	6.478975	5.655416	0	0	99.058197	
2628	37.802822	21.614519	26.459824	0.953581	0.076467	0	6.451345	5.636176	0	0	99.017746	
2629	37.889252	21.472822	26.048164	0.952157	0.065551	0.663024	6.479099	5.658	0	0	99.228058	
2630	37.933598	21.66267	26.220453	0.971907	0.066543	0	6.496029	5.725837	0	0	99.077034	
2631	37.925304	21.63245	26.668936	0.92661	0.033833	0	6.483922	5.66927	0	0	99.34034	
2632	38.075924	21.417978	26.09524	1.001637	0.062095	0	6.467763	5.63529	0	0	98.755951	
2633	37.951458	21.449541	26.294201	0.925483	0.06193	0	6.463784	5.597671	0	0	98.744064	
2634	37.723557	21.488035	25.890991	0.895616	0.094901	0	6.53633	5.622053	0	0	98.251488	
2635	38.054317	21.791065	26.667807	0.969264	0.066198	1.252793	6.513857	5.710269	0	0	101.025566	
2636	38.015442	21.578848	26.104208	1.0266	0.064639	2.988834	6.452363	5.715923	0	0	101.946861	
2637	38.012669	21.691084	26.38497	0.929183	0.07822	0	6.626433	5.729663	0	0	99.452225	
2638	37.829887	21.448313	25.916605	0.88875	0.105168	0	6.491775	5.709598	0	0	98.389534	
2639	37.803909	21.608015	26.307365	0.922298	0.0642	0	6.551599	5.684259	0	0	98.94165	
2640	38.096844	21.753706	26.286562	0.96084	0.090491	0	6.600891	5.684878	0	0	99.474197	
2641	37.928177	21.47016	26.536764	0.930845	0.110237	0	6.504747	5.675041	0	0	99.155975	
2642	38.060856	21.645803	26.472902	1.637888	0.349434	0	6.545805	5.772566	0	0	100.485252	
2643	37.866344	21.207325	26.522522	0.985101	0.098585	0	6.654662	5.820794	0	0	99.155334	
2644	38.009361	21.708164	26.476559	0.877899	0.06536	0	6.563534	5.78477	0	0	99.485641	
2645	37.720783	21.468729	25.80859	0.950896	0.058209	0	6.466738	5.733555	0	0	98.207504	
2646	37.974396	21.646877	26.172064	0.939607	0.062015	0	6.472638	5.80689	0	0	99.074478	
2647	38.153225	21.742188	25.971216	0.992815	0.054462	0	6.593609	5.720558	0	0	99.228065	
2649	37.798313	21.652817	26.312744	0.968306	0.08548	0.054413	6.51654	5.871084	0	0	99.259697	
2653	38.000229	21.655294	25.852058	0.83004	0.069594	0.829055	6.511438	5.920403	0	0	99.668114	
2656	38.223396	21.658854	25.726109	0.871237	0.074077	1.032741	6.502328	6.009047	0	0	100.097778	
2657	38.101097	21.653093	25.551279	0.869371	0.07841	0	6.556488	6.145893	0	0	98.955627	
2659	38.354111	21.689087	26.169134	0.870609	0.063111	0	6.542525	6.046704	0	0	99.735275	
2660	38.068119	21.58107	25.64012	0.830488	0.06119	0	6.637272	6.066955	0	0	98.885223	
2661	38.15543	21.673183	25.780359	0.780643	0.054376	0	6.508117	6.096748	0	0	99.048843	

05NZ12

Line numbers	SiO2	Al2O3	FeO	MgO	MnO	CaO	Total	SiO2	Al2O3	FeO	MgO	MnO	CaO	Total	Notes	
Garnet																
1	38.71	21.91	20.12	4.52	0.9801	13.68	99.92	38.74	21.93	20.14	4.53	0.9808	13.69	100	05NZ12A_grt_LS	Line Start
2	38.13	22.05	23.49	5.78	1.5487	8.96	99.96	38.15	22.06	23.5	5.78	1.5493	8.97	100	05NZ12A_grt_LS	
3	38.45	21.94	25.47	6.71	1.8303	6.06	100.46	38.27	21.84	25.35	6.68	1.8219	6.04	100	05NZ12A_grt_LS	
4	38.1	21.99	25.38	6.69	1.8331	5.96	99.97	38.11	22	25.39	6.7	1.8337	5.96	100	05NZ12A_grt_LS	
5	38.27	22.16	25.59	6.43	1.8216	6.22	100.49	38.08	22.05	25.46	6.4	1.8128	6.19	100	05NZ12A_grt_LS	
6	38.41	22.13	25.31	6.61	1.992	6.07	100.52	38.21	22.02	25.18	6.58	1.9817	6.03	100	05NZ12A_grt_LS	
7	38.33	21.9	25.24	6.46	1.9935	5.95	99.88	38.38	21.92	25.27	6.47	1.9958	5.96	100	05NZ12A_grt_LS	
8	37.79	22.13	25.2	6.5	2.0236	6.07	99.72	37.89	22.2	25.27	6.52	2.0292	6.09	100	05NZ12A_grt_LS	
9	38.06	21.93	25.4	6.51	2.0375	6.05	99.99	38.06	21.93	25.4	6.51	2.0378	6.06	100	05NZ12A_grt_LS	
10	38	21.95	25.17	6.56	2.0342	6.27	99.98	38	21.95	25.17	6.56	2.0345	6.27	100	05NZ12A_grt_LS	
11	38.21	21.95	25.48	6.48	2.0283	6.18	100.33	38.09	21.88	25.39	6.46	2.0215	6.16	100	05NZ12A_grt_LS	
12	38.13	22.05	25.42	6.3	2.0326	6.25	100.19	38.06	22.01	25.38	6.29	2.0288	6.24	100	05NZ12A_grt_LS	
13	38.28	21.94	25.22	6.46	1.9299	6.23	100.06	38.26	21.93	25.21	6.45	1.9287	6.22	100	05NZ12A_grt_LS	
14	32.6	20	25.95	6.53	1.4563	4.33	90.87	35.87	22.01	28.55	7.19	1.6026	4.77	100	05NZ12A_grt_LS	
15	37.9	21.72	25.06	6.41	2.0221	6.24	99.37	38.15	21.86	25.22	6.45	2.035	6.28	100	05NZ12A_grt_LS	
16	37.76	21.96	25.08	6.35	2.0907	6.25	99.49	37.95	22.08	25.21	6.38	2.1015	6.28	100	05NZ12A_grt_LS	
17	37.95	21.86	25.44	6.43	2.185	6.18	100.05	37.93	21.85	25.43	6.43	2.184	6.18	100	05NZ12A_grt_LS	
18	38.03	21.59	25.24	6.32	2.1293	6.15	99.46	38.24	21.7	25.38	6.36	2.1408	6.18	100	05NZ12A_grt_LS	
19	30.34	14.01	14	5.14	1.3075	3.54	68.34	44.4	20.5	20.48	7.52	1.9132	5.18	100	05NZ12A_grt_LS	
20	38.13	21.83	25.14	6.42	2.0891	5.92	99.54	38.31	21.93	25.26	6.45	2.0988	5.94	100	05NZ12A_grt_LS	
21	38.13	21.59	25.19	6.41	2.0849	5.97	99.37	38.37	21.72	25.35	6.45	2.098	6.01	100	05NZ12A_grt_LS	
22	38.21	21.92	25.41	6.3	2.1591	6.18	100.18	38.14	21.88	25.36	6.29	2.1552	6.17	100	05NZ12A_grt_LS	
23	38.25	21.88	25.13	6.36	2.098	6.06	99.76	38.34	21.93	25.19	6.37	2.103	6.07	100	05NZ12A_grt_LS	
24	38.19	22.15	25.33	6.46	2.1737	6.05	100.35	38.06	22.07	25.24	6.43	2.1661	6.03	100	05NZ12A_grt_LS	
25	38.19	21.72	25.41	6.35	2.2507	6.34	100.26	38.09	21.66	25.35	6.33	2.2449	6.32	100	05NZ12A_grt_LS	
26	38.08	21.84	25.85	6.41	2.1104	6.11	100.41	37.92	21.75	25.75	6.39	2.1019	6.09	100	05NZ12A_grt_LS	
27	38.33	22.07	26.12	6.48	2.3553	6.09	101.45	37.79	21.75	25.75	6.39	2.3217	6.01	100	05NZ12A_grt_LS	
28	45.95	21.64	13.63	3.69	1.1776	3.65	89.74	51.2	24.11	15.19	4.11	1.3123	4.07	100	05NZ12A_grt_LS	
29	38.34	22.09	25.11	6.43	2.0491	6.16	100.17	38.27	22.05	25.06	6.41	2.0455	6.15	100	05NZ12A_grt_LS	
30	38.41	22.1	24.99	6.4	2.1237	6.15	100.18	38.34	22.06	24.95	6.39	2.12	6.14	100	05NZ12A_grt_LS	
31	38.08	21.65	25.33	6.33	2.0073	6.08	99.48	38.27	21.76	25.46	6.37	2.0178	6.12	100	05NZ12A_grt_LS	
32	38.07	21.9	25.37	6.4	2.1099	6.22	100.06	38.04	21.88	25.36	6.39	2.1087	6.21	100	05NZ12A_grt_LS	
33	38.44	21.92	25.28	6.35	2.1856	6.16	100.34	38.31	21.85	25.2	6.33	2.1782	6.13	100	05NZ12A_grt_LS	
34	38.08	21.76	25.1	6.47	2.0104	6.21	99.63	38.22	21.84	25.19	6.5	2.0178	6.23	100	05NZ12A_grt_LS	
35	38.31	21.79	25.3	6.33	2.0049	6.27	100.01	38.3	21.79	25.3	6.33	2.0047	6.27	100	05NZ12A_grt_LS	
36	38.42	22.02	25.49	6.44	2.1559	6.36	100.9	38.08	21.83	25.27	6.38	2.1368	6.31	100	05NZ12A_grt_LS	
37	38.25	21.89	25.03	6.49	2.0829	6.27	100.01	38.24	21.89	25.03	6.49	2.0826	6.27	100	05NZ12A_grt_LS	
38	38.04	22	25.15	6.37	2.0658	6.27	99.9	38.08	22.02	25.18	6.38	2.0678	6.27	100	05NZ12A_grt_LS	
39	37.99	21.84	25.39	6.3	2.1128	6.24	99.86	38.04	21.87	25.42	6.31	2.1157	6.24	100	05NZ12A_grt_LS	
40	37.91	21.67	25.54	6.29	2.053	6.32	99.77	37.99	21.72	25.6	6.31	2.0576	6.33	100	05NZ12A_grt_LS	
41	38.13	21.63	25.41	6.38	2.1571	6.4	100.12	38.09	21.61	25.38	6.38	2.1546	6.39	100	05NZ12A_grt_LS	
42	37.76	21.62	25.42	6.24	2.0714	6.22	99.34	38.01	21.77	25.59	6.28	2.085	6.26	100	05NZ12A_grt_LS	
43	38.29	21.61	25.53	6.42	2.1375	6.37	100.36	38.16	21.53	25.44	6.39	2.1299	6.35	100	05NZ12A_grt_LS	
44	37.97	21.77	25.37	6.24	2.1905	6.3	99.84	38.03	21.81	25.41	6.25	2.194	6.31	100	05NZ12A_grt_LS	
45	37.99	22.13	25.49	6.43	2.0311	6.34	100.42	37.83	22.04	25.38	6.4	2.0227	6.32	100	05NZ12A_grt_LS	
46	26.46	12.73	14.36	3.34	1.1783	4.13	62.19	42.54	20.47	23.09	5.37	1.8946	6.65	100	05NZ12A_grt_LS	
47	38.17	21.58	25.63	6.35	1.9921	6.25	99.97	38.18	21.59	25.64	6.35	1.9928	6.25	100	05NZ12A_grt_LS	
48	37.79	21.72	25.55	6.39	2.0345	6.16	99.64	37.93	21.8	25.64	6.41	2.0419	6.18	100	05NZ12A_grt_LS	
49	37.85	21.86	25.63	6.34	2.1308	6.21	100.02	37.84	21.85	25.63	6.34	2.1303	6.21	100	05NZ12A_grt_LS	
50	37.99	21.94	26.16	6.43	2.1298	6.2	100.84	37.67	21.76	25.94	6.38	2.112	6.15	100	05NZ12A_grt_LS	
51	38.09	22.01	26.01	6.39	2.0117	6.12	100.63	37.85	21.87	25.85	6.35	1.999	6.08	100	05NZ12A_grt_LS	
52	37.84	21.72	26.03	6.39	2.0687	6.12	100.17	37.78	21.69	25.98	6.38	2.0652	6.11	100	05NZ12A_grt_LS	
53	38.2	21.79	25.44	6.36	1.9672	6.15	99.91	38.24	21.81	25.47	6.37	1.969	6.15	100	05NZ12A_grt_LS	
54	37.99	21.88	25.78	6.35	1.9969	6.16	100.16	37.93	21.85	25.74	6.34	1.9938	6.15	100	05NZ12A_grt_LS	
55	37.85	21.96	25.62	6.42	2.0529	6.07	99.97	37.86	21.97	25.62	6.42	2.0534	6.07	100	05NZ12A_grt_LS	
56	37.74	21.85	25.73	6.44	2.1008	5.99	99.85	37.8	21.88	25.76	6.45	2.1039	6	100	05NZ12A_grt_LS	
57	37.93	21.95	26.22	6.49	2.0287	6.08	100.7	37.67	21.8	26.04	6.45	2.0147	6.04	100	05NZ12A_grt_LS	
58	38.02	21.83	25.86	6.51	2.0332	6.06	100.3	37.9	21.76	25.78	6.49	2.0271	6.04	100	05NZ12A_grt_LS	
59	38.01	22.18	25.87	6.5	1.9893	6.08	100.63	37.77	22.04	25.71	6.46	1.9768	6.04	100	05NZ12A_grt_LS	
60	38.07	21.96	26.26	6.66	2.0626	6.12	101.14	37.64	21.71	25.97	6.59	2.0395	6.05	100	05NZ12A_grt_LS	
61	36.32	21.32	21.56	5.92	1.6057	6.92	93.64	38.79	22.77	23.02	6.33	1.7148	7.39	100	05NZ12A_grt_LS	
62	37.69	22.36	21.26	4.48	1.5519	13.18	100.52	37.5	22.24	21.15	4.46	1.5439	13.11	100	05NZ12A_grt_LS	
63	38.03	22.31	22.25	4.7	1.5383	11.16	99.99	38.03	22.31	22.25	4.7	1.5385	11.17	100	05NZ12A_grt_LS	
64	61.49	23.08	0.0188	0	0.0166	4.39	89	69.09	25.93	0.0211	0	0.0187	4.94	100	05NZ12A_grt_LS	

15NZ63

Line Numbers	SiO2	TiO2	Al2O3	FeO	MnO	MgO	CaO	Total
Garnet								
8419	37.97185	0.18004	21.21084	26.38137	3.330502	0.749709	10.5525	100.3768
8420	38.65347	0.015619	21.38145	25.68783	1.783051	1.441076	12.19162	101.1541
8421	38.69539	0.020863	21.46063	25.79794	1.763734	1.521664	12.23574	101.496
8422	37.98233	0	21.18241	25.3375	1.741753	1.401879	11.94438	99.59026
8423	40.16015	0.032552	21.93256	26.60684	1.881395	1.499464	12.65808	104.771
8424	38.78597	0.031235	21.7253	25.91957	1.796046	1.491637	12.16697	101.9167
8425	38.33311	0.076482	21.26543	25.34237	2.25891	1.463708	11.93984	100.6799
8427	38.70006	0.01406	21.33359	26.02064	2.860721	1.493474	10.5744	100.9969
8428	38.31157	0.002088	21.23784	26.86485	3.470635	1.561648	9.238692	100.6873
8429	38.26891	0.06412	20.76245	27.7643	3.458975	1.611291	9.389543	101.3196
8430	38.22697	0.049207	21.26457	27.81649	4.062632	1.576616	8.93599	101.9325
8431	38.4338	0.011546	21.31288	27.26402	3.936229	1.524091	8.856246	101.3388
8433	38.22155	0.029473	21.25987	27.45912	4.000489	1.596116	8.420211	100.9868
8434	38.44861	0.030462	21.24488	28.46838	4.063473	1.599762	8.009373	101.865
8435	38.86117	0.010674	21.41527	27.80627	3.759698	1.634908	9.118364	102.6063
8436	37.32503	0	20.82862	26.37013	3.566396	1.503205	9.283576	98.87696
8437	38.35008	0.06118	21.44379	27.94742	3.89356	1.562894	9.04009	102.299
8438	38.25608	0.101277	21.32126	28.17198	4.278647	1.481969	7.737463	101.3487
8439	38.78882	0.063369	21.39211	28.58811	4.455467	1.664494	7.994112	102.9465
8440	38.57585	0.081796	21.36586	28.29179	4.520271	1.474154	7.849673	102.1594
8441	38.40433	0.059864	21.03904	28.39676	4.433574	1.453595	7.828984	101.6162

APPENDIX B: MAD Adobe Illustrator files

https://alabama.box.com/s/ws51012dsuqjy42nedkx2n3k3s1agaab